GEOSCIENCE

Australian Government
Geoscience Australia

EQRM: Geoscience Australia's Earthquake Risk Model

Technical Manual
Version 3.0

D. Robinson, G. Fulford and T. Dhu

Record
2005/01

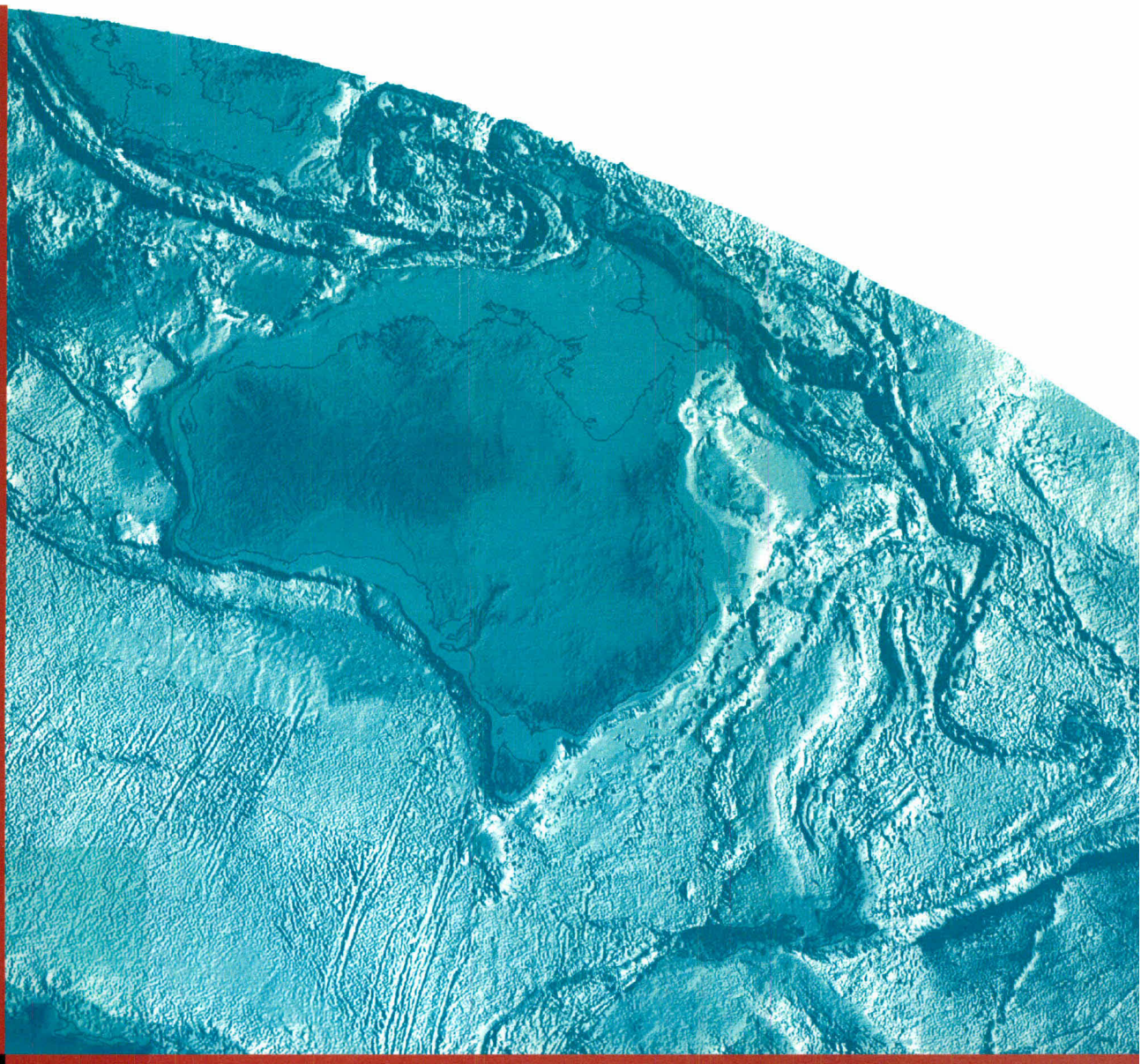

EQRM: Geoscience Australia's Earthquake Risk Model

Technical Manual
Version 3.0

GEOSCIENCE AUSTRALIA
RECORD 2005/01

by

D. Robinson, G. Fulford and T. Dhu

Australian Government
Geoscience Australia

Acknowledgements

The authors wish to thank John Schneider, leader of the Risk Research Group at Geoscience Australia. John's expertise in the areas of earthquake hazard and risk analysis have proven invaluable throughout the project. Without his ongoing support and advice the EQRM would not be half the product that it is today.

Andres Mendez from Aon Re in Chicago is acknowledged for providing software that formed the backbone of the earthquake catalogue generation. This generous contribution, as well as his high level of collaborative support, was fundamental to the project's success.

Bradley Horton is appreciated for the programming support that he provided through a number of contracts with Ceanet. The professionalism with which Bradley conducted his work extended beyond the call of duty on many occasions. Bradley's efforts have lead to great improvements in the useability and robustness of the EQRM. Duncan Gray, Kurt Pudniks and Ken Dale, all of Geoscience Australia, are also acknowledged for their coding efforts in particular modules of the EQRM software.

The authors have sought advice on specific topics from a range of people involved in the earthquake hazard and risk fields. The following are acknowledged for their expertise and assistance; George Walker of Aon Re, Professor John McAneney of Risk Frontiers, Walt Silva of Pacific Engineering and Analysis, Don Windeler and his team at Risk Management Solutions (RMS), Mike Griffith at The University of Adelaide, Gary Gibson of the Seismology Research Centre and Brian Gaull from Guria Consulting.

A number of people at Geoscience Australia have contributed to the development of the EQRM. Members of the Newcastle and Lake Macquarie project team lead by Trevor Jones are acknowledged for their assistance in shaping the early design of the EQRM. Mark Edwards and Ken Dale are thanked for the countless engineering questions that they have fielded over the four year project. Matt Hayne, project leader of the Risk Assessment Methods Project is thanked for creating the productive and supportive environment that allowed this project to flourish. EQRM users, Cvetan Sinadinovski, Annette Patchett, Ken Dale and Augusto Sanabria are thanked for their feedback and for continually inspiring the incorporation of new functionality. Ole Nielsen and Duncan Gray are acknowledged for the provision of software engineering advice and for generally improving the coding abilities of the authors. Angie Jaensch, Greg Michalowski and Fiona Watford are acknowledged for drafting some of the figures. Finally, the authors wish to thank Adrian Hitchman, Ken Dale and Augusto Sanabria for reviewing the drafts of this report. Their reviews lead to substantial improvements to this manual.

Geoscience Australia
Chief Executive Officer: Dr Neil Williams

Department of Industry, Tourism and Resources
Minister for Industry, Tourism and Resources: Senator The Hon. Ian Macfarlane MP
Parliamentary Secretary: The Hon. Bob Baldwin MP
Secretary: Mark Paterson

ISSN 1448-2177
ISBN 1 920871 24 1 (Hardcopy)
ISBN 1 920871 71 3 (Web)

GeoCat No. 61751

Bibliographic reference: Robinson, D., Fulford, G., Dhu, T., 2005. *EQRM: Geoscience Australia's Earthquake Risk Model. Technical Manual Version 3.0.* Geoscience Australia Record 2005/01

Contents

1 Introduction **1**

1.1 Overview 1

1.2 Using this manual 2

1.3 About this manual 3

2 The EQRM application **5**

2.1 Directory structure 5

2.2 EQRM inputs 7

2.2.1 The `setdata` file 7

2.2.2 Parameter files 15

2.2.3 Running the EQRM in MATLAB 16

2.2.4 Compiling and using a stand–alone version of the EQRM in MATLAB R14SP1 18

2.3 Creating a stand–alone executable of the EQRM GUI in MATLAB R14SP1: 18

3 Earthquake source generation **20**

3.1 Overview 20

3.2 Creating an earthquake catalogue for probabilistic seismic hazard analysis 21

3.2.1 Simulated events and the earthquake catalogue 22
3.2.2 Simulated events and virtual faults 23
3.2.3 Location of synthetic earthquakes 25
3.2.4 Overlapping source zones 28
3.2.5 Magnitude selection and event activity 29
3.2.6 Dimensions and position of the rupture plane 32
3.2.7 Azimuth and dip of rupture 38
3.3 Using multiple source zones - Incorporating epistemic uncertainty 38
3.4 Spawning events 40
3.5 Analysing a scenario event 41
3.6 Key functions, flags and parameters 42

4 Grids and building databases **44**

4.1 Overview 44
4.2 Hazard grids 44
4.3 Building databases 45
4.3.1 Building construction types 47
4.3.2 Building usage types 49
4.3.3 Replacement costs 50
4.4 Key functions, flags and parameters 53

5 Attenuation **54**

5.1 Overview 54
5.1.1 Background theory 54
5.1.2 Implementation 56

5.2 Attenuation formulae 57
5.2.1 Toro attenuation formula 58
5.2.2 Gaull attenuation formula 59
5.2.3 Atkinson and Boore attenuation formula 60
5.2.4 Sadigh attenuation formula 60
5.2.5 Somerville attenuation formula 61
5.3 Incorporating aleatory uncertainty 62
5.3.1 Random sampling of a response spectral acceleration . . . 63
5.3.2 Sampling the probability density function of the response spectral acceleration (spawning) 64
5.4 Using multiple attenuation models - Incorporating epistemic uncertainty 66
5.5 Key functions, flags and parameters 69

6 Regolith amplification **71**

6.1 Overview 71
6.1.1 Background theory 71
6.2 The amplification factor input file 72
6.3 Implementation 72
6.4 Incorporating aleatory uncertainty 76
6.5 Key functions, flags and parameters 77

7 Building damage **78**

7.1 Introduction 78
7.2 The capacity spectrum method 79
7.2.1 The building capacity curve 80

Fitting the building capacity curve 81
Variability of the capacity curves 82
7.2.2 Damping the demand curve 82
Modification of elastic damping 83
Hysteretic damping 85
7.2.3 Finding the intersection point 88
7.3 Fragility curves 89
7.3.1 Form of fragility curves 90
7.3.2 Damage state thresholds 90
7.3.3 Variability of the damage states 91
7.3.4 Incremental probabilities 92
7.4 Differences from HAZUS methodology 92
7.4.1 Extra features 93
7.5 Key functions, flags and parameters 95

8 Losses **96**

8.1 Overview 96
8.2 Direct financial loss 96
8.2.1 General financial loss equations: loss for a single building . 96
8.2.2 Aggregated loss and survey factors 100
8.2.3 Cutoff values 100
8.3 Social losses 101
8.4 Key functions, flags and parameters 102

9 Hazard and risk results **104**

9.1 Overview 104

9.2 Calculating hazard and risk 104

9.2.1 Computing the annual exceedance rate 105

9.3 Earthquake hazard results 106

9.3.1 Hazard maps 106

9.3.2 Hazard exceedance curves 107

9.3.3 Uniform hazard spectra 108

9.4 Earthquake risk results 108

9.4.1 Risk exceedance curve 110

9.4.2 Annualised loss 111

9.4.3 Disaggregated annualised loss 112

9.5 Earthquake scenario results 113

9.6 Key functions, flags and parameters 115

A Appendicies **116**

A.1 Creating a stand–alone executable of the EQRM GUI in MATLAB R13: 116

A.2 The default PSHA `setdata` file 119

A.3 The default PSRA `setdata` file 121

A.4 Example of `<site_loc>_par_sourcezones.txt` 123

A.5 Example of `<site_loc>_par_sourcepolys.txt` 124

A.6 Discretising the PDF of a continuous variable 125

A.7 Example of `<site_loc>_par_ampfactors.mat` 127

A.8 Response spectra 128

A.9 Tables of building parameters 130

Chapter 1

Introduction

1.1 Overview

The EQRM application is a computer model for estimating earthquake hazard and earthquake risk. Modelling earthquake hazard involves assessing the probability that certain levels of ground motion will be exceeded. Modelling of earthquake risk involves estimating the probability of a building portfolio experiencing a range of earthquake induced losses. For any number of synthetic earthquakes, the EQRM application can be used to estimate:

1. the ground motion and its likelihood of occurrence (earthquake hazard),
2. the direct financial loss and its likelihood of occurrence (earthquake risk), and
3. less reliably the number of casualties and injuries and their likelihood of occurrence (earthquake risk).

The EQRM application is Geoscience Australia's centerpiece for modelling earthquake hazard and risk. Its use formed the basis for Geoscience Australia's recent reports on Earthquake risk in the Newcastle and Lake Macquarie (Dhu and Jones, 2002) and Perth (Sinadinovski, Edwards, Corby, Milne, Dale, Dhu, Jones, McPherson, Jones, Gray, Robinson and White, 2005) regions.

The process for computing earthquake hazard can be described by the following steps:

1. the generation of a catalogue of synthetic earthquakes (or events) (see Chapter 3),
2. the propagation or attenuation (see Chapter 5) of the 'seismic wave' from each of the events in 1 to locations of interest (see Chapter 4),
3. accounting for the interactions between the propagating 'seismic wave' and the local geology or regolith (see Chapter 6), and
4. accounting for the probability of each event and the estimation of hazard (see Chapter 9).

The process for computing earthquake risk shares the same first three steps as the earthquake hazard. The fourth step and onwards can be described as follows:

4. estimating the probability that the portfolio buildings (see Chapter 4) will experience different levels of damage (see Chapter 7),
5. the computation of direct financial loss as a result of the probabilities computed in 4 (see Chapter 8), and
6. assembling the results to compute the risk (see Chapter 9).

1.2 Using this manual

This manual describes the EQRM application; it has been designed to serve the following three purposes:

1. describe the theory and methodology behind the EQRM application;
2. explain how to use the EQRM application to model earthquake hazard and risk; and
3. provide enough information to assist those who may wish to access individual modules and modify them.

A number of features have been included to assist readers of the manual. These features include:

- **Text highlighting** - Important parameters, file names and code are identified by a typeset font.

- **Index -** An index has been introduced to allow speedy of navigation of the manual.
- **Chapter summary -** Each chapter is concluded with a 'Key functions, flags and parameters' section that summarises the key code related items that were discussed in the chapter.

1.3 About this manual

Chapter 2: The EQRM application introduces the EQRM software. The chapter describes the directory structure and introduces important input parameter files. Setup and operational processes are discussed and the conversion of the EQRM to a stand-alone executable described. Readers who do not wish to familiarise themselves with details of the EQRM application may wish to skip this chapter.

Chapter 3: Earthquake source generation discusses the creation of an earthquake catalogue. At the core of any hazard or risk assessment is the simulation of synthetic earthquakes and the creation of a catalogue of synthetic events. The chapter describes how the simulation of earthquakes can focus around a specific earthquake of interest (a scenario based simulation) or how it can model the effect of 'all foreseeable' events (a probabilistic simulation).

Chapter 4: Grids and building databases describes how calculations of risk and hazard are conducted on a point by point basis. In the case of earthquake hazard, a grid of points is created and hazard computed at each of the grid nodes. Typically a regular grid is used to improve the production of hazard maps, however this is not a requirement. Earthquake risk calculations are also performed on a grid. Each node of the grid represents the centroid of a building within a portfolio of interest. The chapter demonstrates how the grid points are associated with other attributes such as site–class or building construction type.

Chapter 5: Attenuation discusses the propagation (or attenuation) of the motion from each of the synthetic earthquakes in the event catalogue to locations of interest. Different measures of distance between an event and a site of interest are introduced. The chapter also describes the attenuation models that can be used with the EQRM application.

Chapter 6: Regolith amplification discusses how local geology, or regolith, can be incorporated in an earthquake hazard or risk assessment. The chapter illustrates how the presence of regolith can lead to amplification (or de-amplification) of both ground and building motion, and consequently result in higher (or lower) levels of hazard and risk.

Chapter 7: Building damage describes how the EQRM application estimates the probability that each building will experience different levels of damage. The chapter gives a brief discussion of the theory behind making such estimates as well as outlining how to extrapolate the estimates to an entire portfolio of buildings in a region of interest.

Chapter 8: Losses illustrates how to model the direct financial loss as a result of the damage estimates described in *Chapter 7*. The chapter also provides a brief description of how the EQRM application can estimate injuries and casualties.

Chapter 9: Displaying hazard and risk results describes how the results from the EQRM application can be summarised and displayed. There are many ways to display estimates of earthquake hazard and risk. Earthquake hazard is commonly modelled in terms of a probability (often 10%) of a particular ground motion (usually acceleration) being exceeded in some time frame (often 50 years). In the case of a scenario based simulation, earthquake risk can be modelled in terms of dollar estimates of building loss. Such losses can be categorised by building type, geography or any other category of interest. In the case of a probabilistic simulation, earthquake risk is often modelled in terms of one or both of the following:

1. the loss per year averaged over a long period of time, typically 10000 years. This is known as the annualised loss.

2. the probability that different levels of loss will be exceeded. The plot of loss against such exceedance probabilities is referred to as a probable maximum loss curve.

Chapter 2

The EQRM application

This chapter describes the EQRM application. The directory structure, input parameters and directions on how to run the EQRM are all described. Converting the EQRM into a stand-alone executable is also explained at the end of the chapter. Readers who are interested in only the EQRM methodology and not the EQRM software package may wish to skip this chapter.

2.1 Directory structure

The code is currently organised in the following directory structure:

`*/eqrm/datacvt`	'off-line' routines for preparing input data.
`*/eqrm/eqrm_app`	software and default data files comprising the EQRM application.
`*/eqrm/testing_harness`	testing suite to ensure new development meets pre-defined back-compatibility criteria.

The most significant sub-directories of `*/eqrm/datacvt` are:

`*/buildingdb`	tools to assist the preparation of building databases (see Chapter 4).
`*/buildingpars`	tools to assist the preparation of engineering parameters (see Chapter 7).

`*/econsocpars`	tools to assist the preparation of direct financial loss parameters (see Chapter 8).
`*/site_classes`	tools to prepare site class polygons (see Chapter 6).
`*/stats`	tools to extract statistics from building databases (see Chapter 4). Note that these tools were originally written to extract Newcastle information however they can easily be modified to work with other data sets.

The most significant sub-directories of `*/eqrm/eqrm_app` are:

`*/m_code`	EQRM source code, predominately MATLAB functions (see below for more details).
`*/resources`	data files to support the EQRM (see below for more details).
`*/system`	tools and path information directing the EQRM to individual components (e.g. `*/m_code` and `*/resources`).

The most significant sub-directories of `*/eqrm/eqrm_app/m_code` are:

`*/general`	general functions (includes error manager).
`*/startup`	functions to assist with setting up the MATLAB Path (Section 2.2.3).
`*/hazard`	functions for source generation (Chapter 3), attenuation (Chapter 5), amplification (Chapter 6) and hazard calculation (Chapter 9).
`*/c3_gui`	functions to support the `eqrm_param_gui` (Section 2.2.3).
`*/mcc_build_apps`	functions to assist in building a stand–alone executable.
`*/utils`	general utility tools used by other functions.
`*/compare_utils`	important functions for comparing MATLAB binary files (used by the testing suite).
`*/vuln`	functions for building damage (Chapter 7), financial loss (Chapter 8) and risk calculation (Chapter 9).
`*/processing`	post-processing functions for manipulating and plotting EQRM outputs (Chapter 9).
`*/dit`	functions to support the data interrogation tool GUI (output manager: Section 2.2.3).

The most significant sub-directories of `*/eqrm/eqrm_app/resources` are:

`*/data`	parameter files and input data for the EQRM (e.g. attenuation model coefficients, engineering parameters etc.).
`*/c3_gui`	figure files for the `eqrm_param_gui`.
`*/dit_gui`	figure files for the DIT GUI (output manager).

The most significant sub-directories of `*/eqrm/testing_harness` are:

`*/hazard`	input and output data for EQRM hazard back compatibility tests.
`*/vuln`	input and output data for EQRM risk back compatibility tests.

2.2 EQRM inputs

For the purpose of this manual the EQRM inputs are discussed in two separate sections. Section 2.2.1 describes the contents of the `setdata` file, which contains a series of input parameters and flags that must be set by the user. Section 2.2.2 describes other files that are required by the EQRM modules. In most cases these files can be used directly from `*/eqrm/eqrm_app/resources/data`, however the user has the ability to provide alternatives.

2.2.1 The setdata file

The full path to the `setdata` file must be passed to the EQRM when the program is run. It contains a series of input variables (or parameters) that define the manner in which the EQRM is operated. For example; there is a flag to control whether the EQRM models hazard or risk. Other flags can be used to define which attenuation model is selected, whether site amplification is considered or which set of engineering parameters is used. A description of all of the variables in the `setdata` file is given below. The `setdata` file contains a single variable `eqrm_param_T`. For the purpose of this manual the fields of `eqrm_param_T` are segregated into 13 sub-groups as they appear on the EQRM GUI (Section 2.2.3) however no such separation exists in the `setdata` file itself.

Operation Mode:

`run_type` Defines the operation mode of the EQRM:
1 ⇒ hazard;
2 ⇒ risk;
3 ⇒ risk from hazard.

General:

`inputdir`	Directory containing any local input files.
`savedir`	Directory for output files.
`site_loc`	String used in input and output file names.
`ieast`	Direction of increasing longitude: 1 ⇒ increases toward East; -1 ⇒ increases toward West.
`grid_flag`	Define grid type: 1 ⇒ Grid produced in GIS; 2 ⇒ Grid produced by `Input Manager`.
`small_site_flag`	Sampling of sites: 0 ⇒ use all sites; 1 ⇒ use sub-sample defined by `SiteInd`.
`SiteInd`	Vector whose elements represent the site indices to be used in the sub-sample (if `small_site_flag` = 1).
`destring`	Optional string to be used in logfile. Currently only used with risk runs.
`rtrn_per`	Vector whose elements represent the return periods to be considered for hazard.

Source:

`azi`	Predominant azimuth of events.
`d_azi`	Azimuth range for events (i.e. `azi` ± `d_azi`).
`dip`	Dip of virtual faults.
`ntrgvector`	Vector whose elements represent the desired number of simulated events for each generation zone.
`ftype`	Fault type for attenuation models. *Note that this parameter is currently not operational.* 0 ⇒ ss; 0.5 ⇒ ro;

	1 ⇒ rv, nr or no; 2 ⇒ uk.
`wdth`	Width of virtual fault.
`min_mag_cutoff`	Minimum magnitude below which hazard is not considered.
`nbins`	Number of magnitude bins used to sample event magnitudes.

Event Spawn:

`src_eps_switch`	Make copies of events for incorporation of attenuation uncertainty i.e. spawning: 0 ⇒ events NOT copied; 1 ⇒ events copied: logic tree collapsed. 2 ⇒ events copied: logic tree NOT collapsed.
`mbnd`	Only events with magnitude greater than `mbnd` are spawned.
`nsamples`	Creates `nsamples` copies of each spawned event.
`nsigma`	Defines the x-limits of the probability density function to be considered when spawning.

Scenario:

`determ_flag`	Event simulation type: 0 ⇒ standard probabilistic simulation; 1 ⇒ consider a specific scenario event.
`determ_ntrg`	The desired number of copies to be generated (if `determ_flag` = 1).
`determ_azi`	Azimuth of event (if `determ_flag` = 1).
`determ_lat`	Latitude of rupture centroid (if `determ_flag` = 1).
`determ_lon`	Longitude of rupture centroid (if `determ_flag` = 1).
`determ_mag`	Moment magnitude of event (if `determ_flag` = 1).
`determ_r_z`	Depth to event (if `determ_flag` = 1).

Attenuation:

`attenuation_flag` A 2 row matrix containing one column for each attenuation model to be used. The first row contains a pointer to the attenuation model (see below) and the second row contains its weight.
Attenuation Model Pointers:
0 ⇒ Gaull *et al.* (1990);
1 ⇒ Toro *et al.* (1997);
2 ⇒ Atkinson and Boore (1997);
3 ⇒ Sadigh *et al.* (1997);
4 ⇒ Somerville *et al.* (2001);
100 ⇒ Gaull *et al.* (1990) (MMI).

`attn_region` Defines version of selected attenuation model (i.e. region or type of magnitude). Options vary depending on the value of `attenuation_flag` (see Chapter 5).

`var_attn_flag` Variability for attenuation:
0 ⇒ NOT included;
1 ⇒ included.

`var_attn_method` Technique used to incorporate attenuation aleatory uncertainty:
1 ⇒ Sample PDF - spawning;
2 ⇒ random sampling;
3 ⇒ $+2\sigma$;
4 ⇒ $+\sigma$;
5 ⇒ $-\sigma$;
6 ⇒ -2σ.

`resp_crv_flag` Secondary options for choice of response spectral acceleration S_a:
0 ⇒ S_a from attenuation model;
1 ⇒ S_a from attenuation model and cutoff maximum spectral displacement;
2 ⇒ use PGA from attenuation model to scale Australia Standard S_a;
3 ⇒ use PGA from attenuation model to scale

	Australia Standard and cutoff at maximum spectral displacement; 4 ⇒ use PGA from attenuation model to scale HAZUS S_a.
`Rthrsh`	Threshold distance, beyond which motion is assigned to zero.
`periods`	Periods for S_a.
`pgacutoff`	PGA cutoff for re-scaling S_a with PGA greater than `pgacutoff`.
`smoothed_response_flag`	Controls smoothing of S_a: 0 ⇒ No smoothing; 1 ⇒ Smoothing.

Amplification:

`amp_switch`	Amplification associated with local regolith: 0 ⇒ NOT included; 1 ⇒ included.
`var_amp_flag`	Variability for amplification: 0 ⇒ NOT included; 1 ⇒ included.
`var_amp_method`	Technique used to incorporate amplification aleatory uncertainty: 1 ⇒ Sample PDF - spawning; 2 ⇒ random sampling; 3 ⇒ $+2\sigma$; 4 ⇒ $+\sigma$; 5 ⇒ $-\sigma$; 6 ⇒ -2σ.
`MaxAmpFactor`	Maximum accepted value for amplification factor.
`MinAmpFactor`	Minimum accepted value for amplification factor.

Bclasses:

`b_usage_type_flag`	Building usage classification system: 1 ⇒ HAZUS usage classification; 2 ⇒ FCB usage classification.
`hazus_btypes_flag`	Building construction type classification system:

0 ⇒ refined HAZUS building classification;
1 ⇒ HAZUS building classification.

`hazus_dampingis5_flag` Level of damping when `buildpars_flag` = 2:
0 ⇒ Use damping level corresponding to `buildpars_flag`=0;
1 ⇒ Use 5%.

`buildpars_flag` Engineering parameters to be used:
0 ⇒ Australian Engineers Workshop Parameters (AEWP) with Edwards modifications 1;
1 ⇒ AEWP;
2 ⇒ original HAZUS paramaters;
3 ⇒ AEWP with Edwards modifications 2;
4 ⇒ AEWP with Edwards modifications 3.

Bclasses2:

`force_btype_flag` Force all buildings to have the same usage and type classification:
0 ⇒ Use buildings as defined in database;
1 ⇒ Force modification.

`determ_btype` Building type when `force_btype_flag`=1.

`determ_buse` Building usage when `force_btype_flag`=1.

`ignore_post89_flag` Ignore buildings built after 1989:
0 ⇒ include all ages;
1 ⇒ ignore the post 89 buildings.

CSM:

`var_bcap_flag` Variability with building capacity curve:
0 ⇒ NOT included;
1 ⇒ included.

`bcap_var_method` Method used to incorporate variability in capacity curve:
1 ⇒ Random sampling used to adjust the vertical position of the yield and ultimate points;
2 ⇒ Preferred technique: Random sampling applied to ultimate point only and yield

	point re-calculated to satisfy capacity curve 'shape' constraint.
`stdcap`	standard deviation for capacity curve log–normal PDF.
`damp_flags`	Vector to control nature of linear damping (see below for explanation of each element).
`damp_flags(1)`	Damping multiplicative formula to be used - Section 7.2.2: 0 ⇒ Preferred technique: use R_a, R_v, and R_d; 1 ⇒ use R_a, R_v and assign $R_d = R_v$; 2 ⇒ use R_v only and assign $R_a = R_d = R_v$.
`damp_flags(2)`	Modify transition building period i.e. corner period T_{av}: 0 ⇒ Preferred technique: modify as in HAZUS; 1 ⇒ do NOT modify.
`damp_flags(3)`	Smoothing of damped curve: 0 ⇒ Preferred technique: apply smoothing; 1 ⇒ NO smoothing.
`Harea_flag`	Technique for Hysteretic damping: 0 ⇒ NO Hysteretic damping; 1 ⇒ Hysteretic damping via trapezoidal approximation; 2 ⇒ Hysteretic damping via curve fitting.
`SDRelTol`	Tolerance (as a percentage) for SDcr (in nonlinear damping calculations).
`max_iterations`	Maximum iterations for nonlinear damping calculations.

Diagnostics:

`qa_switch_ampfactors`	Diagnostics for `do_amplification` (a few sites only): 0 ⇒ NO diagnostic plots; 1 ⇒ display diagnostic plots.
`qa_switch_attn`	Diagnostics for `do_attenuation` (a few sites only): 0 ⇒ NO diagnostic plots; 1 ⇒ display diagnostic plots.
`qa_switch_fuse`	Diagnostics for `fuse_4hzd`: 0 ⇒ NO diagnostic plots;

	1 ⇒ display diagnostic plots.
qa_switch_map	Diagnostics for do_analysis (works in hazard mode only): 0 ⇒ NO diagnostic plots; 1 ⇒ display diagnostic plots.
qa_switch_mke_evnts	Diagnostics for mke_evnts: 0 ⇒ NO diagnostics and save all events; 1 ⇒ display diagnostic plots and ask user about saving; 2 ⇒ display diagnostic plots and save events inside polygon; 3 ⇒ display diagnostic plots and save all events.
qa_switch_watercheck	No longer used.
qa_switch_soc	Diagnostics for casualty model: 0 ⇒ NO diagnostics; 1 ⇒ plot injuries and casualties.
qa_switch_vun	Diagnostics for capacity spectrum method: 0 ⇒ NO diagnostic plots; 1 ⇒ display building info to screen; 2 ⇒ Do 1 and plot each building's convergence for the 1st earthquake (pause after every iteration); 3 ⇒ Do 1 and plot each building's convergence for the worst earthquake (pause after final convergence); 4 ⇒ Do 1 and plot each building's convergence for the worst earthquake (pause after every iteration).

Loss:

pga_mindamage	minimum PGA(g) below which financial loss is assigned to zero.
ci	Regional cost index multiplier to convert dollar values in building database to desired regional and temporal (i.e. inflation) values.
aus_contents_flag	Contents value for residential buildings and salvageability after complete building damage: 0 ⇒ contents value as defined in building database and salvageability of 50%;

1 ⇒ 60% contents value as defined in building database and salvageability of zero.

Save:

`hazard_map_flag`	Save data for hazard maps: 0 ⇒ do NOT save; 1 ⇒ save.
`save_ecloss_flag`	Save direct financial loss data: 0 ⇒ do NOT save; 1 ⇒ save total financial loss; 2 ⇒ save contents and building loss separately.
`save_socloss_flag`	Save casualty and injury data: 0 ⇒ do NOT save; 1 ⇒ save.
`save_motion_flag`	Save RSA motion when conducting a risk simulation: 0 ⇒ do NOT save; 1 ⇒ save.
`save_probdam_flag`	Save damage state probabilities for each building (*currently not operational*): 0 ⇒ do NOT save; 1 ⇒ save.
`save_deagecloss_flag`	Save loss associated with individual damage types i.e. structural, non-structural (*currently not operational*): 0 ⇒ do NOT save; 1 ⇒ save.

2.2.2 Parameter files

This section identifies the important input files that are used by different components of the EQRM. Input files can be dependent or independent of region. For example the file `newc_par_ampfactors.mat` contains the amplification factors for the Newcastle region (see Section 6), whereas the file `attn_toro_midcontinent_momag.txt` contains attenuation coefficients for the Toro, Abrahamson and Schneider (1997) attenuation model (see Section 5) which are not dependent on region. The EQRM identifies the desired region dependent files using the user defined parameter `site_loc` (see Section 2.2.1).

The EQRM makes use of default data to reduce the need for a large number of

defined input files. Default data files are stored in the directory `*/eqrm/eqrm_app-/resources/data` (see Section 2.1). The EQRM facilitates the use of non-default data by first looking in the user defined `inputdir` (see Section 2.2.1) for required files. If the required files are found in `inputdir` they will be used by the EQRM, if the files are not found in `inputdir` then the default files are used.

Note that default files are available for pre-defined regions only. For example; Newcastle and Perth region default data can be accessed by defining `site_loc` of '`newc`' and '`perth`' respectively.

Table 2.1 summarises the important input files that can be found in the default data area. The files are listed against the chapter where more information can be found.

2.2.3 Running the EQRM in MATLAB

The EQRM has a special startup function (`eqrm_startup`) that adds all the required directories to the MATLAB path. The following instructions describe how to use `eqrm_startup` to set the MATLAB path:

- move to the directory `*/eqrm/eqrm_app/m_code/startup`
- at the command line type
  `>> eqrm_startup('*\eqrm\eqrm_app')`

The EQRM has a special GUI known as the `eqrm_param_gui` that can be used to create a `setdata` file, run the EQRM application or analyse the EQRM outputs. To launch the GUI simply type the following at the command line:

```
>> eqrm_param_gui
```

It is beyond the scope of this manual to discuss the `eqrm_param_gui` further. However it is user friendly and reasonably self explanatory. Alternatively the EQRM can be run from the command line using the function `eqrm_analysis`. To find out how to use `eqrm_analysis` type the following at the MATLAB command line:

```
>> help eqrm_analysis
```

Table 2.1: Default parameter files in */eqrm/eqrm_app/resources/data.

Chapter	Files
Earthquake Source generation	<site_loc>_par_sourcepolys.txt <site_loc>_par_sourcezones.txt
Grids and building databases	aus_mat.txt australia_bndy.txt <site_loc>_par_site.mat <site_loc>_par_site_uniform.mat <site_loc>_par_study_region_box.txt sitedb_<site_loc>.mat suburb_postcode.csv textbtypes.txt textbusageFCB.txt textbuses.txt
Attenuation	attn_atkboore_momag.txt attn_sadigh_coeff_momag_great65.txt attn_sadigh_coeff_momag_less65.txt attn_somer_nonrift_hori.txt attn_somer_nonrift_vert.txt attn_somer_rift_hori.txt attn_somer_rift_vert.txt attn_toro_midcontinent_momag.txt,
Regolith amplification	<site_loc>_par_ampfactors.mat <site_loc>_par_site_class_mask.mat <site_loc>_par_site_class_polys.mat
Building damage	bfactorsdb.mat bfactorsdb_hazus.mat bfactorsdb_wshop.mat bfactorsdb_wshop_update2.mat bfactorsdb_wshop_update3.mat factors-nonstructdam.csv factors-structdam.csv
Losses	rc_perReplCostwrtBuildCEdwardsFCBusage.mat rc_perReplCostwrtBuildCEdwardsHazususage.mat rc_perReplCostwrtBuildCHazusage.mat econ_par.mat

The EQRM has a special Output Manager GUI that can be used to view, analyse and plot EQRM outputs. The Output Manager is also known as the Data Interrogation Tool (DIT). A report generation facility has been included with the Output Manager and can be used to create a LaTeX`*.tex` file with EQRM output figures. The LaTeXfile can be compiled into a `.ps` and/or `.pdf` file if the appropriate MikTeX software is installed.

2.2.4 Compiling and using a stand–alone version of the EQRM in MATLAB R14SP1

Using the MATLAB compiler it is possible to create a stand–alone version of the EQRM that can be used without requiring MATLAB. The instructions for MATLAB R13 are given in Appendix A.1.

2.3 Creating a stand–alone executable of the EQRM GUI in MATLAB R14SP1:

Type the following at the MATLAB command line for the source machine

```
>> cnt_do_mcc_build_to_system('eqrm_param_gui',<*/path>)
```

This process will create the following files in `<*/path>`:

1. `eqrm_param_gui.exe`;
2. a directory named `eqrm_param_gui_mcr`; and
3. `eqrm_param_gui.ctf`.

Prepare the files for transportation as follows:

1. Create a folder entitled `*/testexe`.
2. In `*/testexe` create two folders `*/testexe/system` and `*/testexe/mcr`.

3. Copy `eqrm_param_gui.exe`, `eqrm_param_gui_mcr` and `eqrm_param_gui.ctf` (created above) into `*/testexe/system`.
4. Copy the following files from `*/EQRMROOT/system` into `*/testexe/system`:
   (a) `root_mat_creator_cnt.exe`;
   (b) the directory `root_mat_creator_cnt_mcr`; and
   (c) `root_mat_creator_cnt.ctf`.
5. Copy `_MCRInstaller.exe` from `<MATLABROOT>/toolbox/compiler/deploy-/win32/MCRInstaller.exe` into `*/testexe/mcr`.
6. Copy the directory `*/EQRMROOT/resources` to `*/testexe/resources`.

Installation onto the target machine is achieved as follows:

1. Move the contents of `*/testexe` onto the target machine.
2. Run `_MCRInstaller.exe` on `*/testexe/mcr` by double clicking on it.
3. Set environment path on the target machine
   (a) open the control panel;
   (b) open system;
   (c) select the advanced tab;
   (d) select environment variables;
   (e) create new user variable entitled `path`;
   (f) add the following path names (separated by semi colons) into the value field for `path`;
      - `*/testexe/system`; and
      - `*/testexe/mcr/v71runtime/win32`;
   (g) Log off and log back on.
4. Set the software path as follows
   (a) Open a DOS shell;
   (b) Type `root_mat_creator_cnt.exe`;
   (c) On the 'EQRM root file creation' GUI select the EQRM root directory (i.e. `*/testexe`).
5. Open the EQRM GUI by typing `eqrm_param_gui.exe` at the DOS command prompt.

Chapter 3

Earthquake source generation

3.1 Overview

The EQRM conducts probabilistic seismic hazard analysis (PSHA) and probabilistic seismic risk analysis (PSRA) using an event based approach. This means that the ground motions (hazard) and loss (risk) are computed for each event individually and the results separately aggregated to form probabilistic estimates. The event based approach differs from the traditional approach to PSHA which integrate over all magnitude and distance combinations to attain probability levels for exceeding a particular level of ground motion in a pre-defined period of time. The traditional approach is introduced by Cornell (1968) and summarised by McGuire and Arabasz (1990). A core component of any event based analysis with the EQRM is the generation of a simulated event (or earthquake) catalogue. The generation of the earthquake catalogue is performed by `mke_evnts` which relies upon an existing model for the seismicity in the region. Typically the model of seismicity comes from an interpretation of historical earthquakes, geology and neotectonics. The current version of the EQRM application requires a source zone model that consists of a set of areal source zones with associated Gutenberg-Richter recurrence relationships. Dhu *et al.* (2002) show how the seismic source zones were created for a risk assessment of the Newcastle and Lake Macquarie region.

The EQRM can be used with a single source model containing one or more source zones or multiple source models each containing one or more source zones. For example; Gaull *et al.* (1990) (G90) and Brown and Gibson (2004) (BG04) both present different source zone models for Australia containing 34 and 108 source zones respectively. An Australian hazard or risk assessment can be conducted using the EQRM with either G90 or BG04 independently or by using some weighted

combination of the two of them. Section 3.2 largely focusses on the generation of a synthetic earthquake catalogue from one source zone model, whereas Section 3.3 describes the use of multiple source zone models.

3.2 Creating an earthquake catalogue for probabilistic seismic hazard analysis

The generation of a synthetic catalogue of earthquakes is handled by the function `mke_evnts`. This function function requires one of the following groups of input files to be located within the `inputdir` or `*/eqrm/eqrm_app/resources/data`:

1. `<site_loc>_par_sourcezones.txt` and `<site_loc>_par_sourcepolys.txt`. When the EQRM uses these files directly only a single source zone model can be used. Moreover, the location and magnitude of the earthquakes are controlled by the source zones themselves.

2. `<site_loc>_par_source.mat` containing two variables whose names are `generation` and `source`. This format must be used with the EQRM when considering multiple source zones. Moreover, this format facilitates the generation of synthetic earthquakes (location etc.) using one set of polygons and the assignment of key attributes (such as probabilities) using the actual source zone models. The latter feature is very useful for concentrating earthquake generation in regions of interest (e.g. the central business district). Note that the function `src_zones_to_structure` can be used to create a `<site_loc>_par_source.mat` file by using one or more combinations of the `<site_loc>_par_sourcezones.txt` and `<site_loc>_par_sourcepolys.txt` pair.

The ASCII files `<site_loc>_par_sourcezones.txt` and `<site_loc>_par_sourcepolys.txt` are critical to both of the input combinations (1 and 2) introduced above. The file `<site_loc>_par_sourcezones` contains the parameters that define the seismic activity in each zone and has nine columns separated by tabs or spaces. There is one row for each areal source zone in the source model. The format of `<site_loc>_par_sourcezones.txt` is described in Table 3.1. The ASCII file `<site_loc>_par_sourcepolys.txt` contains the vertices of each of the source zones and it has four columns separated by tabs or spaces. The format of `<site_loc>_par_sourcepolys.txt` is described in Table 3.2. Note that each polygon represents a block of rows containing the information for all vertices in the polygon. Moreover, each polygon must be closed (i.e. the first and last row of each

Table 3.1: Columns in `<site_loc>_par_sourcezones.txt`.

column	description
1	zone identification number (*integer*)
2	area of zone (km^2)
3	f_z - depth to seismogenic region (km)
4	m_{min} - minimum moment magnitude for zone
5	m_{max} - maximum moment magnitude for zone
6	b - slope of Gutenberg-Richter recurrence rate
7	place holder (currently reserved for σ_b)
8	A_{min} - number of earthquakes of magnitude m_{min} or greater per year
9	place holder (currently reserved for $\sigma_{A_{min}}$)

Table 3.2: Columns in `<site_loc>_par_sourcepolys.txt`.

column	description
1	polygon vertex identifier (*integer*)
2	longitude of polygon vertex
3	latitude of polygon vertex
4	zone identification number (*integer*)

polygon block should be the same). Examples of `newc_par_sourcezones` and `newc_par_sourcepolys` are shown in Appendix A.4 and Appendix A.5 respectively. Note that both of these files may also contain metadata in the form of comments (indicated by a %).

3.2.1 Simulated events and the earthquake catalogue

A simulated event is represented by a plane (or rupture) in 3D space that signifies the region where slip has occurred. The geometry of a rupture plane is shown in Figure 3.1. The earthquake catalogue is a *.MAT file that contains a single variable `evntdb`. The variable `evntdb` is an array containing 31 columns and N_s rows, where N_s refers to the number of events in the simulated catalogue. The columns of `evntdb` are defined in Table 3.3. The important parameters of a simulated event are its location, geometry, magnitude and activity (or likelihood of occurrence). The rupture trace is the surface projection of the simulated event along the direction of dip. The position and geometry of the rupture trace is defined by its start (r_s^{lat}, r_s^{lon}) and end (r_e^{lat}, r_e^{lon}) points, its azimuth r_{azi} and its length r_l. The position and geometry of the rupture plane are defined by its width r_w, dip r_{dip} and the position of its centre (or rupture centroid). The

rupture centroid is defined in cartesian coordinates (r_x, r_y, r_z) in km using a local coordinate system with origin at the rupture start point (see Figure 3.1). The orientation of the local coordinate system is such that the $x - axis$ is oriented along the rupture trace with positive direction pointing towards the rupture end point, the $z - axis$ is pointing vertically downwards and the $y - axis$ is oriented along the surface of the 'earth' such that the axes form a right handed triad. The vertical projection of the rupture centroid is also described by its latitude r_c^{lat} and longitude r_c^{lon}. The event magnitude is represented as a moment magnitude and is generated by the process described in Section 3.2.5. The activity (or likelihood of occurrence) of the simulated event is described by the event activity which represents the number of times a given simulated event (conditional on magnitude and position) occurs in one year (see Section 3.2.5).

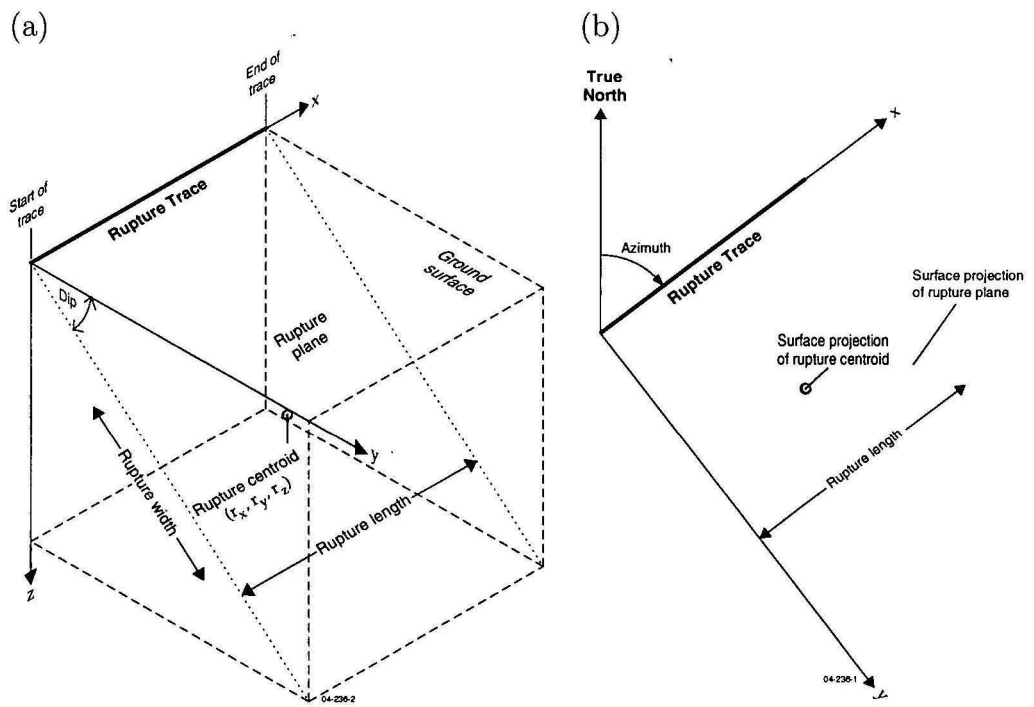

Figure 3.1: Orientation and dimension of the rupture plane in (a) 3D and (b) 2D vertical projection to ground surface.

3.2.2 Simulated events and virtual faults

The terms simulated event, simulated earthquake and simulated rupture are congruent and will be used interchangeably throughout this document. Sometimes the adjective 'simulated' will be omitted for brevity. An adjective 'actual' will

Table 3.3: Columns in `evntdb`. Note that some of the columns are not defined until after `fuse4_hzd` is run (see Section 3.4).

column	description
1	an integer corresponding to the generation source zone from which this event was generated
2	r_s^{lat} - latitude of rupture trace start point (decimal degrees)
3	r_s^{lon} - longitude of rupture trace start point (decimal degrees)
4	r_e^{lat} - latitude of rupture trace end point (decimal degrees)
5	r_e^{lon} - longitude of rupture trace end point (decimal degrees)
6	r_ϕ - azimuth of rupture trace (decimal degrees from True North)
7	r_{dip} - dip of rupture plane ($0 <$ decimal degrees < 90 from the surface)
8	A_{min} - number of earthquakes of magnitude m_{min} or greater per year
9	integer pointer to attenuation model for use with the synthetic earthquake.
10 to 18	place holder (currently not used)
19	w_e - weight derived from event spawning
20	r_ν - event activity (the number of magnitude r_m earthquakes expected per year scaled to the number being simulated)
21	r_m - event magnitude (moment magnitude)
22	r_ε - source epsilon from event spawning
23	r_c^{lat} - latitude of event centroid (decimal degrees)
24	r_c^{lon} - longitude of event centroid (decimal degrees)
25	r_z - event centroid depth z (km from ground surface)
26	r_x - event centroid x (km along rupture trace from the start of trace)
27	r_y - event centroid y (km perpendicular from trace in direction of dip)
28	r_l - length of rupture (km)
29	r_w - width of rupture (km measured along dip)
30	a unique integer for each synthetic earthquake in the generation zone (polygon). Note that the integer count begins again for each generation zone.
31	place holder (currently not used)

be used in place of 'simulated' to refer to a historic earthquake (i.e. one that has actually occurred rather than one that is simulated).

A virtual fault refers to a plane in 3D space upon which an event can occur. The program `mke_evnts` works by first creating a virtual fault and then placing the rupture on the virtual fault (the rupture is not allowed to exceed the bounds of the virtual fault). The introduction of a virtual fault is the mechanism by which the `EQRM` application constrains the location and extent of each rupture. The depth to the top of a virtual fault is defined as the depth to the seismogenic region f_z (see Table 3.1). Other geometrical parameters of virtual faults include the width f_w and length f_l, both of which are hardwired within the program `mke_aseq-4mat` as $f_w = 15km$ and $f_l = 1000km$ respectively. Note that the facility used to constrain synthetic ruptures to virtual faults can also be used to constrain a synthetic rupture to a mapped 'known' fault.

3.2.3 Location of synthetic earthquakes

The location of each event is assigned randomly within the 'generation polygon' where the 'generation polygon' is

1. a source zone from the source zone model when the `<site_loc>_par_source-zones.txt` and `<site_loc>_par_sourcepolys.txt` files are used directly with the EQRM, or
2. a polygon from the `generation` variable when the `<site_loc>_par_sour-ce.mat` option is used.

This assignment is done in such a way that the event has an equal probability of being located anywhere in the 'generation polygon' and is achieved by following a two phase process. The process makes use of a uniform random probability density function and is conducted by the function `mke_aseq4mat`. The user is required to define a vector `ntrgvector` in `setdata` whose i^{th} element represents the desired number of events to be simulated in the i^{th} 'generation polygon'.

The first phase of locating the events involves positioning the start point of each rupture trace (r_s^{lat}, r_s^{lon}). A regular grid is generated over the top of the source zone. The grid is bounded by the minimum and maximum latitude and the minimum and maximum longitude of the source zone itself. The initial number of points in both the northerly and easterly direction is n_{trg} where

$$n_{trg} = max\{1.05 \times ntrgvector(i), 25\} \tag{3.1}$$

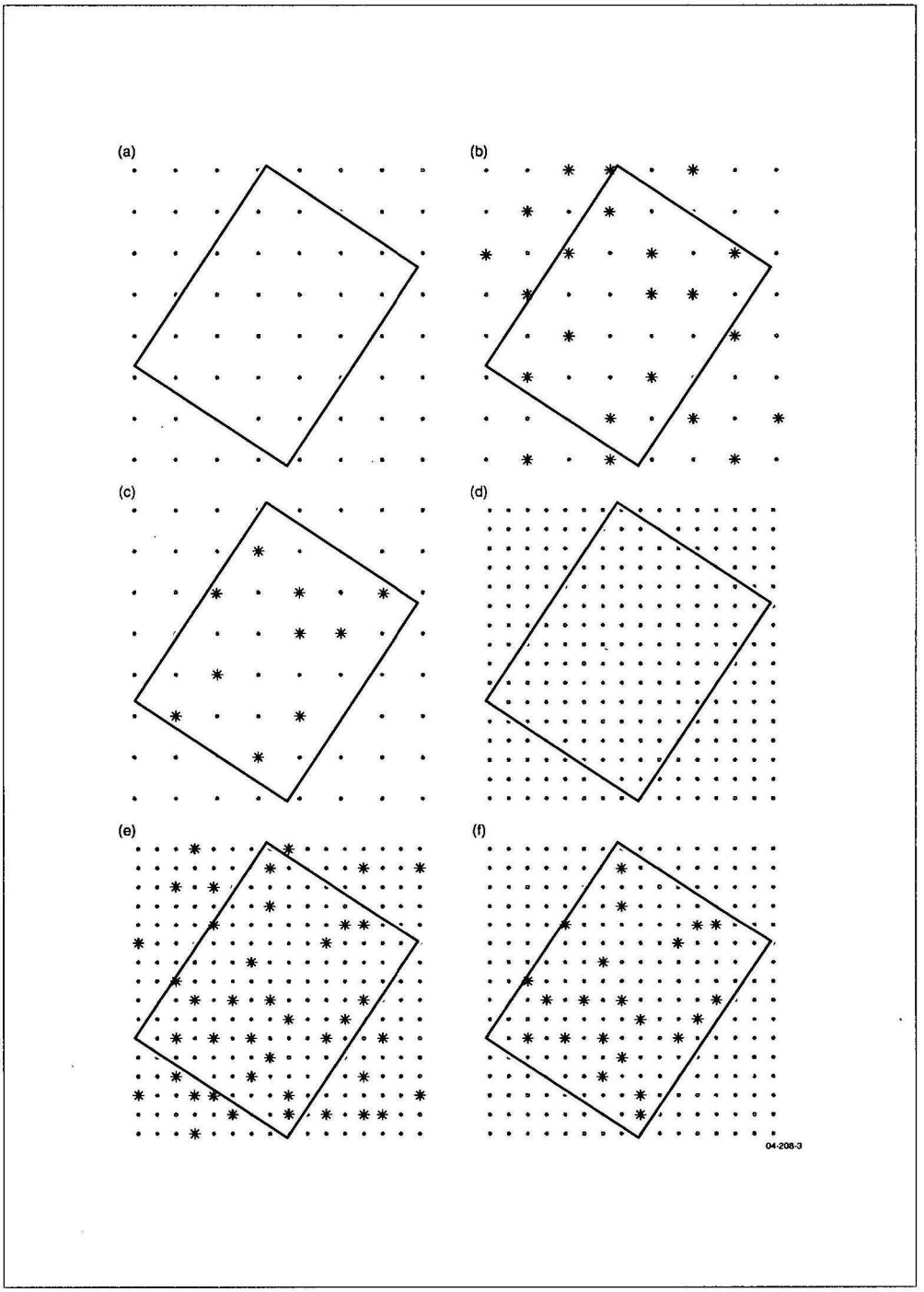

Figure 3.2: Random selection of rupture trace start points for a rectangular 'generation polygon'. (a) to (c) illustrate the first iteration and (d) to (f) the second iteration after contraction of the grid spacing.

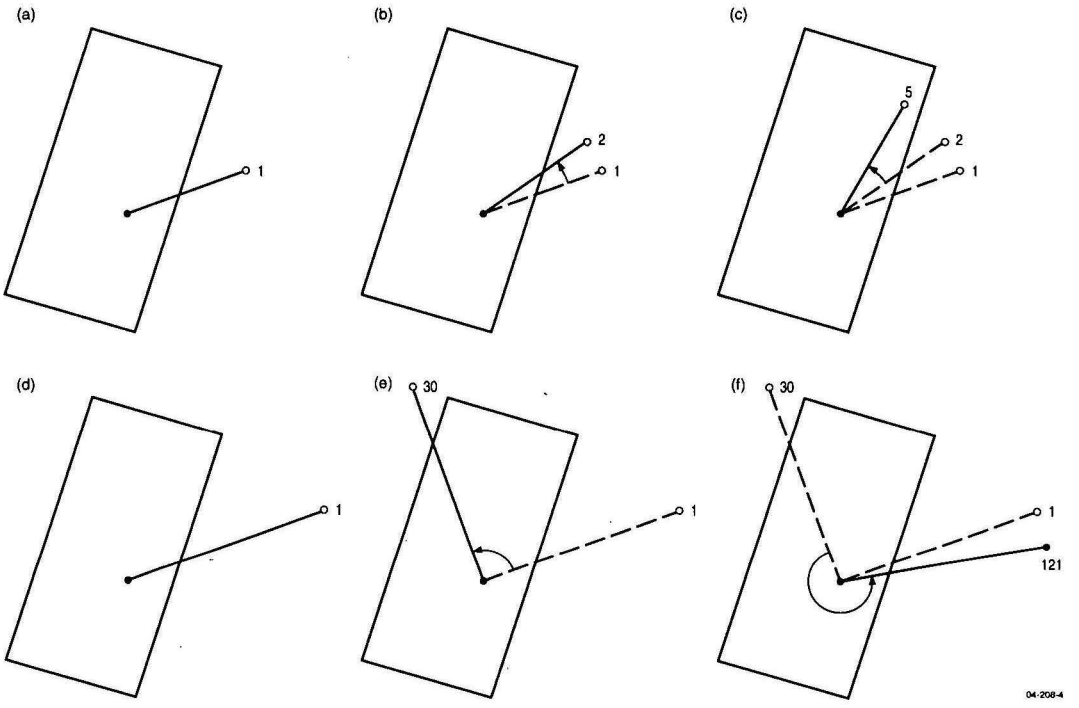

Figure 3.3: Rotation of the rupture trace to move the end of the rupture trace inside the source zone. (a) to (c) illustrate a successful rotation whereas (d) to (f) illustrate a rotation that failed to place the rupture entirely within the source zone. The text alongside each circle represents the rotation iteration i.e. 1 represents the first, randomly chosen, azimuth whereas 30 represents 29 iterative rotations from the 1st azimuth.

i.e. there are a total of n_{trg}^2 points in the grid (Figure 3.2a). The start point of each event is then randomly placed on nodes of the grid using a discrete uniform probability density function (Figure 3.2b). The events that fall within the polygon are distinguished from those that fall outside using the in-built MATLAB function `inpolygon` (Figure 3.2c). The grid is then expanded and contracted in an iterative process until the number of events simulated within the source zone is greater than 90% of the desired number (Figure 3.2d to f). The details of the contraction and expansion of the grid are not important for the purpose of this document. The interested reader is referred to the function `mke_aseq4mat` for further information.

The second phase of locating events involves positioning the end point of the rupture trace. Assume for the moment that both the length and azimuth of the rupture trace are already known (see Section 3.2.6 and Section 3.2.7 respectively for a description of how these are computed). It is then a trivial process to com-

pute the end of the rupture trace (r_e^{lat}, r_e^{lon}) (see function `ll2xy`). If the end of the rupture trace lies within the 'generation polygon' the rupture trace is accepted. The azimuth of each rupture trace whose end lies outside the 'generation polygon' is adjusted by an increment of $+1.5^o$ and `inpolygon` used to identify whether the adjustment has moved the end of the trace inside the source zone. The azimuth of all those events whose end continues to fall outside the 'generation polygon' is then iteratively adjusted by increments of 3^o until:

1. the end of the rupture trace falls within the 'generation polygon', in which case the event is accepted with the adjusted azimuth (Figure 3.3a to c), or
2. the adjustment is 358.5^o, in which case the event is accepted with the final azimuth taken as the true azimuth (Figure 3.3d to f).

Note that it is possible to omit the second phase of the location process (see Section 3.2.7 for an explanation). Alternatively, azi can be determined from the orientation of the Australian stress field and an assumption of the style of faulting. If all faults are assumed to be thrust events, then azi will be set in the direction of the minimum horizontal stress. However, if some faults are strike-slip faults, then a proportion of the faults will be randomly selected and azi will be in the orientation of maximum horizontal stress. The decision to use the Australian stress field is controlled by setting azi to `aust` if all of the events are considered thrust events and `aust_ss` to have 10% of the events randomly assigned as strike-slip events.

The above process is repeated for each of the 'generation polygons' in (1) `<site_loc>_par_sourcezones.txt` when the `<site_loc>_par_sourcezones.txt` and `<site_loc>_par_sourcepolys.txt` input is used or (2) the variable `generation` when `<site_loc>_par_source.mat` is used. Recall that each event is described by a row in `evntdb`. The originating source zone is identified in the first column of the row for each event (see Table 3.3).

It is important to realise that the `EQRM` software does not force the rupture plane, or even the rupture centroid to fall within the source zone. The source zone is only used to constrain the start and end (if $d_{azi} > 0$) of the rupture trace.

3.2.4 Overlapping source zones

The concept of overlapping zones in a source model is useful for accommodating background seismicity. In principle, the code can accommodate overlapping seismic zones, i.e. where two seismic zones share a common geographical region.

However, it should be noted that earthquakes will be distributed randomly in the common region for each zone that exists. That is, a simulation using overlapping source zones (such as that shown in Figure 3.4(a)) may lead to a greater number of simulated earthquakes in the common region than may be warranted by the source model. This only poses a problem if the recurrence relationship (i.e. the a, b parameters) being used has not been modified to account for the 'double counting' in the simulated catalogue (generally this will not have been done). To overcome this problem, it is advisable to define the source zones in such a way that there are no overlapping regions. Figure 3.4 demonstrates two different techniques that can be used to incorporate overlapping source zones in the EQRM. Both of the illustrated techniques are based on creating a doughnut.

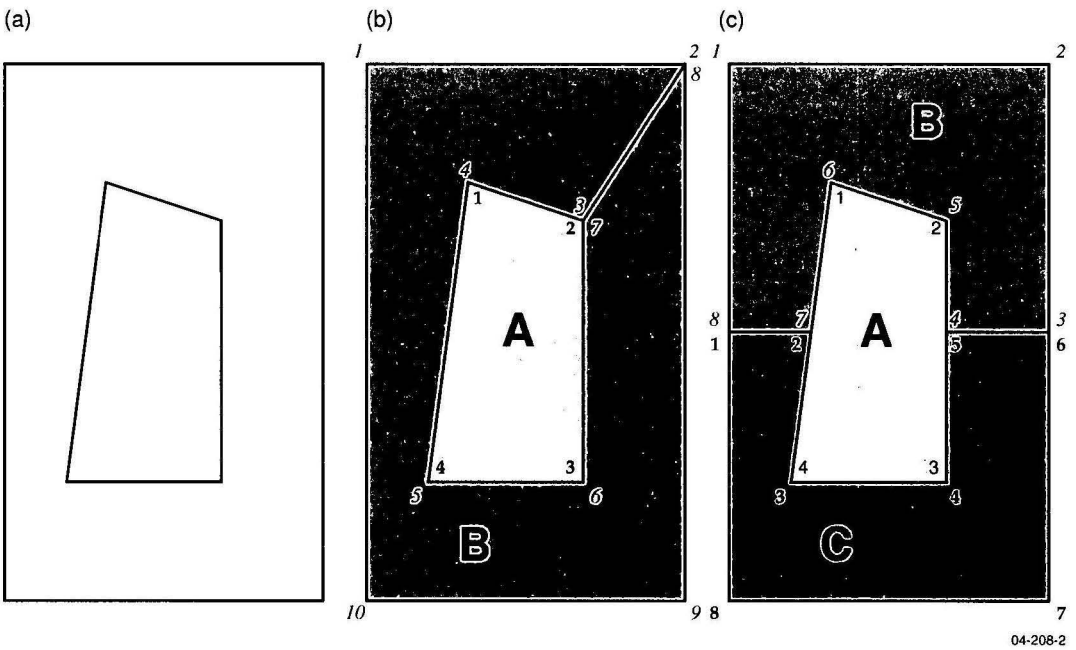

Figure 3.4: Overlapping source zones shown in (a) can be incorporated into the EQRM by cutting out a doughnut (b) or splitting the outer polygon (c). The numbers in different fonts illustrate how the polygon vertices could be listed in the `<site_loc>_par_sourcezones.txt` file.

3.2.5 Magnitude selection and event activity

A 'stratified' Monte-Carlo technique is used to assign the event magnitudes. The stratified nature of the technique ensures that the full range of magnitudes is adequately sampled. The stratified Monte-Carlo technique is illustrated in Figure 3.5 for the general case. This approach is distinctly different to a brute

force Monte-Carlo technique that would preferentially sample the more probable lower magnitude events. Such an approach would require the sampling of a large number of small events to ensure that a handful of large events are sampled.

The algorithm described in this section is the algorithm applied when a single source model is used and the 'generation polygons' are the source zones of the source model. Some minor modifications are required when multiple source models are used or the 'generation polygons' differ from the source zones. These modifications are described in Section 3.3.

The Probability Density Function (PDF) for the event magnitudes is based on the bounded Gutenberg-Richter law (Kramer, 1996). The EQRM application simulates a number N_s of earthquake events. Considering the i^{th} source zone, the algorithm for choosing the magnitude of each event can be summarised as follows:

1. Bound the domain of the PDF with m_{min} and m_{max} (Figure 3.5a).
2. Separate the interval $[m_{min}, m_{max}]$ into N_b bins, and return the bin centroids (Figure 3.5b).
3. For each of the $N_{s,i}$ events randomly select a bin from a discrete uniform distribution, where $N_{s,i}$ refers to the number of events in the i^{th} source zone. This effectively leads to $N_{s,i}/N_b$ earthquakes in each magnitude bin and ensures that the full range of magnitudes is adequately sampled (Figure 3.5c).
4. For each of the $N_{s,i}$ events randomly select a magnitude denoted r_m, from a continuous uniform distribution that spans the complete range of magnitudes in the bin. Note that Step 3 ensures that the entire range of magnitudes is adequately sampled whereas this step ensures that all magnitudes can be attained (Figure 3.5d).
5. For each of the $N_{s,i}$ events calculate the event activity $r_\nu(r_m^*)$, where r_m^* refers to the bin centroid for the event in question and

$$r_\nu(r_m^*) = \frac{N_b}{N_{s,i}} \times \lambda(\texttt{min\_mag\_cutoff}) \times P_{GR}(r_m^* - \Delta < R_m < r_m^* + \Delta). \quad (3.2)$$

The first term in Equation 3.2, $\frac{N_b}{N_{s,i}}$, approximates the reciprocal of the number of synthetic events in the bin. This term ensures that the event activity for each synthetic event scales as the number of generated events is modified and hence 'brings the synthetic results back to the real world'. The second term in Equation 3.2, $\lambda(\texttt{min\_mag\_cutoff})$, represents the number of

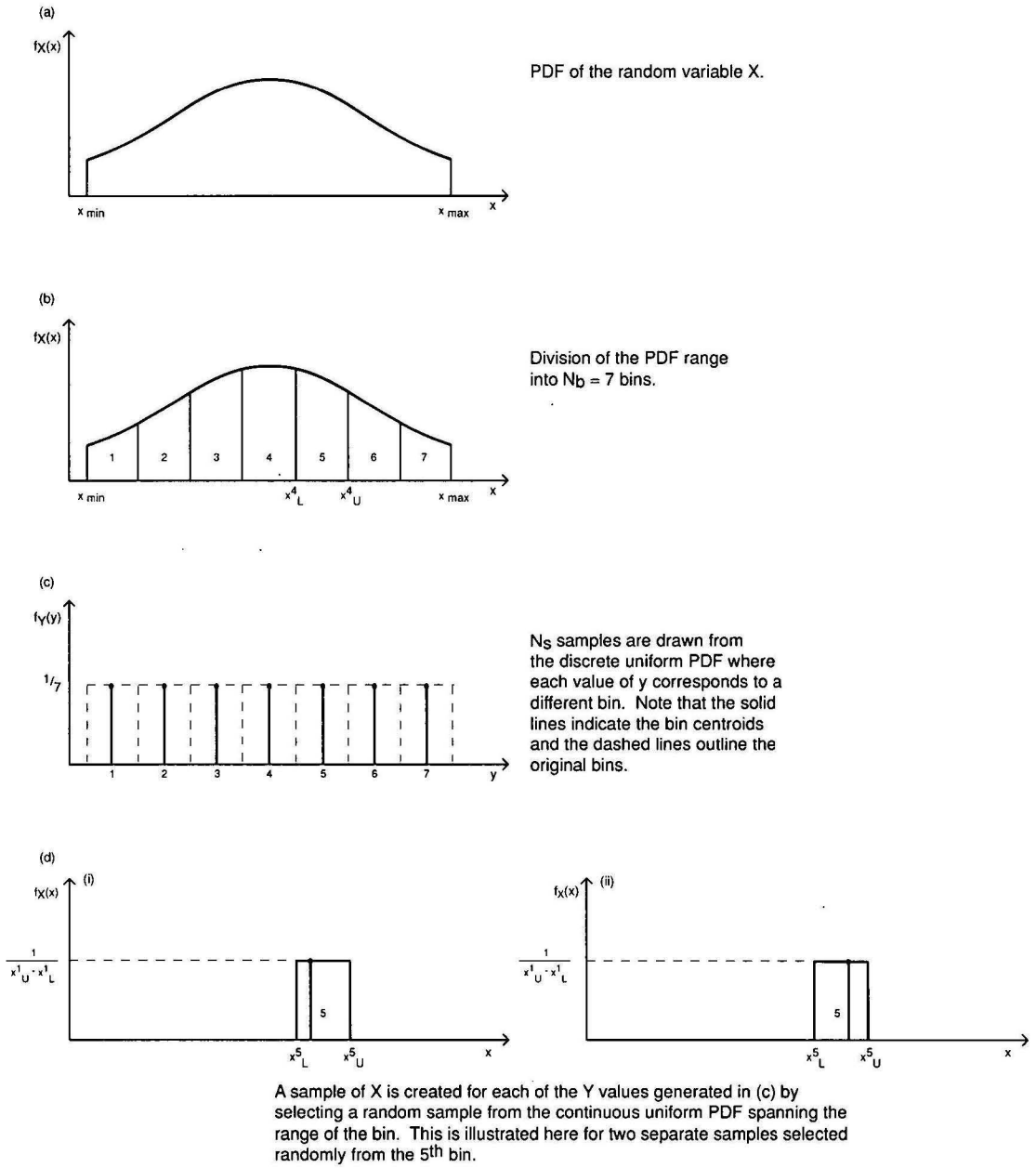

Figure 3.5: Stratified Monte Carlo technique for sampling a PDF. In this case a normal distribution is shown but any PDF can be used.

earthquakes with magnitude greater than or equal to `min_mag_cutoff` and is computed by evaluating the bounded Gutenberg-Richter recurrence relation

$$\lambda(m) = A_{min}\frac{e^{-\beta(m-m_{min})} - e^{-\beta(m_{max}-m_{min})}}{1 - e^{-\beta(m_{max}-m_{min})}}, \tag{3.3}$$

(Kramer, 1996). The final term in Equation 3.2 represents the actual probability that a real event will fall into the r_m^* bin in a given year and is computed by evaluating

$$P_{GR}(r_m^* - \Delta < R_m < r_m^* + \Delta) = \frac{f_M(r_m^*)}{\sum_{j=1}^{N_b} f_M(r_{m,j}^*)} \tag{3.4}$$

(Appendix A.6), where

$$f_M(r_m^*) = \frac{\beta e^{-\beta(r_m^*-m_{min})}}{1 - e^{-\beta(m_{max}-m_{min})}}, \tag{3.5}$$

$$\beta = b\ln(10) \tag{3.6}$$

(Kramer, 1996) and Δ is the half width of the bins. Note that r_ν represents the frequency of occurence in terms of a number per year and can be thought of as the synthetic version of λ for the simulated event catalogue.

Figures 3.6 to 3.8(a) illustrate histograms of the event magnitudes simulated for three different source zone combinations. Note that the fifteen bars in Figures 3.6 and 3.7(a) correspond to the fifteen different magnitude bins. The event activity r_v for the same source zone combinations are shown in Figures 3.6 to 3.8(c).

3.2.6 Dimensions and position of the rupture plane

The width and length of the rupture and position of the rupture centroid are computed by `mag2rup_v` using empirical rules based on the moment magnitude, r_m of the event (Mendez, 2002 [*pers. comm.*]) . The location of the rupture plane is constrained to lie within a virtual fault which is described by the depth to its top (equivalent to the depth to the seismogenic region f_z, see Section 3.1), its length f_l, its width f_w and its dip r_{dip}. Note that by default the dip of the rupture plane is defined to be the dip of the virtual fault. Firstly, the area of the rupture plane A_r is defined as

$$A_r = 10^{r_m - 4.02} \tag{3.7}$$

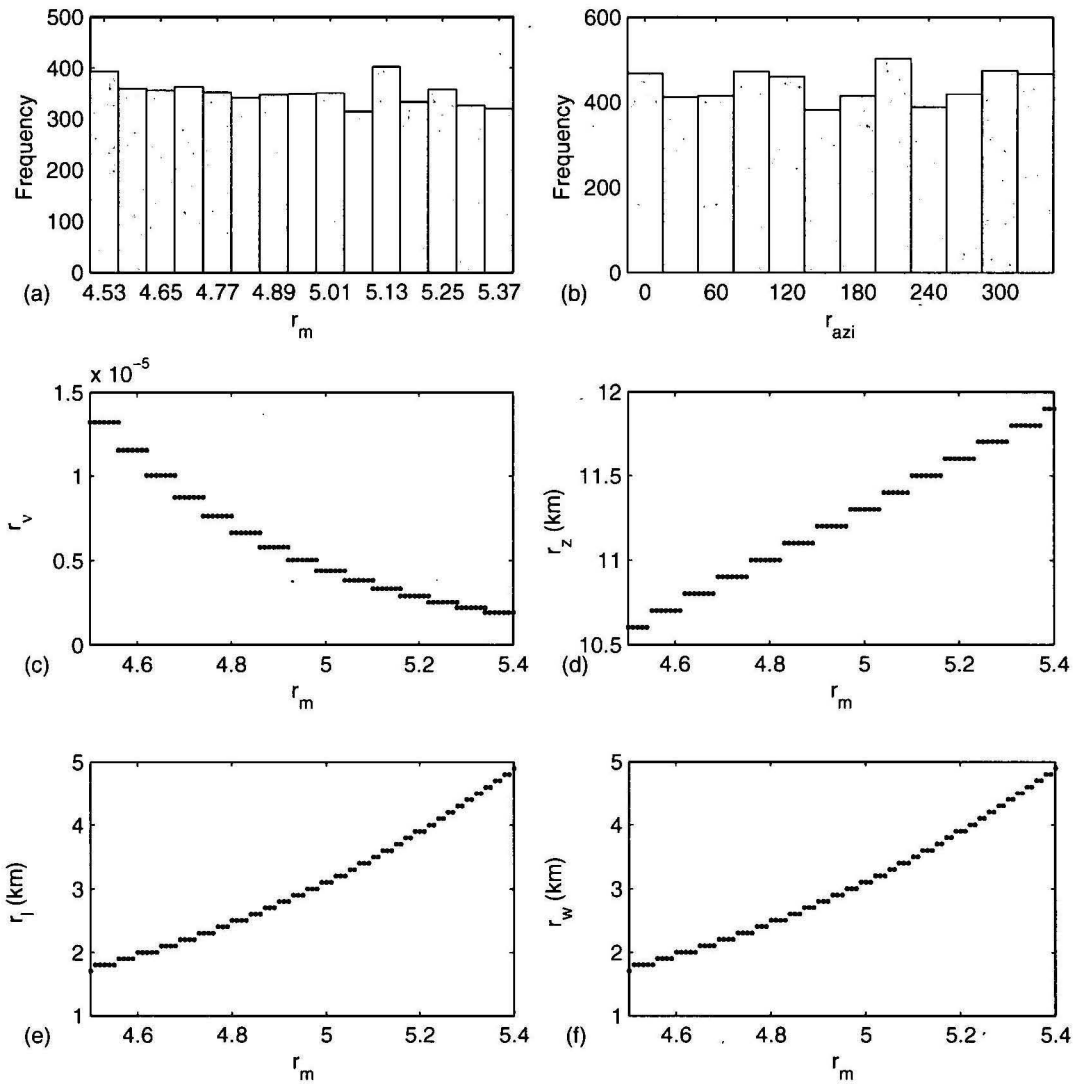

Figure 3.6: Simulated events for the Newcastle Triangle Zone (see Dhu *et al.* 2002). Plots (a) and (b) show histograms of the rupture magnitude r_m and rupture azimuth r_{azi} respectively. Plots (c), (d), (e) and (f) illustrate the relationship between the event magnitude r_m and the event activity r_ν, the depth to the rupture centroid r_z, the length of the rupture r_l and the width of the rupture r_w respectively. The desired number of events $ntrgvector(1)$ was 5000.

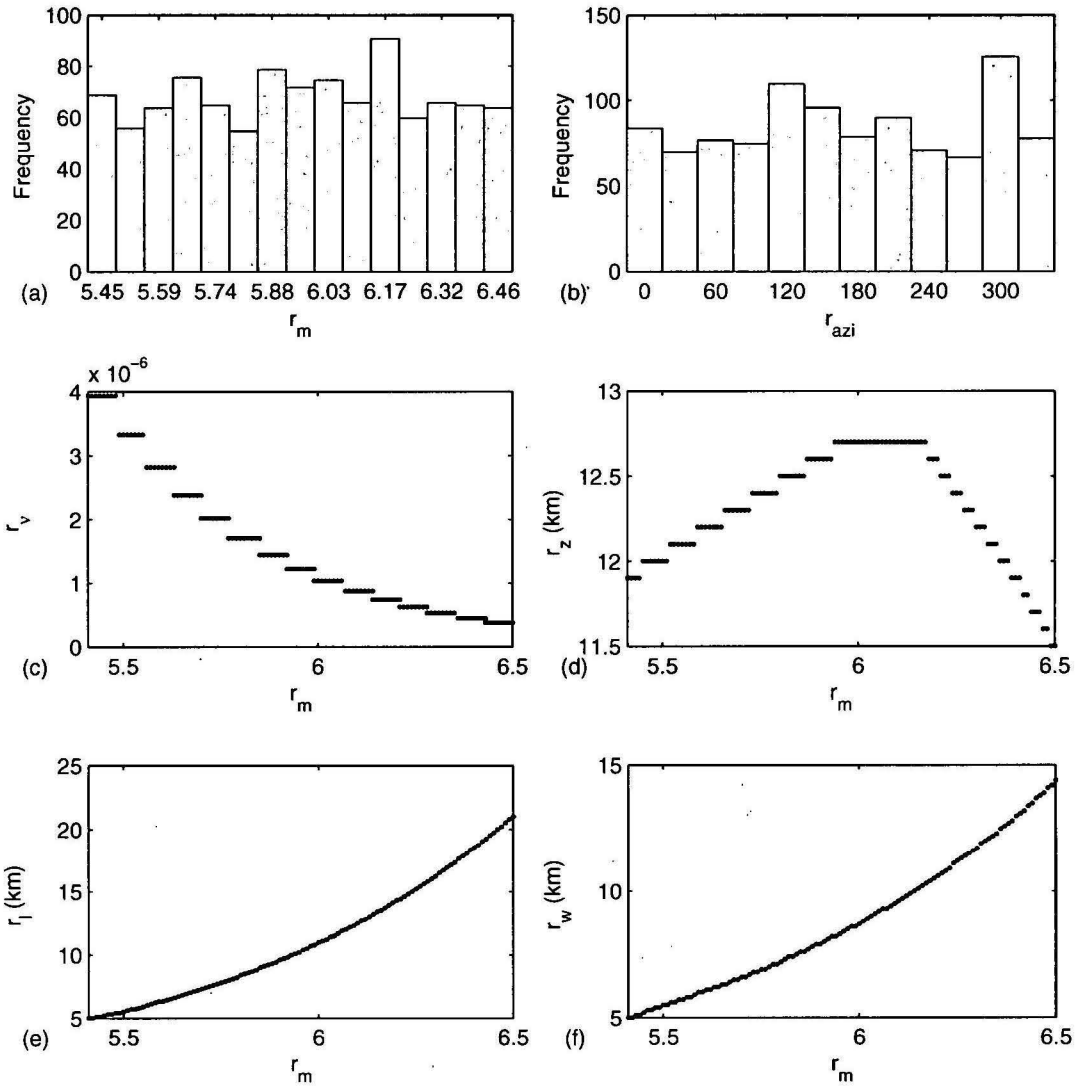

Figure 3.7: Simulated events for the Newcastle Rectangle Zone (see Dhu *et al.* 2002). Parts (a) to (f) are the same as those described in Figure 3.6. The desired number of events $ntrgvector(4)$ was 3000.

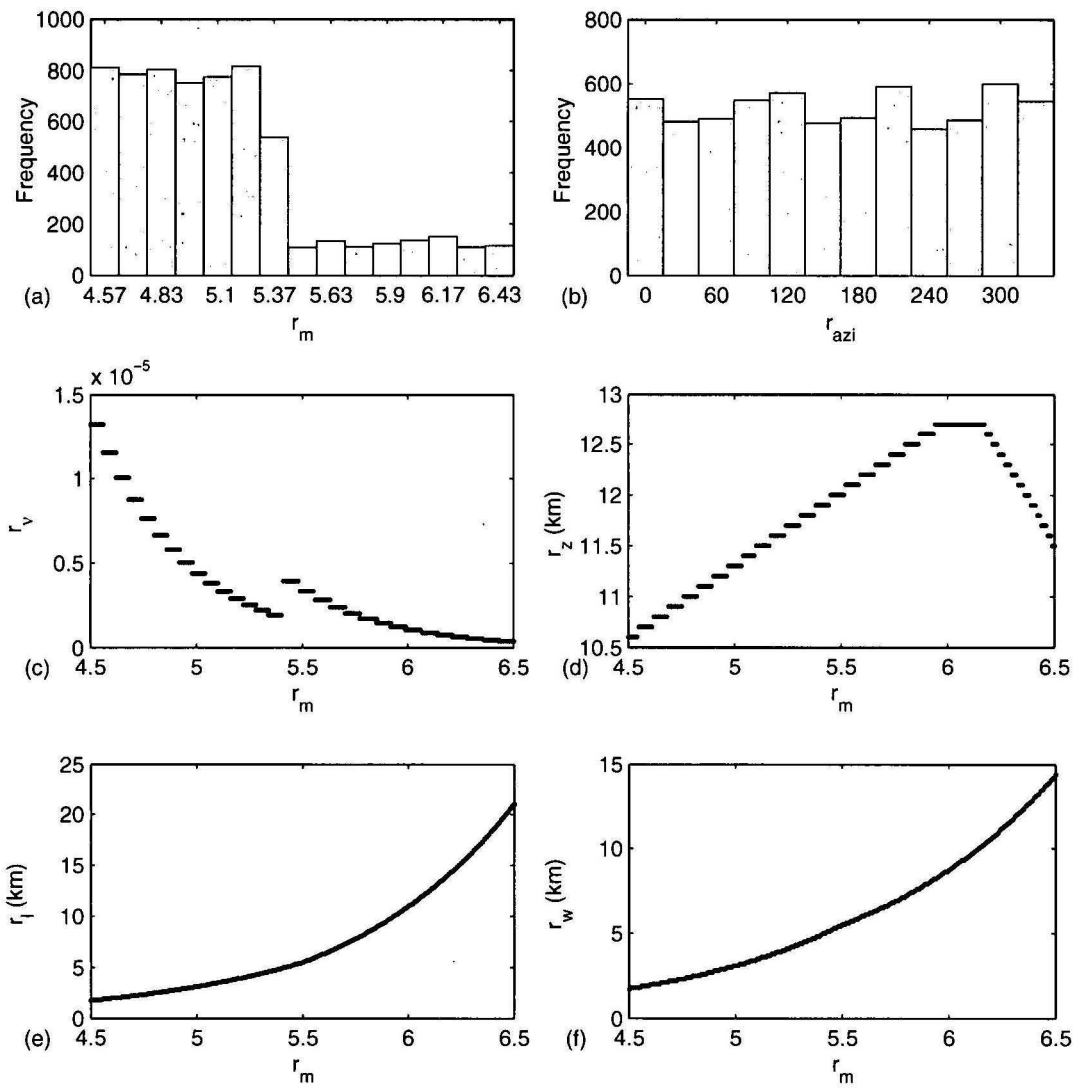

Figure 3.8: Simulated events when the Newcastle Triangle Zone and Newcastle Fault Zone are considered together (see Dhu *et al.* 2002). Parts (a) to (f) are the same as those described in Figure 3.6. The desired number of events was defined by $ntrgvector = [5000, 3000]$ where the source zones 1 and 2 refer to the the Newcastle Triangle Zone (NTZ) and the Newcastle Fault Zone respectively.

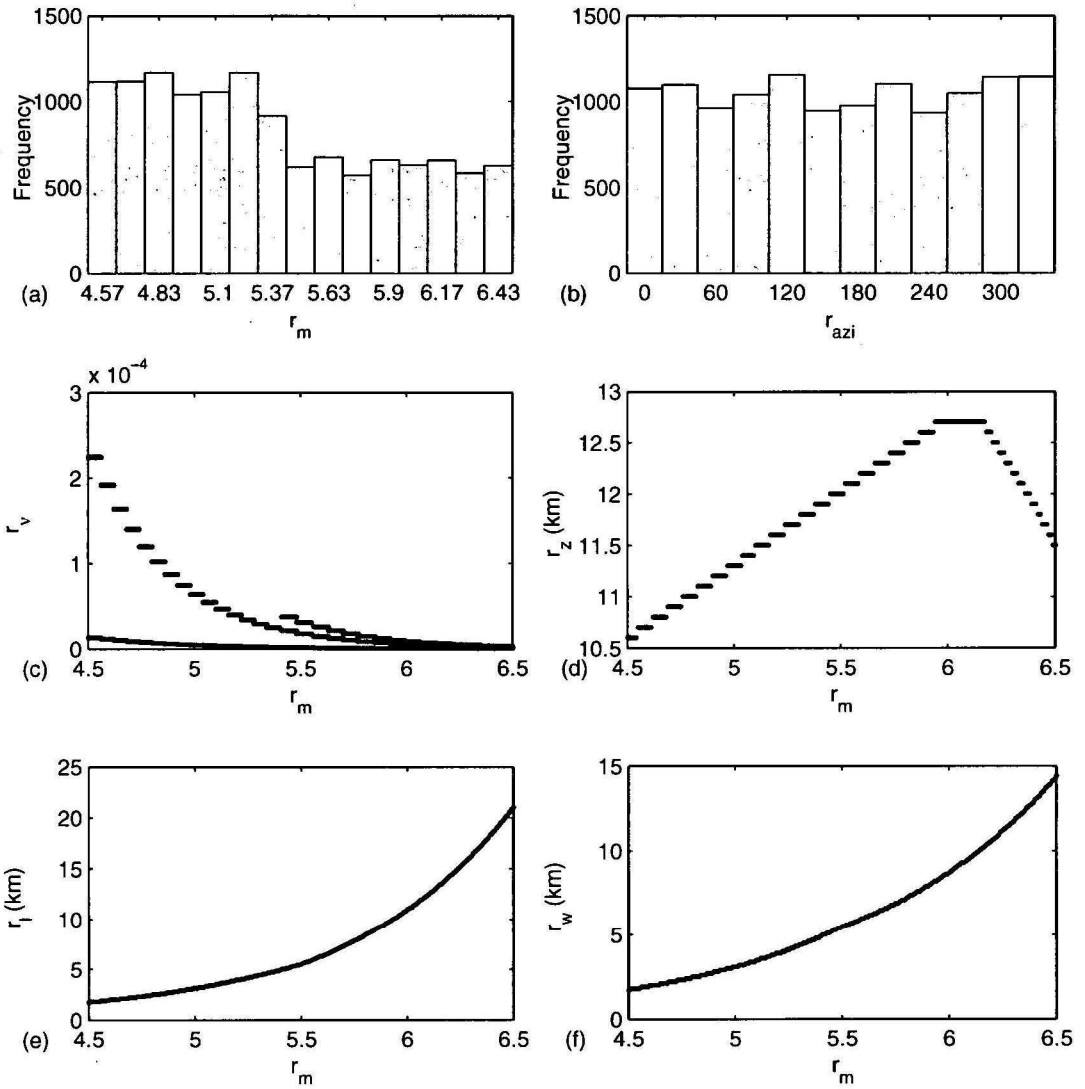

Figure 3.9: Simulated events for all six of the source zones used in the Newcastle and Lake Macquarie study (see Dhu *et al.* 2002). Parts (a) to (f) are the same as those described in Figure 3.6. The desired number of events was defined by $ntrgvector = [5000, 1000, 1000, 3000, 1000, 1000]$ where the source zones 1 to 6 refer to the the Newcastle Triangle Zone (NTZ) the Tasman Sea Margin Zone Subset 1 (TSMZ1), the TSMZ2, the Newcastle Fault Zone, the TSMZ3 and the TSMZ4 respectively.

which represents a subtle change from that defined by Wells and Coppersmith (1994). Empirical relationships for the width r_w and length l_r of the rupture plane were defined by Mendez (2002 [*pers. comm.*]). The width is defined in a two step process as follows

$$f_1 = \begin{cases} 1 & \text{if } r_m \leq 5.5 \\ \frac{1}{\sqrt[4]{1+2(r_m-5.5)\sin(r_{dip})}} & \text{if } r_m > 5.5 \end{cases} \tag{3.8}$$

and

$$r_w = \min\{f_1\sqrt{A_r}, f_w\}. \tag{3.9}$$

Recall from Section 3.2.1 that the rupture centroid (r_x, r_y, r_z) is defined in terms of a local coordinate system. The depth of the rupture centroid is determined in a two step process as follows:

$$f_2 = \begin{cases} 1 & \text{if } r_m \leq 4 \\ 1 + \frac{r_m-4}{2} & \text{if } 4 < r_m \leq 6 \\ 2 & \text{if } r_m \geq 6 \end{cases} \tag{3.10}$$

and

$$r_z = \min\{f_z + \frac{f_2}{3} f_w \sin(r_{dip}), f_z + f_w \sin(r_{dip}) - \frac{1}{2} r_w \sin(r_{dip})\}. \tag{3.11}$$

The other two coordinates of the rupture centroid are given by

$$r_y = r_z \cot(r_{dip}) \tag{3.12}$$

and

$$r_x = \frac{r_l}{2}. \tag{3.13}$$

The depth to the rupture centroid r_z and the length and width of the rupture plane are illustrated for four separate simulations in Figures 3.6 to 3.9(d), (e) and (f) respectively.

3.2.7 Azimuth and dip of rupture

The rupture azimuth of each event may be forced to lie within a user defined range

$$\phi - d_\phi \leq r_\phi \leq \phi + d_\phi$$

where ϕ and d_ϕ are `azi` and `d_azi` in `setdata` respectively. The default values for ϕ and d_ϕ are 180^o and 180^o respectively. Recall that the azimuth is further adjusted through the process described in Section 3.2.3, unless d_{azi} is assigned to a negative number. Note that in the current version of the EQRM application this adjustment process ignores the above azimuth bound. That is, the azimuth of one or more events may be adjusted outside the above range in an attempt to force the event's end point to lie within the source zone. The distribution of simulated azimuth for four different simulations is illustrated in Figures 3.6 to 3.9(b).

The dip of the rupture, r_{dip}, is assigned in `setdata` and may take only a single value for all source zones. The dip of the rupture trace is measured from the ground surface and the direction of dip is such that the plane is located in the region of $y > 0$ in the local coordinate system. Note that it is possible to modify the software to select the dip randomly in a similar fashion to that described for the azimuth above. However, it is worth noting that the effect of a change in dip varies based on the attenuation model (see Section 5). For example, when using an attenuation model that depends on the Joyner-Boore distance, the practical effect of a change in dip can be compensated by a horizontal translation of the rupture trace. In such cases the random location of the rupture trace negates the need to select the dip randomly.

3.3 Using multiple source zones - Incorporating epistemic uncertainty

Recall that Section 3.2 introduced two techniques for passing source models to the EQRM:

1. the `<site_loc>_par_sourcezones.txt` and `<site_loc>_par_sourcepolys.txt` file pair, and
2. the `<site_loc>_par_source.mat` file.

Recall also that the notion of a 'generation polygon' was introduced where the generation polygons are simply the individual source zones when Technique 1 is used, and 'generation polygon' refers to the polygons in the `generation` variable when Technique 2 is used. This definition ensured that the discussion of earthquake location (Section 3.2.3), rupture geometry (Section 3.2.6), azimuth and dip (Section 3.2.7) described above is applicable to both of the two techniques for providing source information to the EQRM. When Technique 2 is used, however, a minor modification must be made to the algorithm described for magnitude and event activity determination (see Section 3.2.5). To explain the differences in the algorithm and to explain the incorporation of multiple source zone models (epistemic uncertainty with source models) the reader will need to understand the contents of the `<site_loc>_par_source.mat` file.

The `<site_loc>_par_source.mat` file contains the following two variables:

1. The `generation` variable is a MATLAB structure containing the fields `zones` and `polys`. The field `zones` is a matrix containing the same format as that described in Table 3.1. The number of rows refers to the number of 'generation polygons' to be used in the generation process. It is common to have 2 'generation polygons' arranged in a doughnut shape with an inner and outer polygon. The inner polygon is typically centered on the region of interest and can be used to simulate a larger number of earthquakes (hence higher spatial concentration) than the outer polygon. The field `polys` is a matrix using the same format as Table 3.2 to describe the vertices of the polygons in the field `zones`.

2. The `source` variable is a MATLAB structure array containing one element for each source zone model to be used. The number of elements in the `source` structure array corresponds to the number of source zone models to be used in the simulation. Each element has fields `zones`, `polys` and `weight`. The fields `zones` and `polys` are similar to those described in 1 above, however this time they represent the individual source source zones for the source model. The field `weight` represents the weight to be applied to the source zone model.

When using Technique 2 the `generation` is used to define the 'generation polygons' and hence the location, geometry, azimuth and dip of the rupture. The variable `generation` is also used to assign magnitudes to each synthetic event using Steps 1 to 4 from Section 3.2.5. Note that a synthetic earthquake generated in this fashion may lie in none, one or multiple source zones from the different source models. The calculation of an event activity involves identifying which zones the earthquake lies within and then computing the weighted sum of

individual event activities for the zones within which it lies. The algorithm for computing the event activity for a single source zone is described in Step 5 of Section 3.2.5. Note that an earthquake must fall within the polygon that defines the source zone and its magnitude must be within the magnitude bounds for the source zone before it is considered to lie within the source zone. More details of this process can be found by looking at the functions `calc_event_activity` for the calculation of event activity and `mke_aseq4mat` for all of processes.

3.4 Spawning events

There is an option within the EQRM application to spawn (or copy) events. Such copies are required by some techniques for incorporating aleatory uncertainty in later stages of the PSHA and PSRA. For example, Section 5.3.1 describes an incorporation of aleatory attenuation uncertainty that does not require spawning of the catalogue whereas Section 5.3.2 describes a process that does require spawning. The option is performed by `fuse_4hzd`. Actually `fuse_4hzd` is an essential component of any earthquake hazard or risk run with the `EQRM` application i.e. it must be run regardless of whether the user wishes to spawn events or not. The spawning of events is controlled by `src_eps_switch` in `setdata`. If `src_eps_switch`$= 1$ or -1 then all events with magnitude greater than m_{bnd} (`mbnd` in `setdata`) are copied $n_{samples}$ (`nsamples` in `setdata`) times with their event activity adjusted according to a weight w_e. If `src_eps_switch`$= 0$ no spawning is undertaken. When spawning the weight w_e is derived by truncating and re-normalising a standard normal distribution to $\pm n_\sigma$ (`nsigma` in `setdata`). The process is summarised below.

We know that the standard normal distribution $N \sim (0, 1)$ has a PDF given by

$$f_X(x) = \frac{1}{\sqrt{2\pi}} e^{\frac{-x^2}{2}} \quad -\infty < x < \infty. \tag{3.14}$$

To truncate and re-normalise $N \sim (0, 1)$ to $\pm n_\sigma$ we must evaluate $P(-n_\sigma\sigma \leq X \leq n_\sigma\sigma)$. The error function

$$erf(x) = \frac{2}{\sqrt{\pi}} \int_0^x e^{-t^2}\, dt. \tag{3.15}$$

is related to the cumulative area under the standard normal distribution via

$$erf(x) = 2P(X \leq x) - 1. \tag{3.16}$$

The function `mke_ctpdf` computes $P(-n_\sigma\sigma \leq X \leq n_\sigma\sigma)$ using the error function as follows

$$\begin{aligned} P(-n_\sigma\sigma \leq X \leq n_\sigma\ \sigma) &= P(X \leq n_\sigma) - P(X \leq -n_\sigma) \\ &= 2P(X \leq n_\sigma) - 1 \\ &= erf(n_\sigma). \end{aligned} \tag{3.17}$$

Then, `mke_ctpdf` computes the truncated and re-normalised PDF by evaluating

$$\tilde{f}_X(x) = \frac{1}{P(-n_\sigma\sigma \leq X \leq n_\sigma\sigma)} \frac{1}{\sqrt{2\pi}} e^{\frac{-x^2}{2}} \quad -n_\sigma\sigma < x < n_\sigma\sigma. \tag{3.18}$$

The observant reader will notice that because the EQRM application works in the discrete world, simply evaluating $\tilde{f}_X(x)$ will not suffice. The approach used by `mke_ctpdf` to discretise $\tilde{f}_X$ and compute the weights $\{w_{e,i}\}_{i=1}^{n_{samples}}$ is identical to that used to compute the event activity r_ν (see Section 3.2.5) and is described in Appendix A.6. That is

$$w_{e,i} = \frac{\tilde{f}_X(x_i)}{\sum_{j=1}^{n_{samples}} \tilde{f}_X(x_j)}. \tag{3.19}$$

Once the weights $\{w_{e,i}\}_{i=1}^{n_{samples}}$ are computed the event activity r_ν for each of the event copies is re-defined as follows:

$$r_{\nu,i} = r_{\nu,original} \times w_{e,i} \quad \text{for } i = 1 \text{ to } n_{samples}, \tag{3.20}$$

for each copy of the original event and its associated weighting. A source epsilon term r_ε is also defined for each copy of the original event i.e. $\{r_{\varepsilon,i}\}_{i=1}^{n_{samples}}$. Each of the $r_{\varepsilon,i}$ are defined such that they correspond to the i^{th} bin centroid from the $n_{samples}$ bin spanning $\pm n_\sigma$ (see Section 5.3.2 for the mathematical definition).

3.5 Analysing a scenario event

The EQRM application (through `mke_evnts`) incorporates an option for considering a particular (or scenario) event. This option is instigated when the user defines `determ_flag`= 1 in `setdata`. The earthquake catalogue takes the same form as that described in Table 3.3. The scenario event is constrained by user defined values for magnitude (`determ_mag`), position (`determ_lat` and `determ_lon`), depth (`determ_r_z`) and azimuth (`determ_azi`).

3.6 Key functions, flags and parameters

Name	Type	Description
`mke_evnts`	Function	Master file for creating an event catalogue.
`mke_aseq4mat`	Function	Handles a significant proportion of the synthetic event generation on behalf of `mke_evnts`.
`m2grpdfb`	Function	Computes the PDF, f_M for the bounded Gutenberg-Richter distribution.
`mag2rup_v`	Function	Computes rupture dimension and 'relative' location based on magnitude.
`fuse_4hzd`	Function	Master file for spawning events.
`mke_ctpdf`	Function	Truncates and discretises $N \sim (0, 1)$.
`azi`	Par	Centre of azimuth range for events.
`d_azi`	Par	Half width of azimuth range.
`dip`	Par	Dip of virtual fault.
`ntrgvector`	Par	Vector whose elements represent the desired number of events to be simulated in each source zone.
`wdth`	Par	Width of virtual fault.
`nbins`	Par	Number of bins for event magnitude sampling.
`src_eps_switch`	Par	Events are (not) spawned if `src_eps_switch` $= 1$ $(= 0)$.
`mbnd`	Par	Only events with magnitude greater than `mbnd` are spawned.
`nsamples`	Par	Creates `nsamples` copies of each spawned event.
`nsigma`	Par	Range of distribution to be considered when spawning.
`determ_flag`	Par	EQRM application used in scenario mode if `determ_flag` $= 1$.
`determ_mag`	Par	Magnitude of scenario event.

`determ_lat`	Par	Latitude of scenario epicenter (corresponds to r_c^{lat}).
`determ_lon`	Par	Longitude of scenario epicenter (corresponds to r_c^{lon}).
`determ_r_z`	Par	Depth to scenario epicenter in km (corresponds to r_z).
`determ_azi`	Par	Azimuth of scenario event (corresponds to r_ϕ).

Chapter 4

Grids and building databases

4.1 Overview

The calculation of earthquake hazard and risk are spatial problems. This chapter describes how grids are required to compute earthquake hazard and how building databases are represented to model earthquake risk. Computationally the EQRM operates by looping over the grid (building database) points one at a time i.e. the hazard or risk is computed iteratively at each point. Tools to assist the user create building databases can be found in `*/eqrm/datacvt`.

4.2 Hazard grids

The term 'hazard grid' merely refers to a set of spatially located points at each of which earthquake hazard can be computed (see Chapter 9 for a definition of earthquake hazard). The set can contain one or more points. Typically however, the grids are uniform and regularly spaced in the horizontal and vertical direction. The EQRM can work with two different hazard grid types, the choice of which is controlled by the `setdata` parameter `grid_flag`.

When `grid_flag` = 1 the EQRM loads the file `<site_loc>_par_site.mat` which contains the following variables:

1. `SiteLocations`: a double array containing a row for each grid point and two columns. The first and second columns contain the latitude and longitude of the grid point respectively.

2. `site_classes`: a character column array containing one row for each grid point. The content of each row is a single letter identifying the regolith site class of the grid point (see Chapter 6).

Typically such a grid originates in the GIS world where a grid of points is created and assigned to site classes. This information is imported into MATLAB where it is manipulated into the above format and saved ready for use. Note that hazard values computed on a `<site_loc>_par_site.mat` must be exported to the GIS environment for plotting (i.e. they can not be plotted by the EQRM).

The `<site_loc>_par_site.mat` is an older format that has been kept for back compatibility. The preferred technique for creating hazard grids is through the `Input Manager`. The `Input Manager`is a GUI, specifically designed to create earthquake hazard grids. It can be accessed through the `eqrm_param_gui` by pressing the `Input Manager`button. The `Input Manager`GUI allows the user to create a grid over a region of interest. To do this the `Input Manager`needs to access a polygon input file that describes the region of interest as a single polygon (e.g. `perth_par_study_region_box.txt`) or as a set of site classes covering the study region (e.g. `perth_par_site_class_polys.mat`). Note that in the first case the EQRM will not access any information about site classes and hence amplification can not be included. The user must indicate how many points are desired in the latitude and longitude directions. The name of the created grid file is `<site_loc>_par_site_uniform.mat` and it can be used with the EQRM by setting `grid_flag` = 2. Its format is more complicated than the above mentioned `<site_loc>_par_site.mat`, however the user does not need knowledge of the format since this is handled by the `Input Manager`. Note that earthquake hazard estimates produced on a `<site_loc>_par_site_uniform.mat` file can be plotted using the EQRM hazard plotting tools (see Chapter 9).

4.3 Building databases

The building database contains attributes for the portfolio of buildings under consideration in the risk assessment. The building database is a MATLAB data file with filename `sitedb_<site_loc>.mat` containing the following variables:

1. `all_postcodes`: a list of all postcodes currently included in the EQRM for use in linking database postcode id numbers.
2. `all_suburbs`: a list of all suburbs currently included in the EQRM for use in linking database suburb id numbers.

Table 4.1: Columns of the building database file `sitedb_<site_loc>.mat`.

Column	Description
1	Integer site identifier for EQRM (typically the same as column 10)
2	Latitude of building
3	Longitude of building
4	Index to building construction type... **expanded** HAZUS list (Section 4.3.1)
5	Index to HAZUS usage classification (Section 4.3.2)
6	Total floor area in square meters (summed over all stories)
7	Survey factor indicating how many 'real' buildings the database entry represents
8	Index to suburb name for building (variable: `all_suburbs`)
9	Index to postcode name for building (variable: `all_suburbs`)
10	Integer site identifier for comparison against original database
11	Logical index stating whether the building is pre- (0) or post- (1) the 1989 Newcastle earthquake
12	Index to building construction type... HAZUS list (Section 4.3.1)
13	Replacement cost of building in dollars per square meter (Section 4.3.3)
14	Replacement cost of contents in dollars per square meter (Section 4.3.3)
15	Index to FCB usage classification (Section 4.3.2)

3. `b_sitemat` a matrix containing one row for each building and 15 columns describing attributes of the building. Details of the columns are given in Table 4.1.

4. `b_soil`: a character column array containing one row for each grid point. The contents of each row is a single letter identifying the regolith site class of the grid point (see Chapter 6).

Typically the building database used with the EQRM represents a subset of the true portfolio of interest. When creating a database that sub-samples a larger portfolio, individual database entries are used to represent more than one 'real' building. Such sub-sampling is undertaken to reduce run times and memory requirements. Results from an EQRM simulation can be re-converted to the full portfolio using the `survey factor`defined in `sitedb_<site_loc>.mat` (see Section 8.2.2).

Tools to assist the creation of building databases for use with the EQRM can be found in `*/eqrm/datacvt/buildingdb`.

4.3.1 Building construction types

Buildings have been subdivided into a number of building types each with their own set of building parameters uniquely defining the median capacity curve and the random variability around the median (see Chapter 7). The building construction types are based upon the HAZUS definitions (FEMA, 1999), with some further subdivisions recommended by Australian engineers for Australian building construction types (Stehle *et al.*, 2001).

In essence, the seven basic HAZUS types are

- Timber frame (W)
- Steel frame (S)
- Concrete frame (C)
- Pre-cast concrete (PC)
- Reinforced masonry (R)
- Unreinforced masonry (URM)
- Mobile homes (MH)

There are further subdivisions of the HAZUS types into subtypes according to numbers of stories in the building. These are given in Table 4.2.

The new Australian sub-types, developed in the Australian engineers workshop, further subdivide some of the HAZUS types (Stehle *et al.*, 2001). In particular, the timber frame category (W1) is subdivided into wall types (timber or brick veneer walls) and roof types (metal or tiled); the unreinforced masonry types (URML and URMM) into roof type (metal, tile or otherwise), and the concrete frame types are subdivided into soft-story or non-soft story types. Soft-story refers to buildings that may have a concrete basement or parking area but wood frame stories.

In total, we currently have 56 possible construction types although some are rarely used. For example; the original Hazus W1 is still there, however this is

Table 4.2: Definitions of the basic HAZUS building construction types.

code	description	Stories
W1	timber frame < 5 000 square feet	(1–2)
W2	timber frame > 5 000 square feet	(All)
S1L	steel moment frame	Low-Rise (1–3)
S1M		Mid-Rise (4–7)
S1H		High-Rise (8+)
S2L	steel light frame	Low-Rise (1–3)
S2M		Mid-Rise (4–7)
S2M		High-Rise (8+)
S3	steel frame + cast concrete shear walls	(All)
S4L	steel frame + unreinforced masonry in-fill walls	Low-Rise (1–3)
S4M		Mid-Rise (4–7)
S4H		High-Rise (8+)
S5L	steel frame + concrete shear walls	Low-Rise (1–3)
S5M		Mid-Rise (4–7)
S5H		High-Rise (8+)
C1L	concrete moment frame	Low-Rise (1–3)
C1M		Mid-Rise (4–7)
C1H		High-Rise (8+)
C2L	concrete shear walls	Low-Rise (1–3)
C2M		Mid-Rise (4–7)
C2H		High-Rise (8+)
C3L	concrete frame + unreinforced masonry in-fill walls	Low-Rise (1–3)
C3M		Mid-Rise (4–7)
C3H		High-Rise (8+)
PC1	pre-cast concrete tilt-up walls	(All)
PC2L	pre-cast concrete frames with concrete shear walls	Low-Rise (1–3)
PC2M		Mid-Rise (4–7)
PC2H		High-Rise (8+)
RM1L	reinforced masonry walls + wood or metal diaphragms	Low-Rise (1–3)
RM1M		Mid-Rise (4+)
RM2L	reinforced masonry walls + pre-cast concrete diaphragms	Low-Rise (1–3)
RM2M		Mid-Rise (4–7)
RM2H		High-Rise (8+)
URML	unreinforced masonry	Low-Rise (1–2)
URMM		Mid-Rise (3+)
MH	Mobile homes	(All)

rarely used in favor of the more detailed classification into W1TIMBMETAL, W1BVTILE, etc. A complete list of all the building construction types is given in Table 4.3. The `setdata` flag `hazus_btypes_flag` can be used to select between the use of the HAZUS building type classification and the Australian engineers extended HAZUS building type classification.

Table 4.3: Complete list of all building construction types (with those that are rarely used in italics).The integers corresponding to each building construction type represent the integer index used in the building database Column 4 for expanded HAZUS types (column 12 for HAZUS only types).

1: W1	15: S5H	29: RM1L	43: C1LSOFT
2: W2	16: *C1L*	30: RM1M	44: C1LNOSOFT
3: S1L	17: *C1M*	31: RM2L	45: C1MMEAN
4: S1M	18: *C1H*	32: RM2M	46: C1MSOFT
5: S1H	19: C2L	33: RM2H	47: C1MNOSOFT
6: S2L	20: C2M	34: *URML*	48: C1HMEAN
7: S2M	21: C2H	35: *URMM*	49: C1HSOFT
8: S2H	22: C3L	36: MH	50: C1HNOSOFT
9: S3	23: C3M	37: W1MEAN	51: URMLMEAN
10: S4L	24: C3H	38: W1BVTILE	52: URMLTILE
11: S4M	25: PC1	39: W1BVMETAL	53: URMLMETAL
12: S4H	26: PC2L	40: W1TIMBERTILE	54: URMMMEAN
13: S5L	27: PC2M	41: W1TIMBERMETAL	55: URMMTILE
14: S5M	28: PC2H	42: C1MMEAN	56: URMMMETAL

The building capacity curves used in the Newcastle and Lake Macquarie study (Fulford *et al.*, 2002) are provided in Appendix A.9, Table A.1. Other examples of the building capacity curves, as well as tools for manipulating them, can be found in the directory `*/eqrm/datacvtbuildingpars`.

4.3.2 Building usage types

The cost models used by the EQRM require knowledge of the building's use in society. For example the value of a factory's contents will vary from the value of a residents house. Similarly, the cost associated with building a hospital and the cost of building a local shop may differ even if the same materials are used because the buildings may be built to different standards. To transfer this information to the EQRM the building database must store information about each building's usage. There are two different schemes that can be used; the

functional classification of building (FCB) usage (Australian Bureau of Statistics, 2001) and the HAZUS usage classification (FEMA, 1999).

The FCB usage is summarised in Table 4.4 and the HAZUS usage classification is summarised in Table 4.5. The `setdata` flag `b_usage_type_flag` can be used to switch between the two usage classifications.

4.3.3 Replacement costs

The replacement cost in dollars per square metre for each building and the replacement cost of the contents of each building are contained within the building database (columns 13 and 14 respectively: see Section 4.3). Typically these costs are a function of the usage classification of the building and are hence also dependent on whether the HAZUS or FCB classification system is used. The EQRM does not cross check how the costings were created. Note that in some instances it may be appropriate to use costings created from one usage classification with the EQRM using the other usage mode (effects cost splits - see below) and in some instance it may not be appropriate to do so. Users are encouraged to familiarise themselves with database metadata to ensure that they are using the EQRM appropriately for their own application.

Table 4.4: Functional classification of building (FCB) (Australian Bureau of Statistics, 2001) and integer index used in the building database column 15.

	Residential: Separate, kit and transportable homes
1	111: Separate Houses
2	112: Kit Houses
3	113: Transportable/relocatable homes
	Residential: Semi-detached, row or terrace houses, townhouses
4	121: One storey
5	122: Two or more storeys
	Residential: Flats, units or apartments
6	131: In a one or two storey block
7	132: In a three storey block
8	133: In a four or more storey block
9	134: Attached to a house
	Residential: Other residential buildings
10	191: Residential: not otherwise classified
	Commercial: Retail and wholesale trade building
11	211: Retail and wholesale trade buildings
	Commercial: Transport buildings
12	221: Passenger transport buildings
13	222: Non-passenger transport buildings
14	223: Commercial carparks
15	224: Transport: not otherwise classified
	Commercial: Offices
16	231: Offices
	Commercial: Other commercial buildings
17	291: Commercial: not otherwise classified
	Industrial: Factories and other secondary production buildings
18	311: Factories and other secondary production buildings
	Industrial: Warehouses
19	321: Warehouses (excluding produce storage)
	Industrial: Agricultural and aquacultural buildings
20	331: Agricultural and aquacultural buildings
	Industrial: Other industrial buildings
21	391: Industrial: not otherwise classified
	Other Non-Residential: Education buildings
22	411: Education buildings
	Other Non-Residential: Religion buildings
23	421: Religion buildings
	Other Non-Residential: Aged care buildings
24	431: Aged care buildings
	Other Non-Residential: Health facilities (not in 431)
25	441: Hospitals
26	442: Health: not otherwise classified
	Other Non-Residential: Entertainment and recreation buildings
27	451: Entertainment and recreation buildings
	Other Non-Residential: Short term accommodation buildings
28	461: Self contained, short term apartments
29	462: Hotels (predominately accommodation), motels, boarding houses, hostels or lodges
30	463: Short Term: not otherwise classified
	Other Non-Residential: Other non-residential buildings
31	491: Non-residential:not otherwise classified

Table 4.5: HAZUS building usage classification (FEMA, 1999) and integer index used in the building database column 5.

	Residential
1	RES1: Single family dwelling (house)
2	RES2: Mobile home
3	RES3: Multi family dwelling (apartment/condominium)
4	RES4: Temporary lodging (hotel/motel)
5	RES5: Institutional dormitory (jails, group housing - military, colleges)
6	RES6: Nursing home
	Commercial
7	COM1: Retail trade (store)
8	COM2: Wholesale trade (warehouse)
9	COM3: Personal and repair services (service station, shop)
10	COM4: Professional and technical services (offices)
11	COM5: Banks
12	COM6: Hospital
13	COM7: Medical office and clinic
14	COM8: Entertainment and recreation (restaurants, bars)
15	COM9: Theaters
16	COM10: Parking (garages)
	Industrial
17	IND1: Heavy (factory)
18	IND2: Light (factory)
19	IND3: Food, drugs and chemicals (factory)
20	IND4: Metals and mineral processing (factory)
21	IND5: High technology (factory)
22	IND6: Construction (office)
	Agriculture
23	AGR1: Agriculture
	Religion/Non/Profit
24	REL1: Church and non-profit
	Government
25	GOV1: General services (office)
26	GOV2: Emergency response (police, fire station, EOC)
	Education
27	EDU1: Grade schools
28	EDU2: Colleges and Universities (not group housing)

4.4 Key functions, flags and parameters

Name	Type	Description
*/datacvt /buildingpars	Dir	Tools for manipulating and preparing engineering parameter files.
*/datacvt /buildingdb	Dir	Tools for manipulating and preparing building databases.
*/datacvt /econsoclosspars	Dir	Tools for manipulating and preparing costing split ratios.
Input Manager	GUI	Tool for creating earthquake hazard grids.
eqrm_param_gui	GUI	Main EQRM GUI.
<site_loc>_par_study _region_box.txt	Par File	Describes study region with a box - can be used to generate hazard grids.
<site_loc>_par_site _class_polys.mat	Par File	Describes study region as a set of site classes - can be used to generate hazard grids.
<site_loc>_par_site _uniform.mat	Par File	Earthquake hazard grid.
sitedb_<site_loc>.mat	Par File	Building database.
b_usage_type_flag	Par	Flag for selecting the usage classification system.
hazus_btypes_flag	Par	Flag for selecting the building construction type classification system.
buildpars_flag	Par	Flag for selecting engineering parameters.
grid_flag	Par	Flag for selecting the type of earthquake hazard grid to be used.

Chapter 5

Attenuation

5.1 Overview

Attenuation models give a measure of the level of motion observed at some distance R from an event of magnitude r_m. Typically the motion of interest is a displacement, velocity or acceleration. It is common to consider both the motion at the ground surface as well as the motion experienced by a range of buildings, typically approximated by single-degree of freedom oscillators (SDOF). Such measures of motion are known as response spectral displacement, the response spectral velocity and the response spectral acceleration for displacement, velocity and acceleration respectively. The most frequently used measure of motion in the EQRM application is the response spectral acceleration which is described in more detail in Appendix A.8. The response spectral acceleration is denoted by $S_a(T_o, r_m, R)$ where the T_o refers to fundamental period (Appendix A.8), r_m refers to earthquake magnitude (Section 3.2.5) and R represents the distance between the event and site of interest and can be any one of R_{hyp}, R_{epi}, R_{rup} or R_{jb} (Section 5.1.1).

5.1.1 Background theory

Different measures of distance are used by different attenuation formulae. They are illustrated in Figure 5.1 and can be summarised as follows (see Abrahamson and Silva (1997) for further information):

- **Hypocentral** distance R_{hyp}: from site to the hypocentre of the fault rupture.

- **Epicentral** distance R_{epi}: from site to the vertical projection of the hypocentre to the ground surface (the epicentre).
- **Rupture distance** distance R_{rup}: from site to closest point on rupture plane.
- **Joyner-Boore** distance R_{jb}: from site to closest point of the vertical projection of the rupture plane.

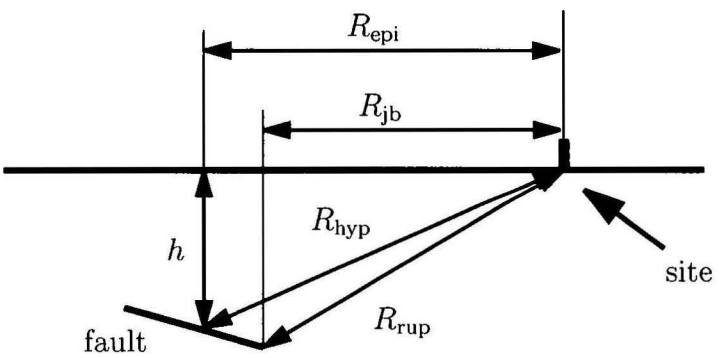

Figure 5.1: Diagram showing the distance measures used in various attenuation formulae.

The earthquake catalogue (see Section 3) simulates events with moment magnitude r_m. However, some of the attenuation formulas require the use of local magnitude r_{m_l} (e.g. Gaull *et al.* 1990). To overcome this obstacle the following conversion is used by `mw2ml`

$$r_{m_l} = \frac{0.473 + \sqrt{0.473^2 - 4 \times 0.145(3.45 - r_m)}}{2 \times 0.145}; \tag{5.1}$$

(Johnston, *pers. comm.*, 2001) which is based on earlier work published by the same author (Johnstone, 1996).

Boore (1983) states that the uncertainties in ground motion predictions (or estimates of the response spectral acceleration $S_a(T_o, r_m, R)$) can be as large as a factor of 2. He goes on to suggest that such uncertainty can be due to variations in source properties, propagation path and local site response. Such uncertainty is commonly segregated into epistemic and aleatory uncertainties (e.g Toro *et al.* 1997). In this case, epistemic uncertainty refers to that uncertainty which results from an incomplete knowledge and data about the physics of the earthquake process, while aleatory uncertainty is the uncertainty which arises from the random nature of the earthquake process. Many authors have assumed that the

PDF of $S_a(T_o, r_m, R)$ for any (T_o, r_m, R) is log-normal (Campbell, 2003). The EQRM assumes that the standard deviation of the PDF is given by the aleatory uncertainty when both aleatory and epistemic uncertainty are provided by the attenuation model. If an attenuation model provides only one measure of uncertainty it is assumed to be the standard deviation. The aleatory uncertainty is then incorporated by sampling the PDF (see Section 5.3.2), whereas epistemic uncertainty is included by considering more than one different attenuation model (see Section 5.4).

5.1.2 Implementation

In the EQRM application the attenuation calculations are conducted within the main driving function `do_analysis` which computes the attenuation for one site at a time for all events and all fundamental (or building) periods. That is, for each site there exists a large matrix of modelled $S_a(T_o, r_m, R)$ (this matrix is `SA` or `SArock` in the code) whose rows correspond to the events (i.e. an r_m-R pair) and whose columns correspond to the T_o. That is

$$SA = \begin{bmatrix} S_a(T_{o,1}, r_{m,1}, R_1) & S_a(T_{o,2}, r_{m,1}, R_1) & \dots & S_a(T_{o,N_T}, r_{m,1}, R_1) \\ S_a(T_{o,1}, r_{m,2}, R_2) & S_a(T_{o,2}, r_{m,2}, R_2) & \dots & S_a(T_{o,N_T}, r_{m,2}, R_2) \\ \vdots & \vdots & \ddots & \vdots \\ S_a(T_{o,1}, r_{m,N_s}, R_{N_s}) & S_a(T_{o,2}, r_{m,N_s}, R_{N_s}) & \dots & S_a(T_{o,N_T}, r_{m,N_s}, R_{N_s}) \end{bmatrix}$$

where N_s refers to the number of events and N_T refers to the number of periods. Note that the r_m-R pair comes from the event catalogue (see Section 3.2.1) and a calculation of distance (see Section 5.1.1). The T_o are determined by the user-defined vector parameter `periods` in `setdata`. Computationally the above calculation of attenuation is conducted in two parts as follows:

1. The preparation of the attenuation coefficients (`prep_attn`) conducted before entering a loop over sites. This preparation involves interpolating the attenuation coefficients to the fundamental periods defined by `periods`.
2. The computation of the $S_a(T_o, r_m, R)$ at each site (`do_attenuation`) conducted site-by-site within a loop over sites.

Each attenuation model returns an estimate of:

1. the mean of $log(S_a(T_o, r_m, R))$ (equivalent to the logarithm of the median of $S_a(T_o, r_m, R)$) and hereafter denoted by $\mu_{log(S_a)}(T_o, r_m, R)$ or $\mu_{log(S_a)}$ for brevity, and

2. the standard deviation of $log(S_a(T_o, r_m, R))$, hereafter denoted by $\sigma_{log(S_a)}(T_o, r_m, R)$ or $\sigma_{log(S_a)}$ for brevity.

Note that the $\sigma_{log(S_a)}$ returned by the different attenuation models differ in the sense that they consider the variability resulting from a range of different 'causes'. A brief discussion of these subtleties is left to the relevant section of each attenuation model (see below). A more detailed explanation of the subtleties can be found in the relevant literature.

The distance between a site and all the events in the earthquake catalogue is computed by `do_alldist`. Recall that in the description of an event (see Table 3.3) there was no mention of an event hypocentre or epicentre. Note that the hypocentre of an actual event is defined as the point at which a rupture begins (Kramer, 1996) and hence is rarely located in the centre of the rupture plane (as illustrated in Figure 2 by Sibson (2003)). There are two obvious techniques that could be used to approximate R_{epi} and R_{hyp}. The first technique approximates R_{epi} and R_{hyp} using R_{jb} and R_{rup} respectively. This technique is conservative since $R_{\text{epi}} \geq R_{\text{jb}}$ and $R_{\text{hyp}} \geq R_{\text{rup}}$. The second technique involves approximating R_{hyp} by using the distance to the rupture centroid and R_{epi} with the distance to the vertical surface projection of the rupture centroid. The `EQRM` application currently uses the first (i.e. conservative) technique. However, it should be noted that this introduces a bias in the results, particularly since the attenuation models themselves are most likely determined from events that have been located as point sources. It is recommended that the technique for such distance approximation is re-considered in the future. In particular, Bommer *et al.* (2005) provide a good discussion of problems associated with using multiple attenuation formulae in PSHA and Scherbaum *et al.* (2004) provide distance metric conversion formulae that may be used to overcome the bias issues discussed above.

5.2 Attenuation formulae

There are many attenuation formulae described in the literature. Campbell (2003) provides an overview of many common attenuation models. A handful of these are available for use within the EQRM application. Analogous to the use of source models, the EQRM allows the user to use one or more attenuation models. This section discusses the individual attenuation formulae. The sampling of attenuation model probability density function (aleatory uncertainty) is discussed in Section 5.3 and the use of multiple attenuation models is described in Section 5.4.

5.2.1 Toro attenuation formula

The Toro *et al.* (1997) attenuation relation used in the EQRM code is based on the Joyner-Boore distance R_{jb} and moment-magnitude. Note that this reference largely describes the variability and not how the coefficients were derived. EPRI (1993) describes how the coefficients were derived.

The Toro *et al.* (1997) attenuation model divides North America into two regions (Gulf and Mid-Continent) and can be used with two different measures of magnitude (local and moment). Currently the EQRM can only use the Mid-Continent – moment magnitude version of the attenuation model. This version of the attenuation model is used because the earthquake mechanism in Mid-Continent USA is believed to be similar to that in Australia (i.e. both are intraplate settings). It is possible to incorporate the other options for the Toro *et al.* (1997) attenuation model in the future by using the `setdata` parameter `attn_region` (see Table 5.2).

The attenuation formula is

$$\begin{aligned}\mu_{log(S_a)}(T_o, r_m, R_{\text{jb}}) = C_1 + C_2(r_m - 6) + C_3(r_m - 6)^2 - C_4 \ln(R_M) \\ - (C_5 - C_4) \max\left[\ln\left(\frac{R_M}{100}\right), 0\right] - C_6 R_M,\end{aligned} \tag{5.2}$$

where

$$R_M = \sqrt{R_{\text{jb}} + C_7^2}. \tag{5.3}$$

The coefficients used in the code, $C_1, \ldots, C_7$, are functions of T_o and are tabulated in Toro *et al.* (1997, Table 2) and in the file `attn_toro_midcontinent_momag.txt` (for the mid-continent region). The preparation of coefficients is undertaken by `attn_prepcoeff_toro` (called by `prep_attn`) and the attenuation computed by `attn_allpervec_toro` (called by `do_attenuation`).

The 'uncertainty parameter' ($\sigma_{log(S_a)}$) can be decomposed as follows:

$$\sigma_{log(S_a)}(T_o, r_m, R_{\text{jb}}) = \sqrt{\sigma_a(T_o, r_m, R_{\text{jb}}) + \sigma_e(r_m)}. \tag{5.4}$$

The aleatory or random uncertainty σ_a can be separated into a source dependant component σ_{a,r_m} (see Toro *et al.* (1997, Table 3) or `attn_preptoro_aleatory1`) and a path dependant component $\sigma_{a,R_{\text{jb}}}$ (see Toro *et al.* (1997, Table 4) or `attn_preptoro_aleatory2`) as follows:

$$\sigma_a = \sqrt{\sigma^2_{a,r_m}(T_o, r_m) + \sigma^2_{a,R_{\text{jb}}}(T_o, R_{\text{jb}})}. \tag{5.5}$$

The EQRM uses the aleatory uncertainty as defined by Equation 5.5.

The epistemic or knowledge uncertainty σ_e is dependant upon source only, that is $\sigma_e = \sigma_{e,r_m}$ (see Toro *et al.* (1997, Page 48) or `attn_preptoro_epistemic`). Note that σ_{a,r_m} is a function of T_o and r_m; $\sigma_{a,R_{\rm jb}}$ is a function of T_o and $R_{\rm jb}$; and σ_{e,r_m} is a function of r_m only.

5.2.2 Gaull attenuation formula

The Gaull *et al.* (1990) attenuation relation, as used in the EQRM code, is based on hypocentral distance $R_{\rm hyp}$ and local magnitude r_{m_l}.The Gaull attenuation model can be used to compute (i) the mean of the logarithm of PGA $\mu_{log(PGA)}$ or (ii) the mean of the logarithm of the Modified Mercalli Intensity $\mu_{log(I_{\rm MMI})}$. The formula is based on empirical intensity data in the Australian region and the PGA extension created using Papua New Guinea data. For the purpose of this attenuation model the Australian region is divided into four sub-regions, Western Australia, Southeastern Australia, Northeastern Australia and Indonesia. In the EQRM application the selection of the Gaull region is controlled by the flag `attn_region` whose functionality is described by Section 5.4 and Table 5.3. The attenuation formulae is:

$$lnY = \ln a - c \ln R_{\rm hyp} + b r_{m_l} \tag{5.6}$$

where a, b and c are constants, r_{m_l} is the local magnitude of the rupture and lnY represents $\mu_{log(PGA)}$ or $\mu_{log(MMI)}$ depending on the value of the constants. The constants are tabulated in Gaull *et al.* (1990, Table 4) and are in the file `attn_allpervec_gaull` (for the PGA case) and `attn_mmi_gaull` (for the $I_{\rm MMI}$ case).

Note that in the case of the Gaull *et al.* (1990) attenuation model (PGA version) there is no need to prepare the attenuation coefficients because the attenuation model is only defined for $T_o = 0sec$ (PGA). To compute $S_a(T_o, r_m, R)$ (more specifically, $\mu_{log(S_a)}$), we can extend the PGA estimate using the Australian Standard Response Spectral Acceleration (Standards Australia, 1993). The actual computation of the Gaull *et al.* (1990) attenuation model is undertaken by `attn_allpervec_gaull` and the 'extension' to a complete S_a is undertaken by `aus_peshnew`.

Gaull *et al.* (1990, Table 4) tabulate the 'uncertainty parameter(s)' ($\sigma_{log(Y)}$) and indicate that they do not depend on r_{m_l} or $R_{\rm hyp}$. Furthermore, when extending the PGA estimate to a complete S_a it is assumed that $\sigma_{log(S_a)}$ is not a function of T_o and that

$$\sigma_{log(S_a)}(T_o) = \sigma_{log(PGA)}. \tag{5.7}$$

Personal discussions with Brian Gaull (2002 and 2003) have revealed that the following values of $\sigma_{log(Y)}$; 0.7 (for PGA) and 0.925 (for I_{MMI}) should be used in preference to the published values of 0.28 and 0.37 respectively.

5.2.3 Atkinson and Boore attenuation formula

The Atkinson and Boore (1997) attenuation relation, as used in the EQRM code, is based on hypocentral distance R_{hyp} and moment magnitude r_m. The formula is

$$\mu_{log(S_a)}(T_o, r_m, R_{\mathrm{hyp}}) = C_1 + C_2(r_m - 6) + C_3(r_m - 6)^2 - ln(R_{\mathrm{hyp}}) - C_4 R_{\mathrm{hyp}}. \quad (5.8)$$

The coefficients used in the code, $C_1, \ldots, C_7$, are functions of T_o and are tabulated in Atkinson and Boore (1997, Table 1) and in the file `attn_atkboore_momag.txt`. The preparation of coefficients is undertaken by `attn_prepcoeff_atkboore` and the attenuation computed by `attn_allpervec_atkboore`.

The uncertainty is dependant on T_o only and is defined by Atkinson (1995). It represents aleatory uncertainty, σ_a and no attempt is made to separate it into into source and path components (see Atkinson 1995, Table 2, or `attn_prep_atkboore_aleatory`).

5.2.4 Sadigh attenuation formula

The Sadigh *et al.* (1997) attenuation relation, as used in the EQRM code, is based on rupture distance R_{rup} and moment-magnitude r_m. Using the convention defined by Campbell (2003) (in accompanying appendix), the attenuation formula is

$$\mu_{log(S_a)}(T_o, r_m, R_{\mathrm{rup}}) = C_1 F + C_2 + C_3 r_m + C_4(8.5 - r_m)^2 + c_5 ln(r_{rup} + C_7 \exp c_8 r_m) + C_r ln(r_{rup} + 2), \quad (5.9)$$

where the parameter F is hard wired in the EQRM to 1 (hence assuming reverse faulting). The coefficients used in the code, $C_1, \ldots, C_7$, are functions of T_o and r_m. They are tabulated in Sadigh *et al.* (1997, Table 2) and they are located in the files `attn_sadigh_coeff_momag_less65.txt` and `attn_sadigh_coeff_momag_great65.txt` for $r_m \leq 6.5$ and $r_m > 6.5$ respectively. The preparation of coefficients is undertaken by `attn_prepcoeff_sadigh` and the attenuation computed by `attn_allpervec_sadigh`.

Sadigh *et al.* (1997) define a magnitude r_m and period T_o dependant 'standard error' $\sigma(r_m, T_o)$ (see Sadigh *et al.* 1997, Table 3) which can be generalised as follows

$$\sigma(r_m, T_o) = \begin{cases} C_{10} - C_{11} r_m & \text{for } 0 < r_m < 7.21 \\ c_{12} & \text{for } r_m \geq 7.21 \end{cases} \tag{5.10}$$

where the coefficients C_{10}, C_{11} and C_{12} are functions of T_o, and are defined in (Campbell, 2003, Table A-14). The coefficients are also included in `attn_sadigh_coeff_momag_less65.txt` and `attn_sadigh_coeff_momag_great65.txt`. The preparation of the coefficients is conducted by `attn_prep_sadigh_uncertainty`. For the purpose of consistency, $\sigma(r_m, T_o)$ is assumed to be the aleatory uncertainty σ_a.

5.2.5 Somerville attenuation formula

The Somerville *et al.* (2001) attenuation relation, as used in the EQRM code, is based on Joyner–Boore distance R_{jb} and moment magnitude r_m. The Somerville *et al.* (2001) attenuation model can be used for rift or nonrift zones and for vertical or horizontal shaking (i.e. four seperate versions). The default setting in the EQRM is nonrift – horizontal however this can be modified by changing `attn_region` (see Section 5.4 and Table 5.3).

The attenuation formula is

$$\begin{aligned} \mu_{log(S_a)}(T_o, r_m, R_{\text{jb}}) = {} & C_1 + C_2(r_m - 6.4) + C_3 ln(R_M) + C_4(r_m - 6.4)) \ln(R_M) \\ & + C_5 R_{\text{jb}} + C_7(8.5 - r_m)^2, \end{aligned} \tag{5.11}$$

for $R_{\text{jb}} < 50$, and

$$\begin{aligned} \mu_{log(S_a)}(T_o, r_m, R_{\text{jb}}) = {} & C_1 + C_2(r_m - 6.4) + C_3 ln(R_M) + C_4(r_m - 6.4)) \ln(R_M) \\ & + C_5 R_{\text{jb}} + C_6(ln(R_M) - ln\sqrt{2536}) + C_7(8.5 - r_m)^2, \end{aligned} \tag{5.12}$$

for $R_{\text{jb}} \geq 50$, where

$$R_M = \sqrt{R_{\text{jb}} + 6^2}. \tag{5.13}$$

The coefficients used in the code, $C_1, \ldots, C_7$, are functions of T_o and are tabulated in Somerville *et al.* (2001, Table 9) and in the file `attn_somer_nonrift_hori.txt` (for the Nonrift – Horizontal case). The preparation of coefficients is undertaken by `attn_prepcoeff_somerville` (called by `prep_attn`) and the attenuation computed by `attn_allpervec_somerville` (called by `do_attenuation`).

Somerville *et al.* (2001) describe five types of uncertainty as follows:

Table 5.1: Different techniques for incorporating attenuation variability in the EQRM.

var_attn_method	Description
1	PDF sampling or spawning (see Section 5.3.2) when src_eps_switch is 1 0 −1
2	random sampling (see Section 5.3.1)
3	$+2\sigma$ from median
4	$+\sigma$ from median
5	$-\sigma$ from median
6	-2σ from median

σ_μ	uncertainty in the median attenuation = 0.2.
σ_σ	uncertainty in the scatter about median attenuation = 0.15.
$\sigma_{modeling}(T_o)$	representing the discrepancy between actual physical processes and the simplified representation of the model.
$\sigma_a(T_o)$	arising from parameters varied in the study of Somerville *et al.* (2001).
$\sigma_b(T_o)$	arising from earlier studies by the same authors.

The terms σ_μ and σ_σ are clearly epistemic uncertainty. Somerville *et al.* (2001) then define $\sigma_{modeling}(T_o)$, $\sigma_a(T_o)$ and $\sigma_b(T_o)$ as contributions to the scatter and as such the aleatory uncertainty is taken to be:

$$\sigma_{a,log(S_a)}(T_o) = \sqrt{\sigma^2_{modeling}(T_o) + \sigma^2_a(T_o) + \sigma^2_b(T_o)}. \tag{5.14}$$

5.3 Incorporating aleatory uncertainty

Incorporating uncertainty is a critical component of any PSHA. The inclusion of aleatory uncertainty in the EQRM for attenuation is facilitated by the flag var_attn_flag. The aleatory uncertainty is based on estimations of $\sigma_{log(S_a)}$ (see Sections 5.2 and 5.1.2) and is incorporated within do_attenuation. Sections 5.3.1 and 5.3.2 describe two of the most commonly used techniques for incorporating attenuation aleatory uncertainty when using the EQRM. The flag to control the uncertainty method is var_attn_method and Table 5.1 illustrates all of the aleatory uncertainty options that are available with the EQRM.

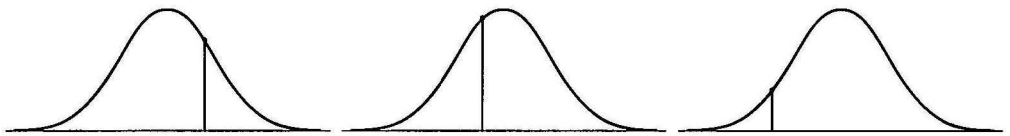

Figure 5.2: Selection of three different random samples from a PDF.

5.3.1 Random sampling of a response spectral acceleration

This technique involves selecting a single 'random' response spectral acceleration (S_a) from its PDF by:

1. Selecting a random number n_{rand} from the standard normal distribution $N \sim (0, 1)$.
2. Computing the S_a as follows

$$log(A_{S_a}(T_o, r_m, R)) = \mu_{log(S_a)} + n_{rand}\sigma_{log(S_a)}, \tag{5.15}$$

   where $\sigma_{log(S_a)}$ is usually assumed to be σ_a.

Random sampling from a PDF is illustrated in Figure 5.2. It is important to note the following about random selection:

1. Two sites that are close to one another may give dramatically different estimates of ground motion for the same event. Earthquake hazard and risk values that are computed using random sampling exhibit a low level of spatial correlation.
2. The number n_{rand} can theoretically take on any value between $\pm\infty$. Therefore it is possible that estimates of S_a using Equation 5.15 can be unrealistically large. Dhu *et al.* (2002) overcame this problem by re-scaling the excessively large S_a to some acceptable level. The re-scaling was performed by the function `pga_cutoff` which computes a re-scaling parameter R_{scale} as follows

$$R_{scale} = \frac{\texttt{pga\_cutoff}}{log(A_{S_a}(0, r_m, R))}. \tag{5.16}$$

   The re-scaling parameter is then applied to the entire S_a as follows

$$log(A_{S_a,new}(T_o, r_m, R)) = R_{scale} \times log(A_{S_a,old}(T_o, r_m, R)). \tag{5.17}$$

3. There is no effort to account for the likelihood (or probability) of selecting a particular n_{rand} i.e. a particular value of the S_a is not weighted against its likelihood. It can be argued that if enough earthquakes are simulated a range of different n_{rand} will be taken (high and low) and the overall hazard and/or risk values will converge to the true ones.

5.3.2 Sampling the probability density function of the response spectral acceleration (spawning)

An alternative technique for incorporating uncertainty relies on sampling the PDF of the S_a. This technique is used by Aon Re (Mendez, *pers. comm.*, 2003) and is often referred to as spawning. An integral component of sampling the PDF is the spawning of events with the event catalogue (see Section 3.4). Essentially the approach involves taking a user defined number of copies of each event. Every event copy is then available for calculation of hazard (or risk) using a different sample from the attenuation PDF.

1. Firstly the user must define a lower magnitude bound m_{bnd}, a number of samples n_{smples} and a PDF range n_σ (see Section 3.4 for a complete definition). Recall that `fuse_4hzd` redefines the event activity r_ν using a weight w_e, derived by truncating and re-normalising a standard normal distribution to $\pm n_\sigma$.

2. The S_a is computed as follows

$$log(A_{S_a,i}(T_o, r_m, R)) = \mu_{log(S_a)} - \epsilon_i \sigma_{log(S_a)} \quad \text{for } i = 1 \ldots n_{smples} \tag{5.18}$$

where

$$\epsilon_i = -n_\sigma + \tfrac{\Delta}{2} + (i-1)\Delta \quad \text{for } i = 1 \ldots n_{smples} \tag{5.19}$$

and

$$\Delta = \frac{2n_\sigma}{n_{smples}}. \tag{5.20}$$

Note that Equations 5.18 and 5.19 ensure that the S_a associated with each of the event copies are evenly spread across the domain of the attenuation PDF (Figure 5.3). Recall from Section 3.4 that the event activities r_ν giving rise to each of the S_a described in Equation 5.18 are modified by `fuse_4hzd` as follows:

$$r_{\nu,i} = r_{\nu,original} \times w_{e,i} \tag{5.21}$$

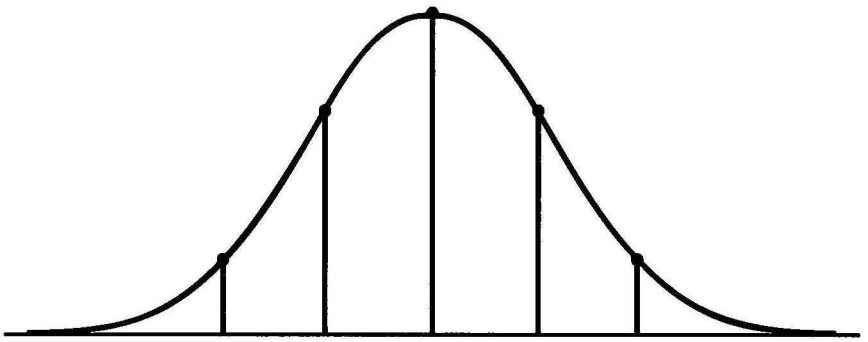

Figure 5.3: Samples drawn from a PDF using the sampling by spawning technique with $n_{smples} = 5$ and $n_\sigma = 2.5$. The width between the vertical bars is Δ. Note that there is one sample for each of the five (spawned) copies of the original event.

For example, assume that there is an event with $r_\nu = 0.05$ that gives rise to $\mu_{log(S_a)} = [0.3g, 0.5g, 0.2g]$ at the periods $T_o = [0s, 0.3s, 1s]$ respectively. Also assume that the estimates of $\mu_{log(S_a)}$ have the following standard deviations $\sigma_{log(S_a)} = \sigma_a = [0.03, 0.04, 0.01]$. Defining $m_{bnd} = 0$, $n_{smples} = 5$ and $n_\sigma = 2.5$ gives

$$\Delta = \frac{2 \times 2.5}{5} = 1, \tag{5.22}$$

and

i	$w_{e,i}$	ϵ_i	r_ν	$log(A_{S_a,i})$
1	0.0545	-2	0.0027	$[0.24g, 0.42g, 0.18g]$
2	0.2442	-1	0.0122	$[0.27g, 0.46g, 0.19g]$
3	0.4026	0	0.0201	$[0.30g, 0.50g, 0.20g]$
4	0.2442	1	0.0122	$[0.33g, 0.54g, 0.21g]$
5	0.0545	2	0.0027	$[0.36g, 0.58g, 0.22g]$

It is important to note the following about spawning:

1. Sub-sampling the PDF provides a smoother (and repeatable) estimate of the S_a than random selection (Section 5.3.1). This equates to a high level of spatial correlation.

2. The range of possible S_a values is bounded by the n_σ.

3. Estimates of all S_a are weighted against an event activity r_ν that accounts for the likelihood of a particular attenuation being observed.

4. The nature of spawning means that the synthetic event catalogue is copied a number of times and hence requires more computation time and memory.

Section 3.4 stated that event spawning is conducted when `src_eps_switch` is 1 or 2. When `src_eps_switch`= 2 the spawned values are treated separately throughout the hazard or risk assessment. When `src_eps_switch`= 1 however, the spawned values are aggregated again before the hazard or risk assessment is made. This idea is illustrated in Figure 5.4.

5.4 Using multiple attenuation models - Incorporating epistemic uncertainty

The use of attenuation models in the EQRM is controlled by the `setdata` parameter `attenuation_flag`. Recall from Section 2.2.1 that `attenuation_flag` is a two row matrix with one column for each attenuation model to be used. The format of `attenuation_flag` is

$$\begin{bmatrix} P_1 & P_2 & \dots & P_n \\ w_{a,1} & w_{a,2} & \dots & w_{a,n} \end{bmatrix},$$

where the integers $\{P_i\}_{i=1}^n$ are pointers to the attenuation model (see Table 5.2) and the real numbers $\{w_{a,i}\}_{i=1}^n$ are weights for the respective attenuation models. Note that the weights w_i must either be all positive or all negative and

$$\left| \sum_{i=1}^{n} w_{a,i} \right| = 1. \tag{5.23}$$

The mechanism for using more than one attenuation model is similar to the mechanism used for spawning (see Section 5.3.2). That is, the event catalogue is copied n times (once for each attenuation model) and the appropriate attenuation model applied to its respective copy. The values of ground motion (loss for risk) can then be treated independently for the hazard/risk calculation (if $\sum_{i=1}^n w_{a,i} = -1$) or aggregated before the hazard/risk assessment is undertaken (if $\sum_{i=1}^n w_{a,i} = 1$). This notion of logic tree collapse is described by Figure 5.4.

(a)

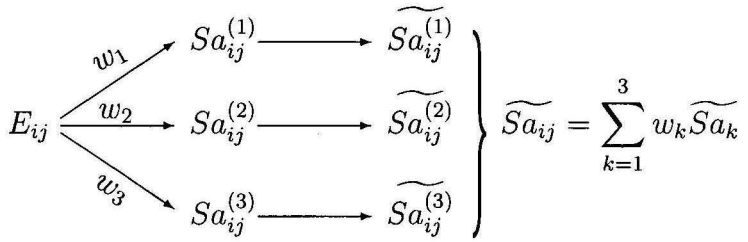

(b)

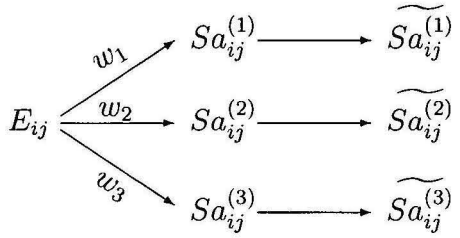

(c)

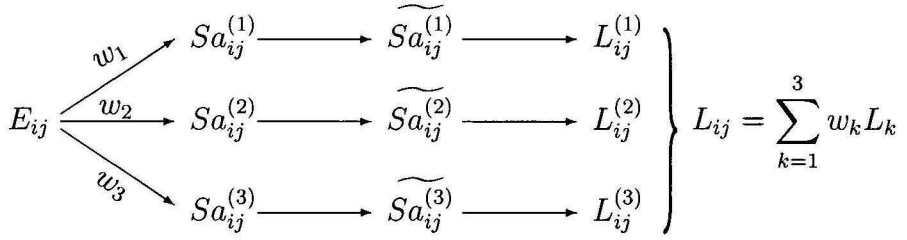

(d)

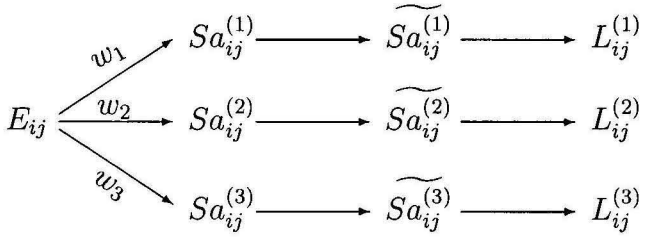

Figure 5.4: The application of spawning to a single synthetic earthquake E_{ij};(a) the collapse of spawned samples for hazard (`src_eps_switch`= 1); (b) hazard spawning without collapse (`src_eps_switch`= 2); (c) the collapse of spawned samples for risk (`src_eps_switch`= 1); and (d) risk spawning without collapse (`src_eps_switch`= 2). The illustrated procedure is repeated for N_s events in the event catalogue and the techniques of Chapter 9 used to assess the hazard or risk.

Table 5.2: Pointers to attenuation models for use in the first row of `attenuation_flag`.

Motion	pointer	model
S_a	0	Gaull *et al.* (1990) PGA with S_a extension
	1	Toro *et al.* (1997)
	2	Atkinson and Boore (1997)
	3	Sadigh *et al.* (1997)
	4	Somerville *et al.* (2001)
I_{MMI}	100	Gaull *et al.* (1990)

Table 5.3: Attenuation region (`attn_region`) options for each of the attenuation models.

attenuation pointer	attenuation model	`attn_region`
0 or 100	Gaull *et al.* (1990)	1 ⇒ Western Australia 2 ⇒ Northeastern Australia 3 ⇒ Indonesia 4 ⇒ Southeastern Australia
1	Toro *et al.* (1997)	1 ⇒ Mid-Continent M_o
2	Atkinson and Boore (1997)	1 ⇒ No published options
3	Sadigh *et al.* (1997)	1 ⇒ No published options
4	Somerville *et al.* (2001)	1 ⇒ Nonrift - Horizontal 2 ⇒ Rift – Horizontal 3 ⇒ Nonrift – Vertical 4 ⇒ Rift –Vertical

5.5 Key functions, flags and parameters

Name	Type	Description
do_analysis	Function	The main driving function for modelling earthquake hazard or risk.
do_alldist	Function	Computes the Joyner-Boore and Rupture Distance from a site to every event.
prep_attn	Function	Prepares the attenuation coefficients by interpolating them to periods of interest T_o.
mw2ml	Function	Converts moment magnitude r_m to local magnitude r_{m_l}.
do_attenuation	Function	Controls the selection of attenuation models for evaluation and assembles outputs.
attn_prepcoeff_toro	Function	Preparation of attenuation coefficients for Toro *et al.* (1997).
attn_allpervec_toro	Function	Computes Toro *et al.* (1997) attenuation.
attn_preptoro_aleatory1	Function	Computes σ_{a,r_m} for use with Toro *et al.* (1997) attenuation.
attn_preptoro_aleatory2	Function	Computes $\sigma_{a,R_{\text{jb}}}$ for use with Toro *et al.* (1997) attenuation.
attn_preptoro_epistemic	Function	Computes σ_{e,r_m} for use with Toro *et al.* (1997) attenuation.
attn_allpervec_gaull	Function	Computes Gaull *et al.* (1990) attenuation.
aus_peshnew	Function	Extends PGA to standard $\mu_{log(S_a)}$.
attn_prepcoeff_atkboore	Function	Preparation of attenuation coefficients for Atkinson and Boore (1997).
attn_allpervec_atkboore	Function	Computes Atkinson and Boore (1997) attenuation.
attn_prep_atkboore_aleatory	Function	Computes σ_a for use with Atkinson and Boore (1997) attenuation.
attn_prepcoeff_sadigh	Function	Preparation of attenuation coefficients for Sadigh *et al.* (1997).
attn_allpervec_sadigh	Function	Computes Sadigh *et al.* (1997) attenuation.

attn_prep_sadigh_uncertainty	Function	Prepares uncertainty coefficients for Sadigh *et al.* (1997) attenuation.
pga_cutoff	Function	Re-scales the S_a such that PGA $\leq$ pgacutoff.
attn_toro_mid continent_momag	Par File	Stores attenuation coefficients for Toro *et al.* (1997) attenuation.
attn_atkboore_momag	Par File	Stores attenuation coefficients for Atkinson and Boore (1997) attenuation.
attn_sadigh_coeff_momag_less65	Par File	Stores attenuation coefficients for Sadigh *et al.* (1997) attenuation.
attn_sadigh_coeff_momag_great65	Par File	Stores attenuation coefficients for Sadigh *et al.* (1997) attenuation.
periods	Par	Periods at which to compute S_a.
attenuation_flag	Par	Defines the attenuation models to be used as well as their respective weights.
attn_region	Par	Flag to assign different attenuation regions for Gaull *et al.* (1990) attenuation.
var_attn_flag	Par	Variability in evaluation of the attenuation model.
var_attn_method	Par	Selects the technique for incorporating variability.

Chapter 6

Regolith amplification

6.1 Overview

Regolith is defined as the soil, geological sediments and weathered rock that overly the un-weathered bedrock. It is well documented that the presence of regolith can increase the level of ground shaking experienced during an earthquake (Borcherdt and Gibbs 1976; Murphy *et al.* 1971). For example, studies in the San Fernando Valley and Los Angeles Basin, U.S.A., have demonstrated that the damage patterns observed during the 1994 Northridge, California earthquake can be strongly correlated to site-response of local regolith (Meremonte *et al.*, 1996). Consequently, including the effect of regolith on earthquake ground shaking is an important component of any seismic hazard or risk analysis.

6.1.1 Background theory

An amplification factor can be used to transfer the earthquake motion from the bedrock to the regolith surface. Amplification factors are influenced by the regolith at the site of interest, the magnitude r_m of the event and the PGA for the event-site combination. For simplicity, the geographical region of interest is usually separated into five or six site-classes inside which the regolith is assumed to be the same. The EQRM application does not compute the amplification factors (or level of amplification). Such calculations must be conducted off-line and the results (or amplification factors) made available to the EQRM application. The interested reader is referred to Robinson *et al.* (2006) for a detailed description of the equivalent linear technique for computing amplification factors. Dhu *et al.*

(2002) discuss the classification of site classes and the application of amplification factors to a probabilistic seismic hazard analysis. Figure 6.1 illustrates the geotechnical cross section for all of the site classes in the Newcastle and Lake Macquarie region, and Figure 6.2 shows an example of the amplification factors use in the same study.

6.2 The amplification factor input file

The amplification factors are saved in a file with a name of the form `<site_loc>_par_ampfactors.mat` where `site_loc` is a variable in `setdata`. For example if `site_loc` = 'newc' then the file is called `newc_par_ampfactors.mat`. The contents of the `<site_loc>_par_ampfactors.mat` include 5 'variable types' that are explained in Table 6.1. Appendix A.7 lists the contents for `newc_par_ampfactors.mat` as used in the Newcastle and Lake Macquarie study (Dhu *et al.*, 2002).

6.3 Implementation

As with the attenuation, the implementation of the amplification factors is conducted within `do_analysis` (for both hazard and risk assessments) in a two step process as follows:

1. The preparation of the amplification factors (`prep_amps`) conducted before entering a loop over sites.
2. Application of the amplification factors to compute $A_{S_a,soil}(T_o, r_m, R)$ at each site (`do_amplification`) conducted within a loop over sites.

The preparation of amplification factors involves interpolating each to the periods defined in the `setdata` parameter `periods` (see Section 5.1.2) and is conducted by the function `prep_amps`. The application of the amplification factors is carried out immediately after the evaluation of the attenuation model and is implemented within `do_amplification`. The process is described for a specific site located within a known Site Class:

1. Bin all of the events in the event catalogue into the bedrock PGA and moment magnitude bins defined by the bin centroids in `pga_bin` and `momag_bin` respectively. Note that the end points of the 'central' bins are assumed to

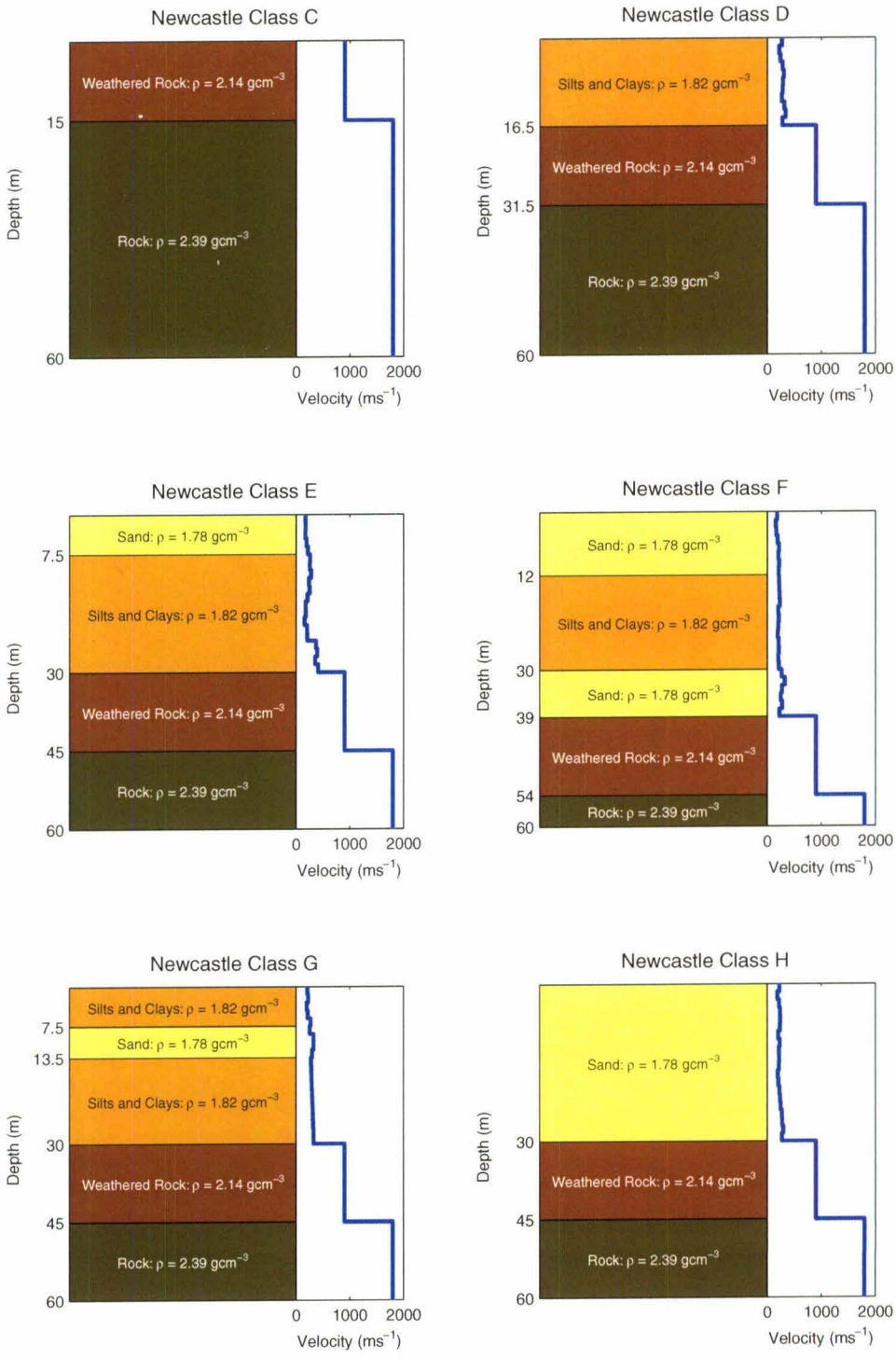

Figure 6.1: Cross sections of the 6 site classes used in the Newcastle and Lake Macquarie study (Dhu *et al.*, 2002).

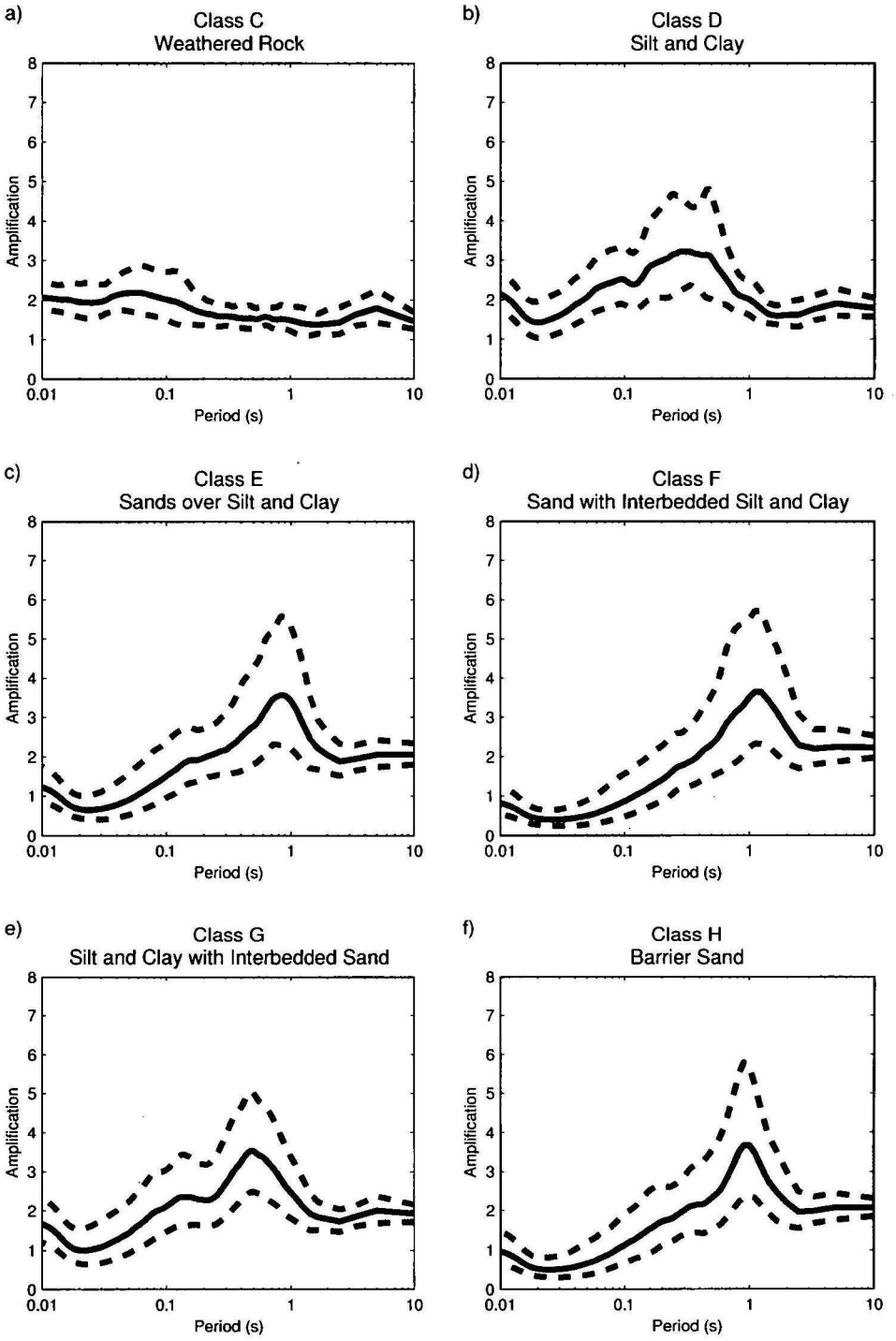

Figure 6.2: Example amplification factors for the site classes shown in Figure 6.1. Note that the amplification factors are for moment magnitude 5.5 and PGA 0.25g.

Table 6.1: Summary of the variables in `<site_loc>_par_ampfactors.mat`. The {1}, {2} and {3} represent input text strings that are pointers to the site class, moment magnitude bin and bedrock PGA bin respectively, for both the amplification factors and their standard deviation. The `<site_loc>_par_ampfactors.mat` file usually contains multiple 'copies' of `ln_site{1}_rockpga{2}_momag{3}` and `stdln_site{1}_rockpga{2}_momag{3}`, whereas it should only contain a single 'copy' of the other variables. All variables are row vectors. The superscript '$*$' shown with some variables refers to the fact that these variables have been 'binned'.

Variable	Description
`amp_period`	Fundamental periods at which the amplification factors (and their standard deviations) are defined.
`ln_site{1}` `_rockpga{2}_momag{3}`	The mean of the logarithm of the amplification factors $\mu_{amp}(T_o, r_m^*, PGA^*)$(at the periods defined in `amp_period`) for the site class {1}, bedrock PGA bin {2} and moment magnitude bin {3}
`momag_bin`	Bin centroids of moment magnitude bins
`pga_bin`	Bin centroids of bedrock PGA bins
`stdln_site{1}` `_rockpga{2}_momag{3}`	The standard deviation of the logarithm of the amplification factors $\sigma_{amp}(T_o, r_m^*, PGA^*)$(at the periods defined in `amp_period`) for the site class {1}, bedrock PGA bin {2} and moment magnitude bin {3}

be half way between the bin centroids. The first and last bins extend to negative and positive infinity respectively.

2. Use a nested loop over all PGA bins (upper loop) and moment magnitude bins (lower loop) and apply the amplification factor as follows:

$$S_{a,soil}(T_o, r_m, R) = F_{amp}(T_o, r_m^*, PGA^*) \times S_{a,bedrock}(T_o, r_m, R), \qquad (6.1)$$

where r_m^* and PGA^* are the centroids of the bins containing r_m and $S_{a,bedrock}(0, r_m, R)$ respectively. The F_{amp} represents the exponential of 'some selection' of amplification factor from the distribution $N \sim (\mu_{log(F)}(T_o, r_m^*, PGA^*), \sigma_{log(F)}(T_o, r_m^*, PGA^*))$. The actual selection made will depend on the method used to incorporate uncertainty (see Section 6.4).

Notice that the use of $N \sim (\mu_{log(F)}, \sigma_{log(F)})$ equates to the assumption that the amplification factors are log-normally distributed.

6.4 Incorporating aleatory uncertainty

In theory, both the random selection and PDF sampling methods described in Section 5.3 could be used to incorporate aleatory uncertainty in amplification factors. Some care will need to be taken if the PDF sampling technique is to be used for incorporating uncertainty at several levels of computation (e.g. for attenuation and amplification) due to the need to spawn the event catalogue (see Section 3.4) at every level. Such iterative spawning may lead to a 'blow-out' in the size of the event catalogue and hence the computation time. sCurrently only the random selection technique is available for use with the amplification factors in the EQRM application.

As with the application of an attenuation model, the EQRM applies `pga_cutoff` to $S_{a,soil}(T_o, r_m, R)$ after applying the amplification factor. This accounts for any unrealistically high selection of amplification factor. A secondary upper cut-off facility exists and involves the use of the `setdata` parameter `MaxAmpFactor`. The `MaxAmpFactor` parameter is applied directly to the amplification factor as follows:

$$F_{new}(T_o, r_m^*, PGA^*) = \begin{cases} F_{old} & \forall \ T_o \text{ s.t. } F_{amp,old} < \texttt{MaxAmpFactor} \\ \texttt{MaxAmpFactor} & \forall \ T_o \text{ s.t. } F_{amp,old} \geq \texttt{MaxAmpFactor} \end{cases} \tag{6.2}$$

or brevity the functional reference to r_m^* and PGA^* in F_{new} and F_{old} in Equations 6.2 and 6.3 refers to the fact that these values represent the bin centroids of `momag_bin` and `pga_bin` respectively. In most simulations the secondary cut-off is not used since `pga_cutoff` handles scaling for an upper bound. Ignoring `MaxAmpFactor` is achieved by setting it to to a very high number (e.g. `MaxAmpFactor`=10000). In contrast, there is another parameter in `setdata` known as `MinAmpFactor` which is commonly utilised within the EQRM application. This parameter stops the selection of any unrealistically low selections of the amplification factor. The `MinAmpFactor` is commonly set to around 0.6. It is applied as follows:

$$F_{new}(T_o, r_m^*, PGA^*) = \begin{cases} F_{old} & \forall \ T_o \text{ s.t. } F_{amp,old} > \texttt{MinAmpFactor} \\ \texttt{MinAmpFactor} & \forall \ T_o \text{ s.t. } F_{amp,old} \leq \texttt{MinAmpFactor} \end{cases} \tag{6.3}$$

Note that a value of $F < 1$ leads to a de-amplification of the bedrock motion.

6.5 Key functions, flags and parameters

Name	Type	Description
`do_analysis`	Function	The main driving function for modelling earthquake hazard or risk.
`prep_amps`	Function	Loads and prepare the amplification factors.
`do_amplification`	Function	Applies the amplification factors and compute `SAsoil`.
`pga_cutoff`	Function	Re-scales the S_a such that PGA $\leq$ `pgacutoff`
`periods`	Par	Periods at which to compute S_a.
`MaxAmpFactor`	Par	Maximum cutoff for all amplification factors (seldom used).
`MinAmpFactor`	Par	Minimum cutoff for all amplification factors (usually 0.6).
`pgacutoff`	Par	The cutoff (or maximum) PGA for use with `pga_cutoff`.

Chapter 7

Building damage

7.1 Introduction

This chapter describes the modelling of building damage. The method is based on the HAZUS methodology (FEMA, 1999) with a few modifications to suit the Monte-Carlo approach used in the EQRM. The modifications are discussed at the end of this chapter.

The Capacity Spectrum Method (FEMA, 1999; Kircher *et al.*, 1997) is used to obtain the peak building displacement and acceleration corresponding to each earthquake. The peak displacement and acceleration are the dependent variables for fragility curves (Kircher *et al.*, 1997) which give probabilities of being in certain damage states, for different types of damage, structural (damage to main structure) and drift-sensitive and acceleration-sensitive non-structural damage (e.g. damage to non-structural internal walls).

The main MATLAB function to calculate building damage is `do_analysis` which reads the earthquake catalogue, applies the attenuation and soil amplification, models the building damage and computes direct financial loss.

The MATLAB function `prep_sites` loads the buildings database file (Chapter 4) and `prep_build_vuln` reads the building parameters file defining engineering parameters. The MATLAB function `do_build_vuln` is a wrapper, called inside the main loop (over sites). The main work is done by `make_build_dam_rand` which calculates the peak values of spectral displacement and acceleration as the intersection of the building capacity curve with the suitably damped demand curve for the vector of all spectral accelerations from each synthetic earthquake.

7.2 The capacity spectrum method

The capacity spectrum method is used to find the peak displacement and peak acceleration for each earthquake-building pair. To use this technique each building is approximated by a single degree of freedom oscillator (SDOF) (Chopra, 2001).

A building's capacity (or response) to an incoming seismic wave, is defined by the capacity curve, a monotonic increasing curve giving the S_a as a function of the spectral displacement S_d. The response spectral acceleration (S_a) normally plotted against building period is plotted against spectral displacement S_d to describe the 'earthquake motion'. When plotted this way the $S_a vs S_d$ plot is known as the demand curve. The peak displacement and acceleration experienced by the building as a result of the 'induced motion' is modelled by the intersection of the capacity curve with the demand curve (Figure 7.1).

The response spectral acceleration curve is normally defined by the attenuation model with 5% damping. The actual damping generated by a building differs from 5% and is a function of the building attributes such as structural type (see Chapter 4). The capacity spectrum method allows for this variation by adjusting the damping (see Section 7.2.2).

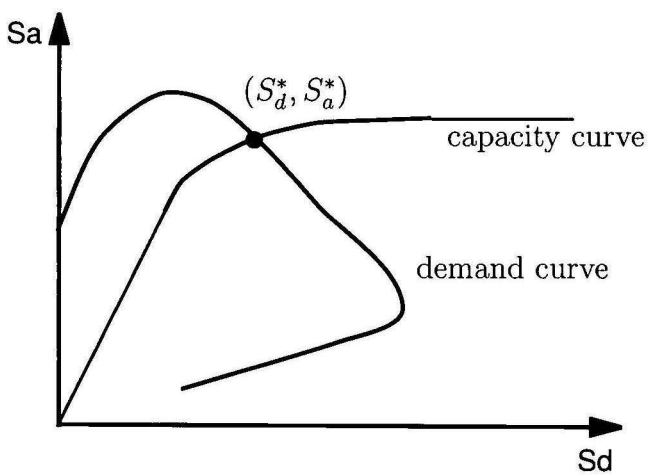

Figure 7.1: The capacity spectrum method.

Figure 7.1 illustrates the intersection of the capacity curve with the demand curve. In the elastic region (or linear component) of the capacity curve the intersection between the capacity curve and the appropriately damped demand curve occurs at a period corresponding to the natural period of the building. If the intersection occurs in the nonlinear plastic deformation region, hysteretic damping results in

a larger component of the earthquakes energy being absorbed through damping in the building. In an equivalent linear approach, this effectively reduces the natural period of the building.

7.2.1 The building capacity curve

The building capacity curve is defined by two points: the yield point (D_y, A_y) and the ultimate point (D_u, A_u). For displacements below the yield point the building response is elastic and the capacity curve represented by a straight line. For displacement amplitudes greater than the yield point nonlinear effects such as plastic deformation cause the rate of increase to reduce. The curve asymptotes towards the ultimate point (see Figure 7.2).

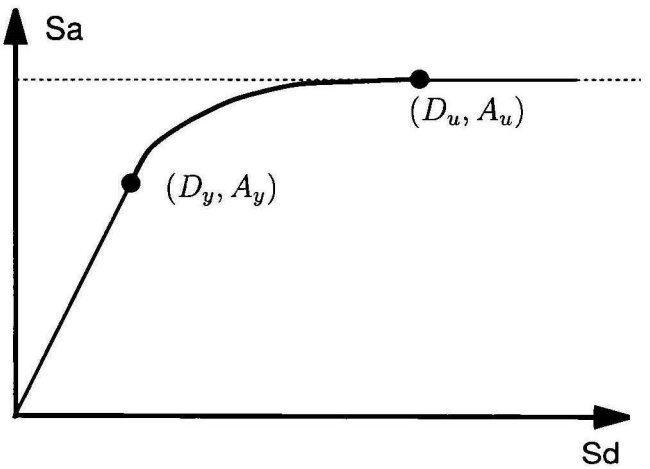

Figure 7.2: The graph of a typical building capacity curve, defined by the yield point (D_y, A_y) and the ultimate point (D_u, A_u). Note that the straight line between the yield point and the origin represents elastic behavior of the building.

The yield point and ultimate point are defined in terms of the building parameters as:

$$\begin{aligned} A_y &= \frac{C_s \gamma}{\alpha_1} \quad [g], \\ D_y &= \frac{1000}{4\pi^2} 9.8 A_y T_e^2 \quad [mm], \\ A_u &= \lambda A_y \quad [g], \\ D_u &= \lambda \mu D_y \quad [mm], \end{aligned}$$

where the building parameters

C_s = design strength coefficient (fraction of the building weight),
T_e = natural elastic building period (seconds),
α_1 = fraction of building weight participating in the first mode,
α_2 = fraction of the effective building height to building displacement,
γ = over-strength factor—yield to design strength ratio,
λ = over-strength factor—ultimate to yield strength ratio,
μ = ductility factor,

are given for several classes of building construction types (Section 4.3.1). Note that the parameter α_2 is not used here, rather it is used to define the appropriate damage ratios (see Equation 7.9).

Fitting the building capacity curve

The capacity curve is composed of three parts: a straight line to the yield point, a curved part from the yield point to the ultimate point, and a horizontal line from the ultimate point.

An exponential function is used to represent the curved part of the building capacity curve. When defining the curved section it is desirable that it has and identical slope to the elastic part at the yield point and that its slope approaches zeros at the ultimate point. We cannot satisfy all these conditions with just three constants, however, we can satisfy the condition of the curves matching at the ultimate point approximately.

The form of the exponential curve is

$$y = c + ae^{-bx}$$

where the constants a, b, and c are given by

$$c = A_u, \quad b = \frac{k}{A_u - A_y}, \quad a = (A_y - A_u)e^{bD_y} \tag{7.1}$$

where $k = A_y/D_y$.

To obtain this, the following equation follows from the curves joining at the ultimate points

$$c + ae^{-bD_u} = A_u.$$

If we neglect the e^{-bD_u} term, then $c = A_u$. From the equation for the yield point we then obtain $A_u - A_y = -ae^{-bD_y}$. From the equation that the slopes match at the yield point we obtain $k = -abe^{-bD_y}$, where $k = A_y/D_y$ is the slope of the elastic linear part of the capacity curve. Eliminating the exponential term from both these equations gives the value of b, and the expression for a follows. The condition that the slope is zero at the ultimate point is consistent with the assumption of neglecting the term e^{-bD_u}. This will be true provided

$$\frac{D_u/D_y}{A_u/A_y - 1} \gg 1.$$

which will be generally true when the ultimate point is far from the yield point.

Variability of the capacity curves

The uncertainty of the peak response of the building to a given ground-shaking is incorporated by using a log-normal distribution of building capacity curves with a log-normal standard deviation parameter $\beta = 0.3$. This value is taken from FEMA (1999) for pre-code buildings with a value of 0.25 recommended for buildings constructed in alignment with building codes. HAZUS gives no explanation or reference to how these values were obtained. It was recommended in the Engineers' workshop, Stehle *et al.* (2001), that a value $\beta = 0.4$ be used for Australian buildings, but there was no justification given for this, so a value of $\beta = 0.3$ has been retained.

The variability of the building capacity curve is described by a log-normal distribution for the vertical component of the ultimate point. That is, $A_u = \bar{A}_u \times e^{\beta\phi}$, where $\bar{A}_u$ is the median value of A_u and ϕ is a random number selected from a standardised normal distribution (see `bcap_rand`).This sampling is analogous to the random sampling technique used elsewhere in the EQRM (e.g. Section 5.3.1) because the median of a log-normally distributed random variable (e.g. $barA_u$) is the same as the exponential of the mean of the log (e.g. $exp(\mu_{ln(A)})$). This is illustrated in Figure 7.3. The yield point (D_y, A_y) on the random capacity curve is chosen from the equations $D_u = \lambda\mu D_y$, with $D_u = \bar{D}_u$, and $D_y = 9.8A_yT_e^2$.

7.2.2 Damping the demand curve

The Response Spectral Acceleration curve (S_a), as obtained from an attenuation formula, is specified for 5% damping. Recall that S_a describes the response of an idealised (SDOF) building. The response of the actual building is incorporated by modifying the damping. This is undertaken in the following two parts:

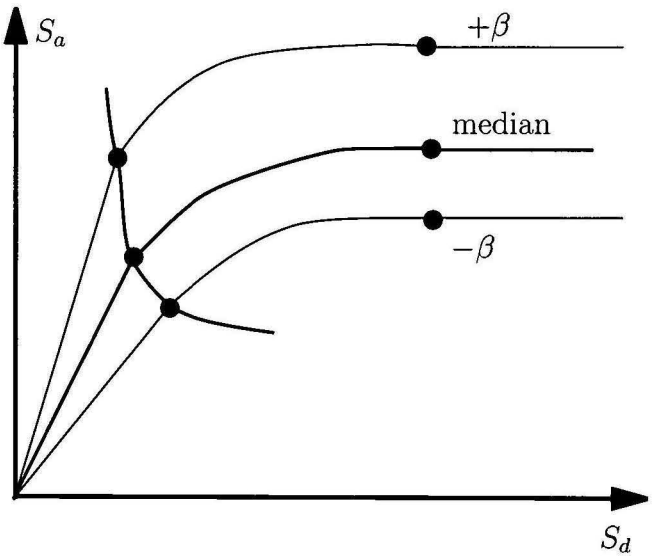

Figure 7.3: Illustration of the random selection of a building capacity curve from a log-normal distribution of building capacity curves. The median, 84th percentile ($+\beta$) and 16th percentile ($-\beta$) are shown.

1. modification of elastic damping, and
2. hysteretic damping.

Modification of elastic damping

The HAZUS approach uses 5% damping for all buildings. However, the modifications suggested at the Australian buildings workshop (Stehle *et al.*, 2001) suggest using elastic damping values higher than 5% with corresponding hysteretic damping coefficients made smaller. The values of the elastic damping have been determined from Newmark and Hall (1982).

Damping formulae are the same as used in FEMA (1999), which are obtained from Newmark and Hall (1982). These are empirically derived formulae, as multiplicative factors, defined for three regimes according to building period. The three regimes correspond to the acceleration-sensitive, velocity-sensitive and displacement-sensitive areas of the response spectrum, denoted R_a, R_v and R_d respectively. The effect of elastic damping on the demand curve is illustrated in Figure 7.4.

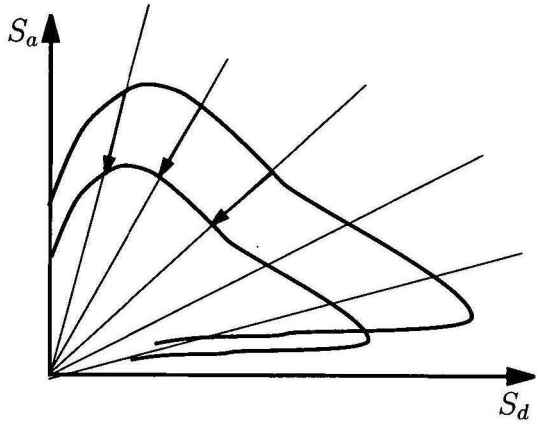

Figure 7.4: Damping of the demand curve.

The damping formula are:

$$R_a = \frac{2.12}{3.21 - 0.68\ln(100B_T)}, \quad 0 \le T < T_{av} \tag{7.2}$$

$$R_v = \frac{1.65}{3.21 - 0.68\ln(100B_T)}, \quad T_{av} \le T < T_{vd} \tag{7.3}$$

$$R_d = \frac{1.39}{1.82 - 0.27\ln(100B_T)}, \quad T \ge T_{vd} \tag{7.4}$$

where B_T is the effective damping, expressed as a decimal (not a percentage). Note that when $B_T = 0.05$, (5% damping) then $R_a = R_v = R_d = 1$.

In the code the flag `damp_flags(1)=1` can be used to set $R_d = R_v$, (HAZUS doesn't use R_d), or `damp_flags(1)=2` sets R_a and R_d to R_v. This might be used used if there are problems with convergence. The default value `damp_flags(1)=0` uses all 3 factors.

The transition building periods (corner periods), T_{av} and T_{vd}, are given (according to HAZUS) as

$$T_{av} = \frac{S_a(T_o = 1.0)}{S_a(T_o = 0.3)}, \qquad T_{vd} = 10^{(r_m - 5)/2} \tag{7.5}$$

where r_m is the moment magnitude. These are called corner periods because, in an 'ideal' tripartite plot (i.e. S_v vs building period, in log-log space), these periods correspond to corners (Newmark and Hall, 1982).

HAZUS also modifies T_{av} to $T_{av\beta}$ where

$$T_{av\beta} = \frac{R_a}{R_v} T_{av}.$$

It is not clear to the authors why this is needed. According to discussions with Mark Edwards (*pers. comm.*, 2002) it is needed to account for the damping that has already occurred. However, since the damping ratios are applied to the original 5% spectra, at each stage of the iteration, it should not be needed.

In the code, the flag `damp_flags(2)=0` (default value) is used to modify T_{av} to $T_{av\beta}$, at each iteration, whereas `damp_flags(2)=1` does not do the modification. The corner periods are calculated in the file `calc_corner_periods`.

Note that the formulae for the corner periods are chosen (by HAZUS) to be consistent with the artificial standardised demand curve that HAZUS uses. Therefore they are not necessarily appropriate for response curves that are computed from attenuation formulae. It is believed that they will be a reasonable approximation. However, because our response spectra are not consistent with the corner periods there may be some problems with discontinuities leading to convergence problems with the iterative approach used to deal with inelastic behavior (see Section 7.2.2). To try and minimise this a small amount of smoothing of the demand curve is applied near the corner periods.

For future work, it may be worth investigating using damping formula which vary continuously as a function of period. Also, in Newmark and Hall (1982) formula are given for a variability component of the damping. A random damping factor has not yet been implemented. It would not be difficult, but it first needs to be determined whether it is already taken into account by the random capacity curves.

Tables of the elastic damping parameter values, for different building construction types, are given in the Appendix A.9; Table A.3.

Hysteretic damping

When the intersection point occurs in the inelastic region the damping applied to the response spectral acceleration also has an additional component due to hysteresis. This hysteretic damping accounts for the fact that the buildings ability to absorb energy changes after it has been pushed into the inelastic region. The effective damping term B_T has an elastic component B_E and a component due to hysteretic damping B_H . This latter component is zero when the intersection point is in the elastic region. The hysteretic damping term is determined from the area enclosed by the hysteresis curve A_H, as shown in Figure 7.5. The effective damping is given by

$$B_T = B_E + B_H, \tag{7.6}$$

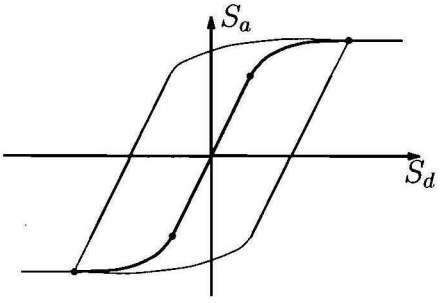

Figure 7.5: Hysteresis area.

where

$$B_H = \frac{A_H}{2\pi DA} \tag{7.7}$$

and B_E is defined by the process described in Section 7.2.2.

Recall that the curved part of the hysteresis boundary is approximated by

$$y = ae^{-bx} + c,$$

where

$$c = A_u, \qquad b = \frac{k}{A_u - A_y}, \qquad a = (A_y - A_u)e^{bD_y},$$

and the slope of the elastic part is,

$$k = \frac{A_y}{D_y}.$$

The area is calculated by subdividing into three separate areas (see Figure 7.6)

$$A_H = 2(A_1 - A_2 + A_3).$$

We also define the coordinates (see Figure 7.7)

$$x_2 = D - \frac{A}{k}, \qquad x_1 = 2x_2 + \frac{y_1}{k}, \qquad y_1 = A_u - A_y.$$

The sub-areas are calculated as

$$A_1 = cx_1 + \frac{a}{b}(1 - e^{-bx_1})$$
$$A_2 = \frac{y_1^2}{2k}$$
$$A_3 = 2A_y(D - D_y).$$

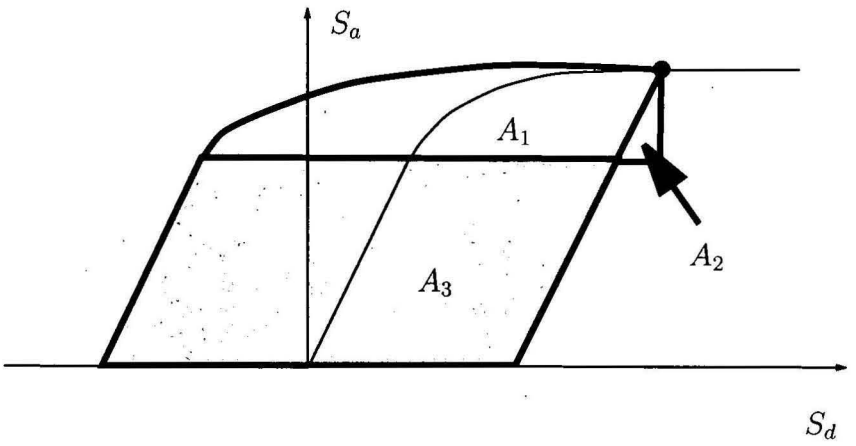

Figure 7.6: Diagram showing the sub-areas used for the hysteresis area calculation.

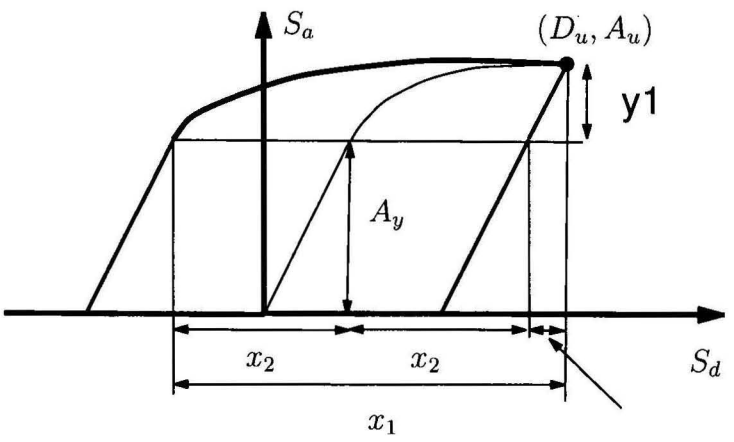

Figure 7.7: Coordinates used for hysteresis area calculation.

The calculation of the hysteretic area is implemented in the MATLAB function `hyst_area_rand`. Note that this function has arguments to deal with a randomly sampled capacity curve. Currently the code calculates hysteretic damping for all events including those in the elastic region (where the hysteretic damping is zero), because the calculations are vectorised. Furthermore the code iterates until the most nonlinear event has converged or the maximum iteration limit is reached. Some efficiencies might be gained by first filtering out those events in the elastic region, and then later filtering out those events which have converged.

Tables of the hysteretic damping coefficients κ_L, κ_M and κ_L are given in Ap-

pendix A.9. Table A.3 provides the hysteretic damping coefficients κ_L, κ_M and κ_L corresponding to parameters used in the Newcastle and Lake Macquarie study (Fulford *et al.*, 2002).

7.2.3 Finding the intersection point

The algorithm used to find the intersection point of the suitably damped demand curve with the building capacity curve is quite simple. However, it is vectorised over all the synthetic earthquakes. The intersection point is generally not found exactly, rather it is approximated.

The algorithm can be summarised, as follows:

1. Locate points on demand curve and building capacity curve which bound the intersection point, as shown in Figure 7.8.
2. Use linear interpolation to find a first approximation to the intersection point.
3. Use a vertical step to force the intersection to lie on the building capacity curve.

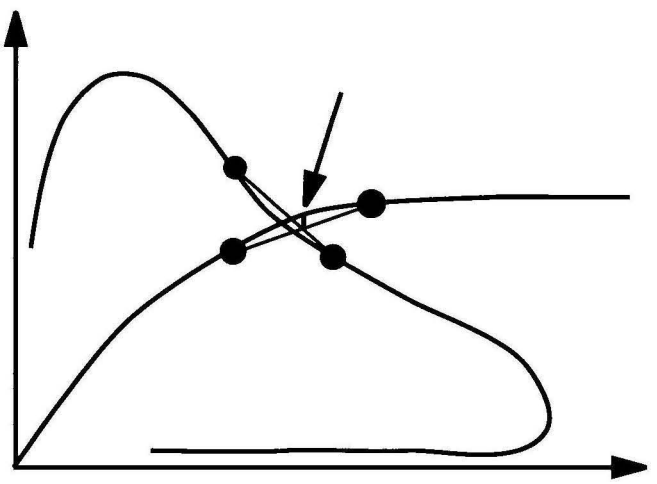

Figure 7.8: Illustration of the algorithm used to approximate the intersection point of the demand SA curve and the building capacity curve.

It is important that the approximation to the intersection point lies on the building capacity curve for the calculation of of the hysteretic area.

Further refinements could be made to improve the accuracy of the location of the intersection point. These might involve iterative procedures which use the tangent of the capacity curve intersecting the line between the two points on the demand curve, to iteratively spiral into the true intersection point. However, a more sophisticated scheme, such as this, may be difficult to code since it would have to account for all possible variations in the form of the demand curve (after soil amplification and damping) and might not always converge. Therefore further refinements are probably not warranted since the current scheme appears to be sufficiently accurate.

7.3 Fragility curves

Fragility curves give the cumulative probability of a particular building being in or exceeding a given damage state given a seismic demand parameter, such as building peak displacement or acceleration. There are separate fragility curves for each of the 4 cumulative damage states: Slight, Moderate, Extensive and Complete and the 3 types of damage: (a) Structural Damage (based on peak displacement), (b) Non-structural damage-drift sensitive (also based on peak displacement) and (c) Non-structural damage-acceleration sensitive (based on peak acceleration).

FEMA (1999, page 5-12, Table 5.2) provides a table showing typical non-structural components of buildings as drift sensitive or acceleration sensitive. FEMA (1999, page 5-13 to 5-23) also provide qualitative descriptions of what the damage states for structural and non-structural damage correspond to. For example *slight structural damage* for wood framed construction corresponds to small cracks in door and window openings and *complete structural damage* corresponds to an immediate danger of structure collapse.

In FEMA (1999, pages 5-19) it is stated that non-structural (acceleration sensitive) damage to components at or near ground level may be better characterised by peak ground acceleration (PGA) rather than peak spectral acceleration S_a^*. To this end, HAZUS suggests a combined use of PGA and S_a^* to model damage for near ground components. Currently the EQRM considers only S_a^* when computing damage, however the HAZUS suggestion could easily be incorporated into future version of the EQRM.

7.3.1 Form of fragility curves

Each fragility curve is determined by two parameters: the threshold value of displacement (or acceleration) and a variability parameter. The form of the fragility curve is a cumulative log-normal distribution,

$$F(s_{dam} \| \bar{S}^*, \epsilon) = \ln \left[\Phi \left(\frac{S^*}{\bar{S}^*}; \epsilon \right) \right] \tag{7.8}$$

where s_{dam} refers to the damage state of interest, Φ is the standard cumulative normal distribution function,

$$\Phi(x) = \frac{1}{\sqrt{2\pi}} \int_{-\infty}^{x} e^{-t^2} \, dt,$$

S^* denotes either peak spectral displacement, S_d^* or peak spectral acceleration, S_a^*, $\bar{S}^*$ is the median damage state threshold value of S^* and ϵ is a variability parameter.

The value ϵ represents the uncertainty of the damage state. It is the square root of the variance of the logarithm of the data (i.e. the log-standard deviation). A zero value for ϵ means the the curve approximates a step function, and so below the threshold value the building is not in the given damage state and above the threshold it is definitely in the damage state. The larger the value of ϵ the more spread out the curve is, reflecting our less certain knowledge of what state the building is in (Figure 7.3.1).

7.3.2 Damage state thresholds

The damage state thresholds are the median values that determine the damage states.

For structural damage and non-structural drift-sensitive damage the damage state thresholds are determined from provided drift ratios for each building construction type. For non-structural acceleration-sensitive damage the damage state thresholds are obtained from specified acceleration thresholds. These are tabulated for different versions of the engineering parameters in `buildfacts-<version>.xls`, in directory `*/datacvt/buildpars`. For example

$$S_T = \alpha_2 h \delta \tag{7.9}$$

is used to compute the median damage state threshold for structural damage, where δ is the drift ratio, h is the provided height of the building for the given

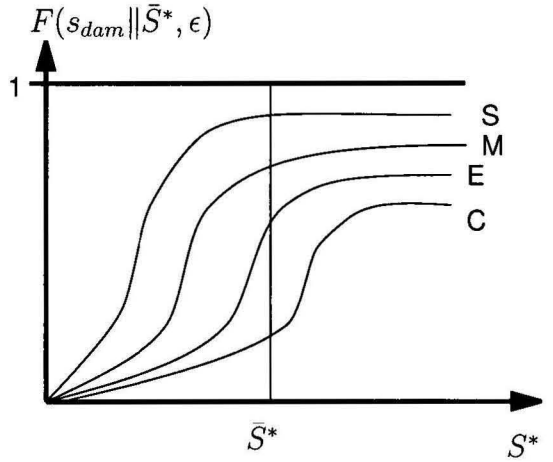

Figure 7.9: A typical fragility curve, giving the cumulative probability of being in or exceeding a certain damage state as a function of the peak displacement (or acceleration).

building construction type and α_2 is a building construction parameter corresponding to the fraction of the building height (roof) at the location of push-over mode displacement. The parameters α_2 and h are given in Table A.1. Note that h is given in feet, however, in the code this is converted into mm (since S_d is considered throughout the code in mm). Tables of drift ratios, and acceleration values, for different sets of building parameters are given in the Appendix A.9.

7.3.3 Variability of the damage states

The uncertainty of a building being in a given damage state for a given peak displacement, is characterised by the variability parameter ϵ in equation Equation 7.8. As this uncertainty becomes smaller, the fragility curve steepens and becomes more like a step function, as shown in Figure 7.10.

We follow FEMA (1999) in setting

- for structural damage $\epsilon = 0.4$,
- for non-structural, drift sensitive damage $\epsilon = 0.5$,
- for non-structural, acceleration sensitive damage, $\epsilon = 0.6$.

Note that HAZUS does not give any references to the derivation of these values.

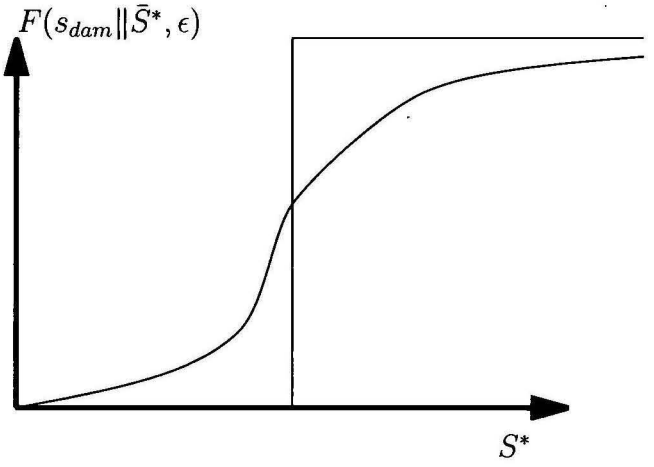

Figure 7.10: As the variability of a fragility curve is reduced the fragility curve steepens and becomes more like a step function.

7.3.4 Incremental probabilities

The fragility curves give the probability of being in the given damage state or lower. That is, they are cumulative probabilities. For our Monte Carlo simulation approach we need the incremental probabilities of the building being in the given damage state. For example, suppose we have the fragility curve for the extensive damage state, $\Pr(d \leq E)$. To find $\Pr(d = E)$, we calculate

$$\Pr(d = E) = \Pr(d \leq E) - \Pr(d \leq M).$$

This is illustrated in Figure 7.11.

7.4 Differences from HAZUS methodology

A key difference in our implementation of the Capacity Spectrum Method to that used by HAZUS is using the full response spectrum for intersecting with the building capacity curve rather than a design spectra based on only a few building periods. For example, the HAZUS approach only uses periods 0.3 and 1.0 seconds. Our approach has the advantage that the full structure of the response spectrum and all the available information for the soils amplification factors, at all periods, is taken into account rather than at only two periods (Chapters 5 and 6). There are also some minor differences in the way that demand curve damping is applied.

Another difference is in how the fragility curves are used. In HAZUS, the fragility curves incorporate not only the variability of the damage state thresholds, but

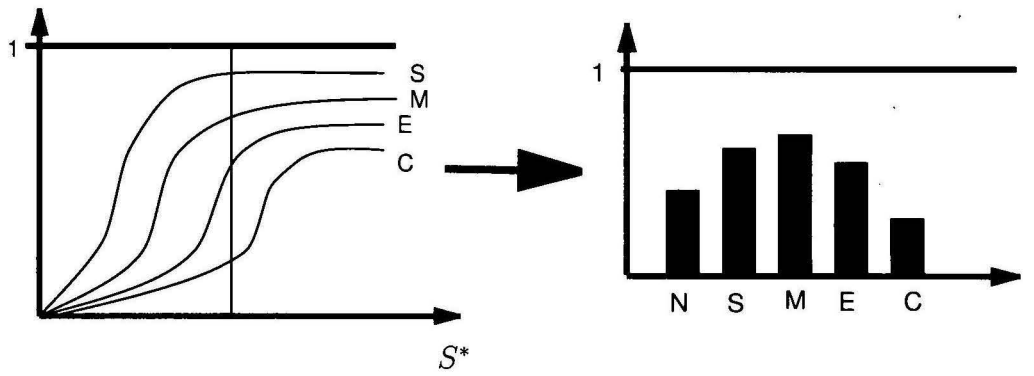

Figure 7.11: Converting the cumulative probabilities in the fragility curves to incremental probabilities describing the probability that the building component is in a given damage state.

also the variability of the capacity curve and the ground-shaking. A 'convolution procedure', as described in Kircher *et al.* (1997), is used to convolve the various log-normal probability distributions for ground-shaking and building capacity curve by calculating intersection points for a range of randomly selected demand and capacity curves, then fitting a log-normal distribution. In the EQRM the fragility curves includes only the variability for being in the given damage state and not the variability associated with ground shaking or building type. The variability associated with the fragility curve is defined by a cumulative log-normal distribution with variability parameters 0.4, 0.5 and 0.6 for structural damage, non-structural damage (drift sensitive) and non-structural damage (acceleration sensitive), respectively. The variability associated with ground shaking (Sections 5.3 and 6.4) and building type (Section 7.2.1) are incorporated elsewhere in the Monte-Carlo simulation.

7.4.1 Extra features

The risk component of the EQRM also has a number of extra features or alternative operation modes that are not offered by the HAZUS methodology. Two of the more significant extra features are:

1. The use of **uniform hazard spectra** instead of demand curves. This effectively drives the risk calculation by hazard values rather than individual earthquakes. The process is discussed further in Patchett *et al.* (2005). The EQRM can be used in this fashion by setting the `setdata` parameter `run_type` to 3.

2. The use of **Modified Mercali Intensity (MMI) damage curves** rather than the capacity spectrum method. When the user selects $100 \leq$ `attenuation_flag` ≤ 199 the EQRM will use an MMI attenuation model (currently only Gaull is coded) and will compute risk using in-built damage curves that relate percentage damage to MMI. Note that the damage curves are exponential in shape and that the percentage damage estimates represent damage to the entire structure rather than components of the structure. Edwards *et al.* (2004) provide an example of the use of damage curves with the EQRM.

7.5 Key functions, flags and parameters

Name	Type	Description
*/datacvt/buildpars	Dir	Directory containing tools to assist the preparation of engineering parameters.
do_analysis	Function	Higher order function of EQRM responsible for computing hazard and/or risk.
prep_locations	Function	Loads and prepares earthquake hazard grids and building databases.
prep_build_vuln	Function	Loads and prepares engineering and financial loss parameters.
do_build_vuln	Function	Models building damage, financial loss and social loss.
make_build_dam_rand	Function	Models building damage.
build_cap_rand	Function	Calculates building capacity curve as a function of spectral displacement S_d.
make_fragility	Function	Calculates the fragility curve and outputs probabilities of being in various damage states.
calc_corner_periods	Function	Calculates the corner periods of the demand curve.
cvt_bfactors	Function	Converts Excel building paramter files to required *.MAT format.
hyst_area_rand	Function	Incorporates hysteretic damping (called by nonlin_damp_rand).
buildfacts _<version>.mat	Par File	Excel version of engineering parameters used by EQRM (e.g. buildfactors.xls or buildfactors-wshop.xls). Note that these Excel files are converted to the EQRM required *.MAT files using cvt_bfactors.
run_type	Par	Defines the operation mode of the EQRM (Section 2.2.1).
damp_flags	Par	Vector to control nature of linear damping (Section 2.2.1).
qa_switch_vun	Par	Controls diagnostics for capacity spectrum method (Section 2.2.1).

Chapter 8

Losses

8.1 Overview

The EQRM considers two types of loss:

1. **direct financial loss** defined as the cost involved in replacing damaged building components and/or contents; and
2. **social loss** defined as the number (or probability) of casualties and injuries as a result of a simulated scenario.

This chapter describes the direct financial and social loss modules.

8.2 Direct financial loss

8.2.1 General financial loss equations: loss for a single building

Recall that the capacity spectrum method assumes that each building comprises three main components, namely a structural, non-structural drift sensitive and non-structural acceleration sensitive component. Section 7 described how the damage experienced by each building is computed separately for each of the components. It is therefore necessary to partition the replacement cost of the building

Table 8.1: Examples of costing splits for the FCB and HAZUS usage classification.

FCB Usage Classification	
111 - W1BVTILE:	
structural	23.44%
non-structural drift sensitive	50.00%
non-structural acceleration sensitive	26.56%
491 - C1MSOFT:	
structural	15.32%
non-structural drift sensitive	34.23%
non-structural acceleration sensitive	50.45%
HAZUS Usage Classification	
RES1 - W1BVTILE:	
structural	23.44%
non-structural drift sensitive	50.00%
non-structural acceleration sensitive	26.56%
COM5 - URMLMETAL:	
structural	13.79%
non-structural drift sensitive	34.48%
non-structural acceleration sensitive	51.72%

into the replacement cost for each of the three components. The proportion chosen for each building component is a function of the buildings construction and usage type as well as the usage classification system. For example Table 8.1 illustrates the proportion of the replacement value corresponding to a couple of different buildings for both the HAZUS and FCB classification system. The `setdata` flag `b_usage_type_flag` can be used to select the usage classification system and consequently the desired cost proportions.

Let $P_{i\alpha}$ denote the probability of being in a damage state $\alpha = (1, 2, 3, 4) = (S, M, E, C)$ corresponding to Slight, Moderate, Extensive and Complete damage, where the index $i = (1, 2, 3) = (s, n_d, n_a)$ corresponds to the type of damage: drift sensitive structural damage (s), drift sensitive non-structural damage (n_d) and acceleration sensitive non-structural damage (n_a). Contents damage is factored in later.

We also define L_i as the financial loss corresponding to the 3 building components

(structural damage, $i = s = 1$; drift-sensitive non-structural damage, $i = n_d = 2$; acceleration-sensitive non-structural damage $i = n_a = 3$; and L_4 as the financial loss due to damage of contents.

Let R_i denote the replacement cost component of the building per unit floor area, for $i = (1, 2, 3) = (s, n_d, n_a)$. Thus $R = R_1 + R_2 + R_3$ is the total replacement cost (per unit floor area) of the building (excluding contents). The financial loss, for a single building, excluding contents, is then given as the weighted sums of the probabilities

$$L_1 = C_0 \sum_{\alpha=1}^{4} f_{\alpha,1} R_1 A P_{\alpha,1} = \sum_{\alpha=1}^{4} f_{\alpha,1} g_1 R A P_{\alpha,1},$$
$$L_2 = C_0 \sum_{\alpha=1}^{4} f_{\alpha,2} R_2 A P_{\alpha,2} = \sum_{\alpha=1}^{4} f_{\alpha,2} g_2 R A P_{\alpha,2}, \text{and}$$
$$L_3 = C_0 \sum_{\alpha=1}^{4} f_{\alpha,3} R_3 A P_{\alpha,3} = \sum_{\alpha=1}^{4} f_{\alpha,3} g_3 R A P_{\alpha,3},$$

where A is the floor area of the building (in m^2). Note that R is the replacement cost of the building, $f_{\alpha,i}$ is a repair cost fraction of replacement cost for the given damage state, g_i is the damage component replacement value as a fraction of the replacement value, and C_0 is a regional cost factor. The total loss of the building, excluding contents, is $L = L_1 + L_2 + L_3$.

Note that for percentage loss (loss divided by the value of the building) the quantity $c_0 R$ cancels.

For example, the total repair cost for a building (excluding contents) in damage state $\alpha = 3 = E$ is $f_{3,1} R_1 + f_{3,2} R_2 + f_{3,3} R_3$. The probabilities $P_{\alpha,i}$ correspond to the probability of the building component $i = (s, n_d, n_a)$ being in damage state $\alpha = (S, M, E, C)$.

The regional cost factor, C_0, is a normalising factor to calibrate the replacement costs if necessary. For example in the Newcastle risk assessment (Fulford *et al.*, 2002) the HAZUS cost values were used (see Table 8.2) and converted to the Newcastle region using $C_0 = 1.4516$. In this particular case the C_0 was computed by assuming that a $100\,\mathrm{m}^2$ brick veneer residential house (RES1, W1BVTILE) had a replacement cost of AUS$1,000 per m^2 (this value of $1000 having been obtained from NRMA web site for the NSW region). In other studies, such as the Perth Cities case study, the replacement costs (see Table 4.1) were defined for the region and no further correction was required. Note that the parameter C_0 is `ci` in the `setdata` file.

The repair cost factors $f_{\alpha,i}$ are the proportions of the replacement costs (for each building component $i = (1, 2, 3) = (s, n_d, n_a)$ per floor area. For structural damage,

$$f_{\alpha,1} = (2\%, 10\%, 50\%, 100\%), \tag{8.1}$$

for non-structural damage (drift-sensitive),

$$f_{\alpha,2} = (2\%, 10\%, 50\%, 100\%), \tag{8.2}$$

and for non-structural damage (acceleration-sensitive)

$$f_{\alpha,3} = (2\%, 10\%, 30\%, 100\%), \tag{8.3}$$

These values are taken from FEMA (1999). For example, the repair cost for the acceleration-sensitive components in the extensive damage state are given by the product $f_{33}R_3$, so that if the replacement cost for complete damage is \$500 per square metre, the repair cost would be $30/100 \times$ \$500.

The directory `*/eqrm/datacvt/econsoclosspars` contains tools to assist the preparation of direct financial loss parameters. The files `RcPerWrtBuildCFCB-usageEdwards.xls` and `RcPerWrtBuildCHazususageEdwards.xls` contain the replacement cost component of the building per unit floor area R_i for the FCB and HAZUS usage types respectively. The MATLAB function `per_replace-_cost_wrt_bc_usage` converts these excel files to `*.MAT` that can be used by the EQRM. The EQRM assumes the replacement cost components to be independent of the construction type. There are a few exceptions, which have not been implemented. These are based on the tables given in FEMA (1999), in particular, Table 25.2a (page 15-12), Table 13.3 (page 15-14) and Table 15.4 (page 15-15). In principle the tools in `*/eqrm/datacvt/econsoclosspars` allow the replacement cost components to be a function of both usage and construction type. Note that `per_replace_cost_wrt_bc_usage` attributes proportions of the building's total value to its different components. Recall form Table 4.1 that the replacement costs for each building is stored with the building database.

The contents damage, L_4, is based only on the probabilities for acceleration sensitive non-structural damage being in Slight, Moderate, Extensive or Complete states, and on the total contents repair costs R_4 defined by the building database (see Table 4.1). The cost L_4 is then added to the building damage cost L to get the overall loss L^* which includes contents.

As with the building components, the loss for contents damage, is expressed as a weighted sum of probabilities of the acceleration sensitive components for each damage state,

$$L_4 = C_0 \sum_{\alpha=1}^{4} f_{\alpha,4} R_4 P_{\alpha 3}, \tag{8.4}$$

where $P_{\alpha 3}$ is the probability of the acceleration sensitive component of the building being in damage state $\alpha = (1, 2, 3, 4) = (S, M, E, C)$ and $f_{\alpha,4}$ is the repair cost fraction of the replacement value for the contents in damage state $\alpha = (S, M, E, C)$. This factor is expressed as a percentage in Table 8.2 and has been taken from FEMA (1999, Table 15.6, page 15-21). Furthermore, for contents damage,

$$f_{\alpha 4} = (1\%, 5\%, 25\%, 50\%). \tag{8.5}$$

These values assume that 50% of the contents in complete damage can be salvaged with similar proportions for lesser damage (FEMA, 1999). If the `setdata` parameter `aus_contents_flag` is set to 1 the following modifications are made as to suggested by George Walker (Aon Re):

1. HAZUS usage only: The contents value of usage types 1 to 10, 24 and 29 (see Table 4.5) are re-assigned to 60% of R_4.
2. $f_{\alpha 4}$ is re-assigned to $(2\%, 10\%, 50\%, 100\%)$ which assumes that no contents will be salvaged from complete damage of Australian buildings.

8.2.2 Aggregated loss and survey factors

Each building in the database represents a sample from its surrounding area. There is a building survey factor associated with each building, which represents the additional number of buildings that are represented by the modelled building (see Table 4.1). Typically the extra buildings are of the same type and are located in close proximity to the modelled building.

The aggregated loss is therefore the weighted sum of the losses of each building in the database with its corresponding survey factor.

The aggregated financial loss values are saved to a file of form `<site_loc>-_db_savedecloss.mat`. If the `setdata` parameter `save_ecloss_flag` = 1 a combined loss for the building and contents is saved; whereas if `save_ecloss_flag` = 2 the losses for the building and contents are saved separately.

8.2.3 Cutoff values

The damage and financial loss models estimate small (but finite) damage for very small ground accelerations. This arises due to the asymptotic nature of the fragility curves. A cutoff value has been implemented in the code to prevent such

small values being calculated. The cutoff is in terms of PGA and is controlled by the `setdata` parameter `pga_mindamage`. For all those events having peak ground acceleration (pga) values smaller than `pga_mindamage` at the building location, the financial loss is set to zero. Typically it is assumed that no damage worth reporting occurs for ground accelerations smaller than `pga_mindamage` $= 0.05g$.

8.3 Social losses

The EQRM includes a module for computing the injuries and casualties associated with a scenario simulation (see Section 3.5). The code for considering social losses associated with probabilistic simulations has not yet been written. The social loss module is activated by setting the `setdata` parameter `save_socloss_flag` to 1. When activated, the social loss module produces a file `<site_loc>_db_savedsocloss.mat` that can be processed by the MATLAB script `newc89plothistsoc`.

For the Newcastle 1989 simulation the results are slightly greater than those observed in the actual earthquake (e.g. median of 45 casualties vs 13 casualties actually recorded). Further investigation of the model is recommended before it is widely used. Firstly, a check on the accuracy of the distribution of the population would be useful. Secondly, some thought should be given to a model which distributes the population randomly. It is expected that this will result in a greater spread of the distribution of injuries.

Chapter 13 of FEMA (1999) provides a detailed description of the methodology behind social loss calculations.

8.4 Key functions, flags and parameters

Name	Type	Description
*/eqrm/datacvt /econsoclosspars	Dir	Tools to assist the preparation of direct financial loss parameters.
per_replace_cost _wrt_bc_usage	Function	Converts the RcPerWrtBuildCFCB-usageEdwards.xls and RcPerWrt-BuildCHazususageEdwards.xls to the required format for the EQRM.
socloss	Function	Function for calculating injury probabilities.
newc89plothistsoc	Script	MATLAB script to plot injury probabilities (for Newcastle scenario only).
RcPerWrtBuildCFCB usageEdwards.xls	Par File	Replacement cost component of the building per unit floor area for the HAZUS usage classification.
RcPerWrtBuildCHazus usageEdwards.xls	Par File	Replacement cost component of the building per unit floor area for the FCB usage classification.
ci	Par	Regional cost index multiplier.
aus_contents_flag	Par	Contents value for residential buildings and salvageability after complete building damage.
pga_mindamage	Par	minimum PGA(g) below which financial loss is assigned to zero.
save_ecloss_flag	Par	Options for saving direct financial loss data.
save_socloss_flag	Par	Options for saving casualty and injury data.
<site_loc>_db _savedecloss.mat	Output	Output file containing the loss estimates for an EQRM risk simulation.

Table 8.2: Calculated replacement costs (AUD m^2) of building usage types.

	Structural	NS-drift	NS-accel	Contents %	ex-contents	total
RES1	234	500	266	50	1000	1500
RES2	172	266	266	50	703	1055
RES3	172	531	547	50	1250	1875
RES4	172	547	547	50	1266	1898
RES5	234	500	516	50	1250	1875
RES6	219	484	484	50	1187	1781
COM1	234	219	344	100	797	1594
COM2	172	141	219	100	531	1062
COM3	172	359	531	100	1062	2125
COM4	219	375	547	100	1141	2281
COM5	250	625	937	100	1812	3625
COM6	266	656	969	150	1891	4727
COM7	203	484	719	150	1406	3516
COM8	156	562	859	100	1578	3156
COM9	141	406	609	100	1156	2312
COM10	219	62	78	50	359	539
IND1	125	94	578	150	797	1992
IND2	125	94	578	150	797	1992
IND3	125	94	578	150	797	1992
IND4	125	94	578	150	797	1992
IND5	125	94	578	150	797	1992
IND6	125	94	578	100	797	1594
AGR	94	16	94	100	203	406
REL	266	437	641	100	1344	2687
GOV1	187	344	516	100	1047	2094
GOV2	266	594	875	150	1734	4336
ED1	219	562	375	100	1156	2312
ED2	172	937	453	150	1562	3906
RES1-T	199	425	226	50	850	1275
RES1-DB	258	550	292	50	1100	1650

Chapter 9

Hazard and risk results

9.1 Overview

Earlier chapters have described how to generate synthetic earthquakes, propagate (or attenuate) the response spectral acceleration and compute loss. This chapter describes how to 'aggregate' the above information to estimate earthquake hazard and earthquake risk. A number of diagrams are used to demonstrate the common techniques for visualising earthquake hazard and risk.

9.2 Calculating hazard and risk

Consider a random variable Y such that;

- Y refers to the response spectral acceleration S_a at a particular site in the case of hazard, or
- Y indicates the loss, either at a particular simplicity we will assume that Y represents the aggregated loss as a percentage of building stock value.

A common way to represent Y is in terms of a probability of exceedance in one one year. To achieve this we assume that earthquakes occur as a Poisson process (McGuire and Arabasz, 1990). This means that the earthquake process has no memory; or in other words, the probability of an earthquake today does not

depend on whether or not an earthquake occurred yesterday. Mathematically, this assumption can be represented as follows:

$$\Pr(T, Y \geq y) = 1 - e^{\lambda_Y(y)t}, \tag{9.1}$$

where t is a time interval in years (typically 1 year) and $\lambda_Y(y)$ is the annual exceedance rate. The return period is given by Equation 9.2:

$$R_Y(y) = \frac{1}{\lambda_Y(y)}. \tag{9.2}$$

9.2.1 Computing the annual exceedance rate

Chapter 3 described the Monte-Carlo approach used to generate earthquakes. Chapters 5 to 8 describe how to compute an S_a or loss value for each of the synthetic events. It follows, therefore that there exists a set of N_s numbers $\{Y_i\}_{i=1}^{N_s}$ with corresponding event activities $\{r_{\nu_i}\}_{i=1}^{N_s}$ (see Section 3.2.5), where N_s is the number of simulated events.

The annual exceedance rate $\lambda_Y(y)$ is computed from the event activity through the following process:

1. re-order the values $\{Y_i\}_{i=1}^{n}$ from largest to smallest and re-order the corresponding event activities such that the $Y_i - r_{\nu_i}$ pairs are not separated.

$$\begin{bmatrix} y_1 \\ y_2 \\ \vdots \\ y_n \end{bmatrix}, \begin{bmatrix} r_{\nu_1} \\ r_{\nu_2} \\ \vdots \\ r_{\nu_n} \end{bmatrix} \rightarrow \begin{bmatrix} y_{1^*} \\ y_{2^*} \\ \vdots \\ y_{n^*} \end{bmatrix}, \begin{bmatrix} r_{\nu_1^*} \\ r_{\nu_2^*} \\ \vdots \\ r_{\nu_n^*} \end{bmatrix} \tag{9.3}$$

2. evaluate $\lambda_Y(y)$ by computing the cumulative sum of event activities.

$$\begin{bmatrix} \lambda_{Y_{1^*}} \\ \lambda_{Y_{2^*}} \\ \vdots \\ \lambda_{Y_{n^*}} \end{bmatrix} = \begin{bmatrix} r_{\nu_1^*} \\ r_{\nu_1^*} + r_{\nu_2^*} \\ \vdots \\ r_{\nu_1^*} + r_{\nu_2^*} + \ldots + r_{\nu_n^*} \end{bmatrix}, \tag{9.4}$$

The asterisk in Equations 9.3 and 9.4 refer to re-ordered values.

9.3 Earthquake hazard results

The EQRM estimates the earthquake hazard $E_H(R_Y)$ at the return periods R_Y defined in the `setdata` vector `rtrn_per` by interpolating the values $\{\lambda_{Y_i^*}\}_{i=1}^{N_s}$ and $\{Y_i^*\}_{i=1}^{N_s}$ to the values $1/R_Y$ (see Equation 9.2). In the case of earthquake hazard the random variable Y refers to the response spectral acceleration and is therefore a function of building period T_o. The earthquake hazard information is saved in the output file `<site_loc>_db_hzd.mat`. It is important to emphasise that only the hazard information is saved, the information for individual synthetic earthquakes is discarded. This means that the earthquake hazard information can not be de-aggregated in terms of causative events.

The EQRM offers three tools for visualising the earthquake hazard:

1. the earthquake hazard map,
2. the hazard exceedance curve, and
3. the uniform hazard spectra.

9.3.1 Hazard maps

Earthquake hazard maps can be used to illustrate the earthquake hazard across a spatial region. The earthquake hazard $E_H(R_Y)$ is plotted for a specific building period T_o and return period R_Y. Figure 9.1 provides an example of a hazard map for the Newcastle and Lake Macquarie region.

It is necessary to draw a number of hazard maps corresponding to different T_o and R_Y in order to understand the hazard across a spatial region. Traditionally return periods considered for building design correspond to a 2% and/or 10% probability of exceedance within 50 years. An exceedance probability of 10% in 50 years equates to a return period of roughly 500 years and an exceedance probability of 2% in 50 years corresponds to roughly 2500 years.

The EQRM post processing tool `plot_hzd_map` can be used to generate hazard maps. The tool `create_gis_output` can be used to export the data in `<site_loc>_db_hzd.mat` to a convenient file for plotting in GIS.

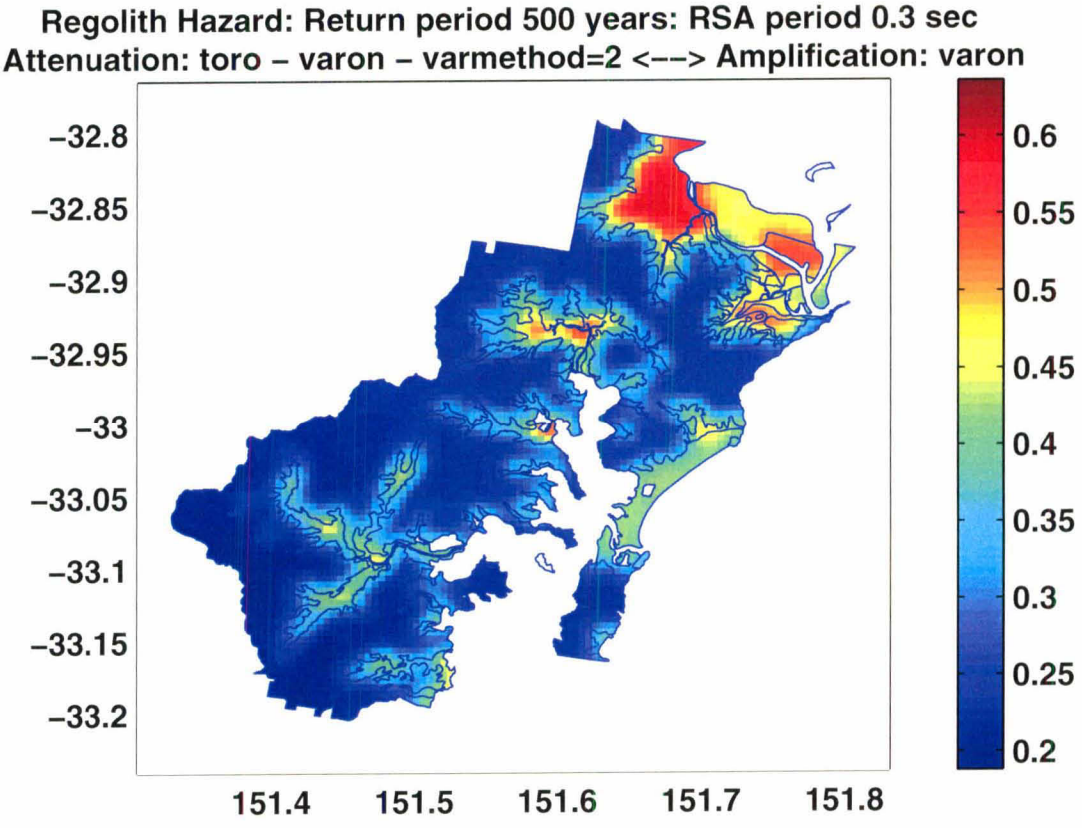

Figure 9.1: Newcastle and Lake Macquarie hazard map for return period of 500 years and S_a period of 0.3 seconds

9.3.2 Hazard exceedance curves

The exceedance probability curve for hazard (also known as the hazard exceedance curve or hazard curve) represents a technique for visualising the earthquake hazard at a single location. The hazard exceedance curve expresses $P(Y \geq y)$ at a single location as a function of the earthquake hazard ($Y = S_a$). Note that unlike the hazard map, the hazard exceedance curve presents the hazard corresponding to the 'full' range of probability levels (return periods). Figure 9.2 provides an example of a hazard exceedance curve for the Newcastle central business district. The EQRM post processing tool `plot_singlesite_hzd` can be used to generate hazard exceedance curves.

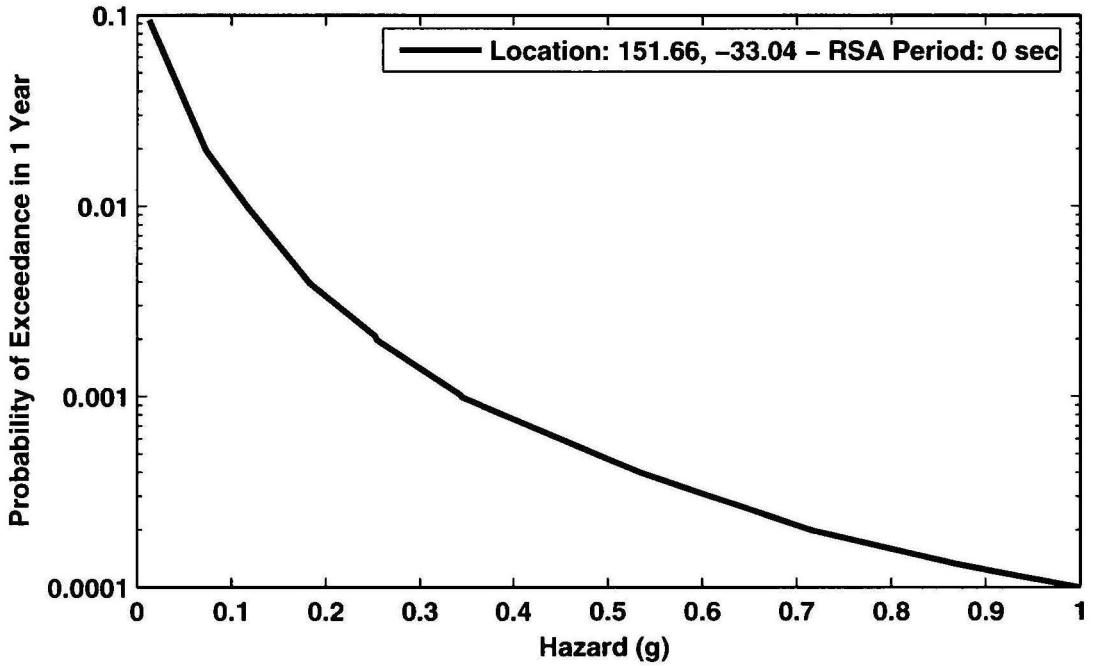

Figure 9.2: Peak ground acceleration hazard exceedance curve for the Newcastle central business district.

9.3.3 Uniform hazard spectra

The uniform hazard spectra represents another technique for visualising the earthquake hazard at a single location. The hazard for a specified probability level (return period) is plotted for all S_a periods. Figure 9.3 provides an example of an uniform hazard spectra for the Newcastle central business district. The EQRM post processing tool `plot_singlesite_hzd` can also be used to generate uniform hazard spectra.

9.4 Earthquake risk results

The EQRM returns the loss for each earthquake-building pair. This information is saved in the file `<site_loc>_db_savedecloss.mat` along with other information such as building values, the event activity for each synthetic earthquake and the distance between the building-earthquake pair. It is important to note that this technique for data storage is fundamentally different to the technique used for storing the earthquake hazard outputs. Recall that the earthquake hazard outputs store only the earthquake hazard values and not the S_a at each site. Sav-

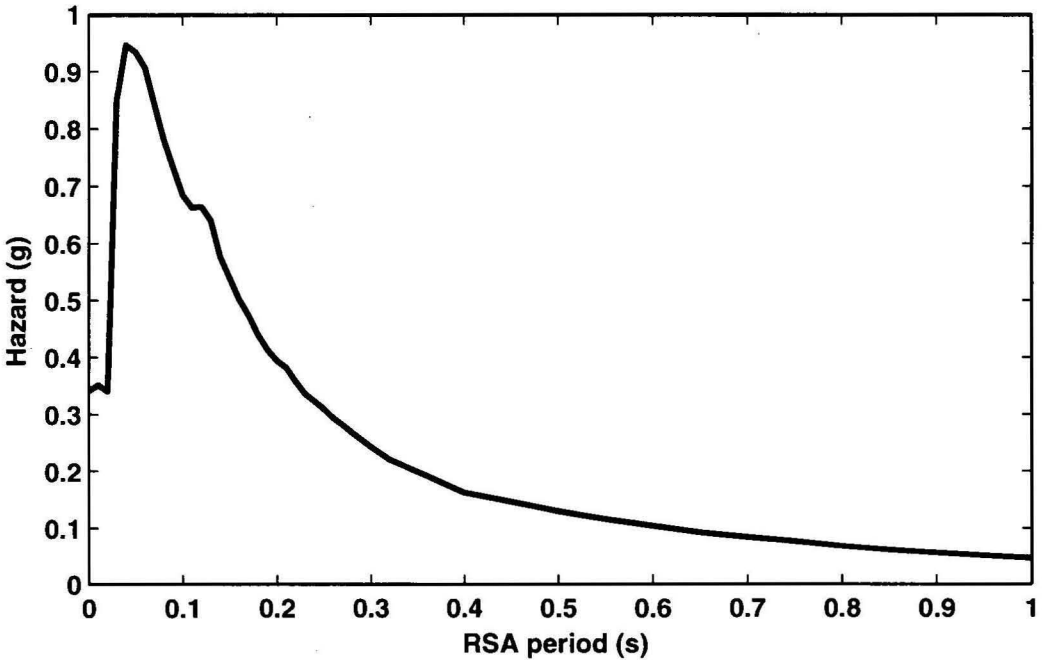

Figure 9.3: Uniform hazard spectra for return period of 500 years for a single site on regolith in the Newcastle region.

ing the information for each earthquake-building pair provides greater flexibility for risk visualisation and allows the de-aggregation of risk results into a variety of forms. As a result risk output files are typically much larger than hazard outputs and computer memory can become problematic. When the EQRM runs out of memory in a risk simulation the user needs to reduce the number of synthetic earthquakes and/or the number of buildings in the building catalogue. If reducing the number of earthquake-building pairs is not possible the EQRM can be run in a cut-down mode that saves risk results rather than earthquake-building pairs by assigning the `setdata` parameters `save_ecloss_flag` to 3.

The EQRM is equipped with tools for visualising earthquake risk in the following forms:

1. the risk exceedance curve (PML),
2. annualised loss, and
3. a variety of disaggregated annualised loss values.

The manner in which the `<site_loc>_db_savedecloss.mat` is processed will vary slightly depending on the plotting tool being used. However, all of the plotting

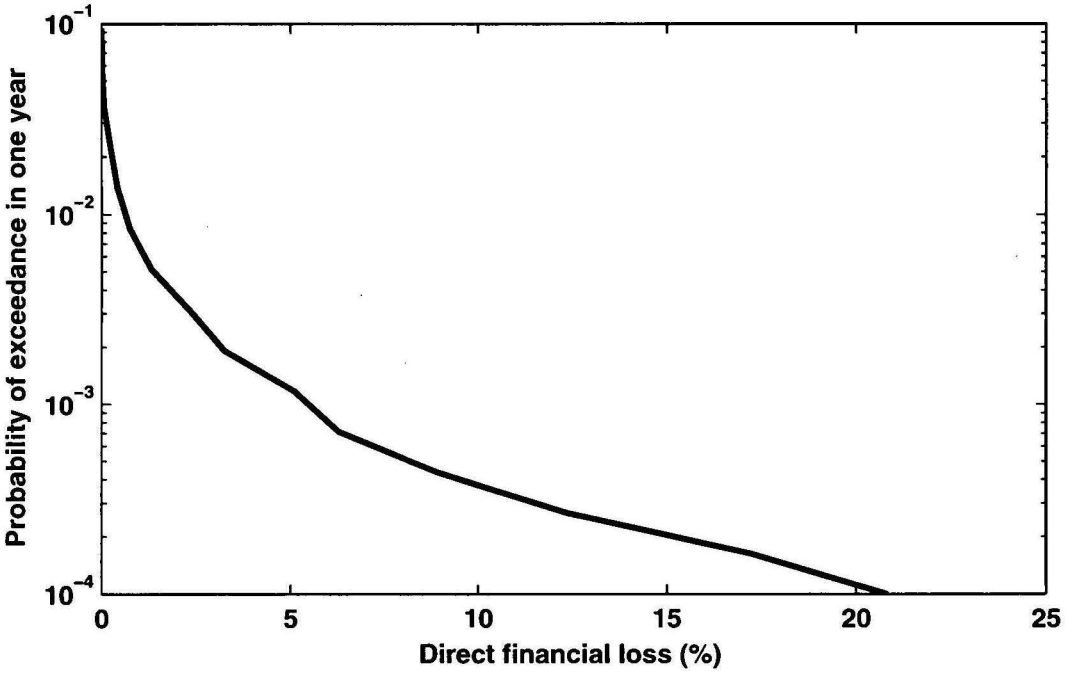

Figure 9.4: Risk exceedance curve for all the buildings in the Newcastle and Lake Macquarie portfolio.

tools make use of the basic process described by Equations 9.3 and 9.4 where the random variable Y describes the loss. A plot manager (or wrapper) `wrap_risk_plots` has been developed to manage the plotting of all risk results. Essentially `wrap_risk_plots` intelligently calls the individual plotting tools by reducing the repetition of common operations.

9.4.1 Risk exceedance curve

The exceedance probability curve for risk is analogous to the exceedance probability curve for hazard. The curve represents the maximum loss that is expected to be exceeded for given levels of probability. Unlike the hazard exceedance curve the risk exceedance curve need not be presented for a single site. It is more common to represent the percentage loss for an entire portfolio of buildings, however risk exceedance curves for single buildings can also be constructed. The risk exceedance curve expresses $P(Y \geq y)$ as a function of the earthquake risk $Y = E_L$, where E_L may be the percentage loss to the portfolio or the loss to a single building. Figure 9.4 provides an example of a risk exceedance curve for the Newcastle and Lake Macquarie portfolio. The EQRM post processing tool `wrap_risk_plots` can be used with the individual plotting tool `plot_pml` to plot

a risk exceedance curve.

9.4.2 Annualised loss

The annualised loss represents the loss per year averaged over all of the synthetic earthquakes. It can be computed by integrating underneath the risk exceedance curve. Since this is not necessarily intuitive the proof is given below.

Consider the risk exceedance curve as the probability of a loss being exceeded in a one year time frame $P(Y \geq y)$. Let $f_{E_L}(\ell)$ denote the PDF (probability density function) of the aggregate loss and $F_{E_L}(\ell)$ denote the CDF (cumulative distribution function). Let us define $F_{E_L}(\ell)$ as the CDF,

$$F_{E_L}(\ell) = \int_0^{\ell} f(x)\, dx.$$

and $G(\ell)$ as the exceedence probability function,

$$G_{E_L}(\ell) = 1 - F_{E_L}(\ell) = \int_{\ell}^{\infty} f_{E_L}(y)\, dy.$$

The mean of the random variable E_L or annualised loss is given by the expectation

$$E(L) = \int_0^{\infty} y f_{E_L}(y)\, dy.$$

Using integration by parts, and using $f_{E_L}(y) = -G'_{E_L}(\ell)$, we get

$$E(L) = \int_0^{\infty} -yG'_{E_L}(y)\, dy = \big[- yG_{E_L}(y)\big]_0^{\infty} + \int_0^{\infty} G_{E_L}(y)\, dy.$$

Assuming $xG_{E_L} \to 0$ as $x \to \infty$ (which is true for an exponential distribution, or distribution which behaves asymptotically as exponential) we have

$$E(L) = \int_0^{\infty} G_{E_L}(y)\, dy$$

which demonstrates that the mean value of the loss is the area under the risk exceedance curve (PML).

The EQRM post processing tool `wrap_risk_plots` can be used with the individual plotting tool `calc_annloss` to compute the annualised loss.The annualised loss associated with the PML in Figure 9.4 is 0.03%.

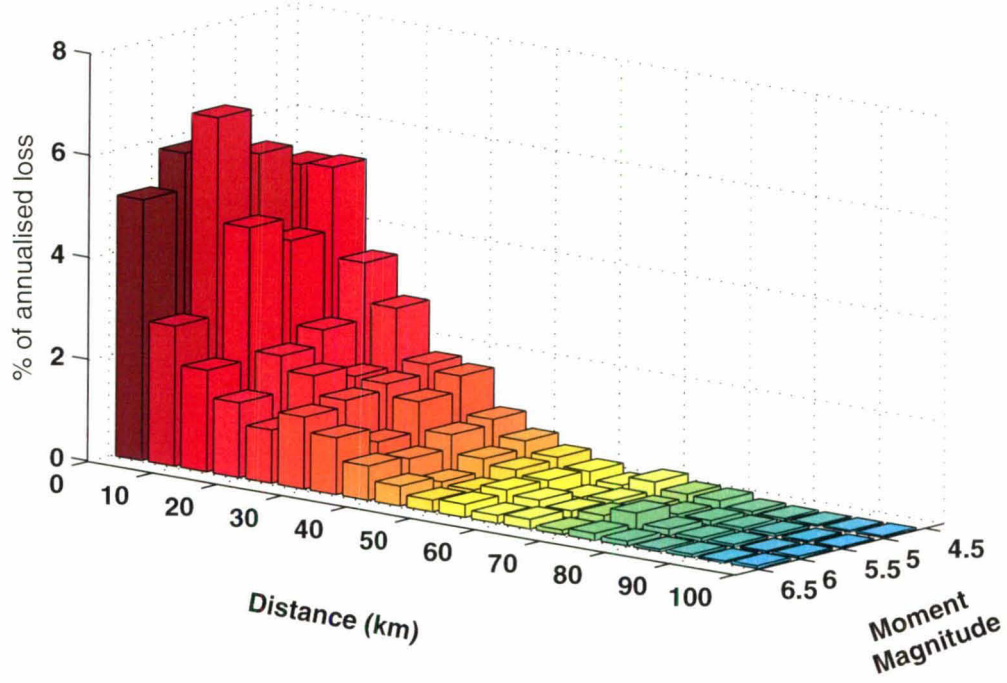

Figure 9.5: Annualised loss disaggregated by distance and magnitude for the Newcastle and Lake Macquarie region.

9.4.3 Disaggregated annualised loss

Storing the loss results for all of the earthquake-building pairs allows the de-aggregation of annualised loss into a range of classes. The EQRM offers several tools to assist the de-aggregation into common classes all of which are managed through the plotting tool `wrap_risk_plots`. These are described as follows:

1. **disaggregation by distance and magnitude** allows the visualisation of magnitude-distance combinations which have the greatest influence on risk assessments. Figure 9.5 illustrates the disaggregation by distance and magnitude for risk in the Newcastle and Lake Macquarie region. The individual plotting tool `calc_annloss_deagg_distmag` can be used with `wrap_risk_plots` to de-aggregate the risk by distance and magnitude.

2. **disaggregation by building construction type** separates the annualised loss into the four major construction types; wood framed, un-reinforced masonry, concrete and steel framed. Figure 9.6 illustrates the annualised

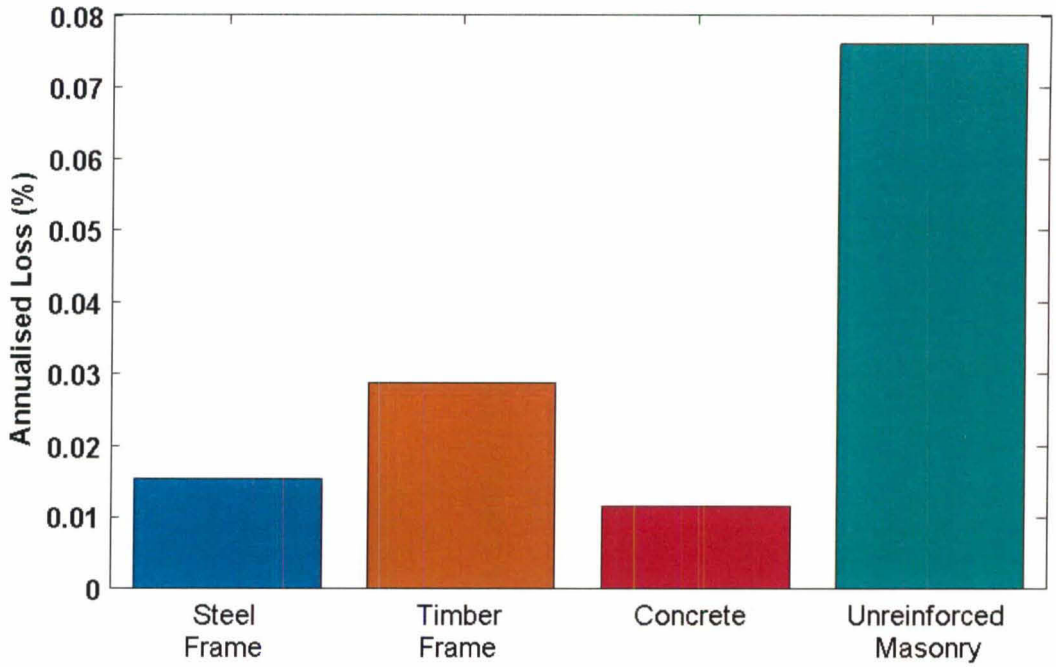

Figure 9.6: Annualised loss disaggregated by building construction type for the Newcastle and Lake Macquarie region.

loss disaggregated by structural type for the Newcastle and Lake Macquarie region. The individual plotting tool `calc_annloss_deagg_structural` can be used with `wrap_risk_plots` to de-aggregate the risk by structural type.

3. **disaggregation by suburb** separates the annualised loss into different suburbs and allows the visualisation of how earthquake risk varies spatially. The individual processing tool `calc_annloss_deagg_sub` can be used with `wrap_risk_plots` to de-aggregate the risk by suburb. Note that `calc_annloss_deagg_sub` produces a CSV file that can be plotted in GIS or some other environment.

9.5 Earthquake scenario results

The output for an earthquake scenario loss simulation is also stored in the file `<site_loc>_db_savedecloss.mat`. The format for this file is exactly the same as the format for the probabilistic risk output. Note, however, that each of the earthquakes in `<site_loc>_db_savedecloss.mat` represent different realisations

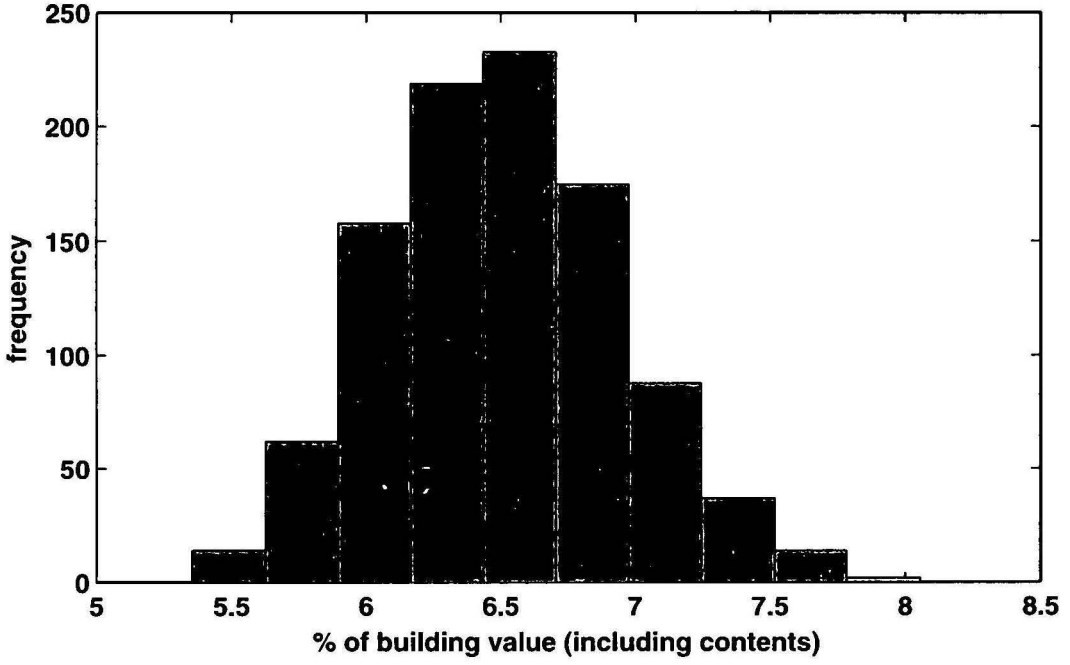

Figure 9.7: Histogram of loss estimates for a synthetic Newcastle 1989 earthquake.

of the same scenario (see Section 3.5). The primary technique for visualising an EQRM scenario output is via a histogram such as that shown in Figure 9.7 for a simulation of the Newcastle 1989 earthquake. Each bar of the histogram in Figure 9.7 represents the frequency of realisations which predicted a loss value within the bars domain. Histograms such as Figure 9.7 can be produced using the individual plotting tool `calc_scen_loss_stats` with `wrap_risk_plots`. Note that `calc_scen_loss_stats` also produces basic statistics for the scenario realisations such as the mean and median.

9.6 Key functions, flags and parameters

Name	Type	Description
<site_loc>_db_hzd.mat	Output	EQRM output file for a probabilistic earthquake hazard run.
<site_loc>_db_savedecloss.mat	Output	EQRM output file for a probabilistic (or scenario) risk run.
rtrn_per	Par	Vector whose elements represent the return periods to be considered.
plot_hzd_map	Function	Post processing tool for plotting probabilistic earthquake hazard maps.
create_gis_output	Function	Post processing tool to export probabilistic earthquake hazard data.
plot_singlesite_hzd	Function	Post processing tool for plotting hazard exceedance curves or uniform hazard spectra.
wrap_risk_plots	Function	Post processing tool to handle user interaction with risk processing/plotting tools.
plot_pml	Function	Post processing tool for plotting and computing the PML.
calc_annloss	Function	Post processing tool for computing the annualised loss.
calc_annloss_deagg_distmag	Function	Post processing tool for plotting the annualised loss disaggregated by distance and magnitude.
calc_annloss_deagg_structural	Function	Post processing tool for plotting the annualised loss disaggregated by building structural type.
calc_annloss_deagg_sub	Function	Post processing tool for computing the annualised loss disaggregated by suburb.
calc_scen_loss_stats	Function	Post processing tool for analysing and plotting loss data for earthquake scenario runs.

Appendix A

Appendicies

A.1 Creating a stand–alone executable of the EQRM GUI in MATLAB R13:

Type the following at the command line

- `>> mcc -v -B sgl eqrm_param_gui -d <destination directory>`

OR
Use the `eqrm_tools` GUI by typing

- `>> eqrm_tools`

and following the instructions. This process will create the following files in `<destination directory>` (`*\eqrm\eqrm_app\system` if `eqrm_tools` is used):

1. `eqrm_param_gui.exe`;
2. a directory named `bin` (containing `FigureMenuBar.fig` and `FigureToolBar.fig`); and
3. a number of a files with `.c` extension.

Prepare the files for transportation as follows:

1. Create a folder entitled *\testexe.
2. In *\testexe create two folders entitled *\testexe\system and *\testexe\mglbin.
3. Copy eqrm_param_gui.exe and bin (created above) into *\testexe\system.
4. Copy the following files from *\eqrm\eqrm_app\system into *\testexe\system:
   (a) cnt_error_dlg.fig,
   (b) root_mat_creator_cnt.exe,
   (c) root_mat_creator_cnt.fig,
   (d) uigetfolder_win32.dll and
   (e) uigetfiles_cnt.dll.
5. Copy mglinstaller.exe from <MATLAB>\extern\lib\win32 into *\testexe\mglbin.
6. Run mglinstaller.exe on *\testexe\mglbin by double clicking on it.
7. Copy <MATLAB>\toolbox\matlab\iofun\dataread.dll into *\testexe\mglbin\toolbox\matlab\iofun\dataread.dll.
8. Copy *\eqrm\eqrm_app\resources into *\testexe.

Installation onto the target machine is achieved as follows:

1. Move the contents of *\testexe onto the target machine.
2. Set environment path on the target machine
   - open the Control Panel.
   - open System.
   - select the Advanced tab.
   - select Environment Variables.
   - either create a new user variable entitled path or edit the existing path variable.
   - add the following path names (separated by semicolons) into the value field for path:

- `*\testexe\mglbin\bin\win32`,
- `*\testexe\system`, and
- `*\texmf\miktex\bin`.

- Log off and log back on.

3. Set the software path as follows

   - Open a DOS shell.
   - Type `root_mat_creator_cnt.exe`.
   - On the 'EQRM root file creation' GUI select the EQRM root directory (i.e. `*\testexe`).

4. Open the EQRM GUI by typing `eqrm_param_gui.exe` at the DOS command prompt.

A.2 The default PSHA setdata file

run_type	1
hazard_map_flag	1
savedir	'./'
inputdir	'./'
var_attn_method	2
var_amp_method	2
nsamples	5
nsigma	2.5
mbnd	4
determ_ntrg	167
attn_region	1
site_loc	'newc'
SiteInd	[1, 1125, 2250, 3374, 4499, 5624, 6748, 7873, 8998, 10122, 11247, 12371, 13496, 14621, 15745, 16870, 17995, 19119, 20244, 21369]
destring	'no description string set'
small_site_flag	0
ieast	1
nbins	15
ftype	2
wdth	15
dip	35
azi	180
d_azi	180
min_mag_cutoff	4.5
ntrgvector	[5000,1000,1000,3000,1000,1000]
src_eps_switch	0
Rthrsh	800
rtrn_per	[10 50 100 200 250 474.56 500 974.79 1000 2474.9 2500 5000 7500 10000]
grid_flag	2
attenuation_flag	[1; 1]
var_amp_flag	1
var_attn_flag	1
amp_switch	1
MaxAmpFactor	10000

MinAmpFactor	0.6
pgacutoff	2.0
qa_switch_watercheck	0
qa_switch_mke_evnts	0
qa_switch_fuse	0
qa_switch_ampfactors	0
qa_switch_attn	0
qa_switch_map	1
periods	[0 0.05 0.1 0.2 1/3.3 0.5 1];
determ_flag	0
determ_mag	5.35
determ_lat	-32.95
determ_lon	151.61
determ_r_z	11.5
determ_azi	340
force_btype_flag	0

A.3 The default PSRA setdata file

run_type	2
hazard_map_flag	0
b_usage_type_flag	1
SiteInd	[2997 2657 3004 3500]
inputdir	'./'
var_attn_method	2
var_amp_method	2
nsamples	5
nsigma	2.5
mbnd	4
attn_region	1
site_loc	'newc'
destring	'no description string set'
small_site_flag	0
save_ecloss_flag	1
save_socloss_flag	1
save_probdam_flag	0
save_deagecloss_flag	0
savedir	'./'
periods	linspace(0,10/3,20)
ieast	1
nbins	15
ftype	2
wdth	15
dip	35
azi	180
d_azi	180
min_mag_cutoff	4.5
ntrgvector	[500,100,100,300,100,100]
src_eps_switch	0
Rthrsh	400
rtrn_per	[10 50 100 200 250 474.56 500 974.79 1000 2474.9 2500 5000 7500 10000]'
attenuation_flag	[1; 1]
var_amp_flag	1
var_attn_flag	1

var_bcap_flag	1
bcap_var_method	3
stdcap	0.3
amp_switch	1
MaxAmpFactor	10000
MinAmpFactor	0.6
pgacutoff	2.0
ci	1.4516
qa_switch_watercheck	0
qa_switch_mke_evnts	0
qa_switch_fuse	0
qa_switch_ampfactors	0
qa_switch_attn	0
qa_switch_vun	0
qa_switch_soc	0
qa_switch_map	0
Harea_flag	1
resp_crv_flag	0
damp_flags	[0, 0, 0]
smoothed_response_flag	0
pga_mindamage	0.05
grid_flag	2
hazus_btypes_flag	0
buildpars_flag	1
SDRelTol	1.0
max_iterations	7
hazus_dampingis5_flag	0
aus_contents_flag	0
determ_flag	0
determ_ntrg	167
determ_mag	5.35
determ_lat	-32.95
determ_lon	151.61
determ_r_z	11.5
determ_azi	340
force_btype_flag	0
determ_btype	34
determ_buse	1

A.4 Example of <site_loc>_par_sourcezones.txt

```
%%%%%%%%%%%%%%%%%%%%%%%%%%%%%%%%%%%%%%%%%%%%%%%%%%%%%%%%%%%%%%%%%%%%%%%%%%%%
% Important recurrence parameters for the Newcastle source combination 1
%
% The format of the table is:
% (i) ZoneID  (ii) Area (km^2)     (iii) h (focal depth) (km) (iv) Ml(min)
% (v) Ml(max) (vi) b               (vii) sigma-b              (viii) Amin
% (ix) sigma-a
%
% i.e. the format is the same as Table 2 from probabilistic earthquake
% risk maps of oz Gaull et al, 1990, Australian Journal of Earth Sciences
%
% Note on GR relationship:
%       Incremental:    N(m) = a -bm            (1)
%       Cumulative:    Lambda(m) = A - Bm       (2)
%           where A = a - log10(ln(10)*b) and B = b
%
% Source of values:
% * it is advisable to include some description of the source of the
% parameters here e.g.*
%
%    Source zone parameters as used in the Newcastle and Lake Macquarie
%    report.
%
%
%                                                  David Robinson
%                                                  15/04/02
%%%%%%%%%%%%%%%%%%%%%%%%%%%%%%%%%%%%%%%%%%%%%%%%%%%%%%%%%%%%%%%%%%%%%%%%%%%%
```

1	5054.035	7	3.3	5.4	1.0	0.106	0.568	0.244
2	57731.425	7	3.3	5.4	1.14	0.025	2.53	0.034
3	56703.105	7	3.3	5.4	1.14	0.025	2.48	0.029
4	3046.615	7	5.41	6.5	1.0	NaN	0.0016	NaN
5	72204.957	7	5.41	6.5	1.118	0.024	0.014	NaN
6	44149.044	7	5.41	6.5	1.118	0.024	0.0086	NaN

A.5 Example of <site_loc>_par_sourcepolys.txt

```
%%%%%%%%%%%%%%%%%%%%%%%%%%%%%%%%%%%%%%%%%%%%%%%%%%%%%%
% Digitised polygons for the Newcastle region.
%
% The format of the table is:
% vertexID  X-coord Y-coord zoneID
%
% Source of Values: the first three polygons as used in
% the Newcastle and Lake Macquarie Report.
%
%                       David Robinson
%                       15/04/02
%%%%%%%%%%%%%%%%%%%%%%%%%%%%%%%%%%%%%%%%%%%%%%%%%%%%%%
```

0	151.150	-32.400	1
1	152.170	-32.750	1
2	151.430	-33.450	1
3	151.150	-32.400	1
4	149.500	-31.000	2
5	149.500	-32.400	2
6	151.150	-32.400	2
7	152.170	-32.750	2
8	152.760	-32.750	2
9	152.800	-32.700	2
10	153.110	-32.000	2
11	153.290	-31.000	2
12	149.500	-31.000	2
13	149.500	-35.000	3
14	149.500	-32.400	3
15	151.150	-32.400	3
16	151.430	-33.450	3
17	152.170	-32.750	3
18	152.760	-32.750	3
19	151.350	-34.400	3
20	151.150	-34.740	3
21	151.100	-35.000	3
22	149.500	-35.000	3

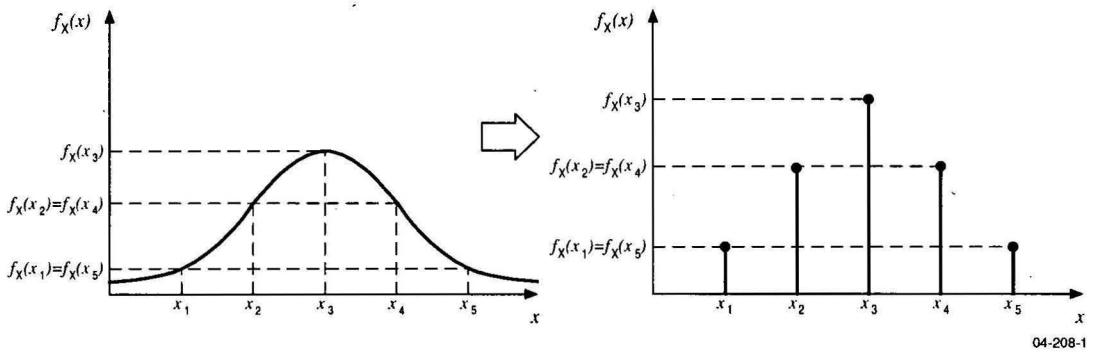

Figure A.1: Discrete sampling of the PDF of a continuous random variable X.

A.6 Discretising the PDF of a continuous variable

At many stages the EQRM application relies upon sampling the probability density function (PDF) of a continuous random variable. The discrete nature of most numerical computations requires a discrete sampling of the PDF. This Appendix describes how the discrete sampling of the PDF is conducted within the EQRM application.

Consider a continuous random variable X whose PDF is given by $f_X(x)$ (see Figure A.1). Assume that N samples $\{x_j\}_{j=1}^N$ are taken and that the samples are separated by a distance 2Δ (5 samples are shown in the figure). In the continuous case the probability that X lies between $x_i \pm \Delta$ where $1 \leq i \leq N$ is given by:

$$P(x_i - \Delta < X < x_i + \Delta) = \int_{x_i-\Delta}^{x_i+\Delta} f_X(x)\, dt. \tag{A.1}$$

In the discrete case the associated probability can be approximated by:

$$P(x_i - \Delta < X < x_i + \Delta) = \frac{f_X(x_i)}{\sum_{j=1}^{N} f_X(x_j)}. \tag{A.2}$$

Another valid approximation could be obtained by numerically integrating Equation A.1, however it is the Equation A.2 approximation that is used by the EQRM.

Note that the denominator in Equation A.2 ensures that

$$\sum_{i=1}^{N} \frac{f_X(x_i)}{\sum_{j=1}^{N} f_X(x_j)} = 1 \tag{A.3}$$

which is analogous to

$$\int_{-\infty}^{\infty} f_X(t)\, dt = 1. \tag{A.4}$$

A.7 Example of <site_loc>_par_ampfactors.mat

amp_period	1x88	704	double array
ln_siteC_rockpga0050_momag45	1x88	704	double array
ln_siteC_rockpga0050_momag55	1x88	704	double array
ln_siteC_rockpga0050_momag65	1x88	704	double array
ln_siteC_rockpga0100_momag45	1x88	704	double array
ln_siteC_rockpga0100_momag55	1x88	704	double array
ln_siteC_rockpga0100_momag65	1x88	704	double array
ln_siteC_rockpga0250_momag45	1x88	704	double array
ln_siteC_rockpga0250_momag55	1x88	704	double array
ln_siteC_rockpga0250_momag65	1x88	704	double array
ln_siteC_rockpga0500_momag45	1x88	704	double array
ln_siteC_rockpga0500_momag55	1x88	704	double array
ln_siteC_rockpga0500_momag65	1x88	704	double array
ln_siteD_rockpga0050_momag45	1x88	704	double array
⋮	⋮	⋮	⋮
ln_siteD_rockpga0500_momag65	1x88	704	double array
ln_siteE_rockpga0050_momag45	1x88	704	double array
⋮	⋮	⋮	⋮
ln_siteE_rockpga0500_momag65	1x88	704	double array
ln_siteF_rockpga0050_momag45	1x88	704	double array
⋮	⋮	⋮	⋮
ln_siteF_rockpga0500_momag65	1x88	704	double array
ln_siteG_rockpga0050_momag45	1x88	704	double array
⋮	⋮	⋮	⋮
ln_siteG_rockpga0500_momag65	1x88	704	double array
ln_siteH_rockpga0050_momag45	1x88	704	double array
⋮	⋮	⋮	⋮
ln_siteH_rockpga0500_momag65	1x88	704	double array
momag_bin	1x3	24	double array
pga_bin	1x4	32	double array
stdln_siteC_rockpga0050_momag45	1x88	704	double array
⋮	⋮	⋮	⋮
stdln_siteC_rockpga0500_momag65	1x88	704	double array
stdln_siteD_rockpga0050_momag45	1x88	704	double array
⋮	⋮	⋮	⋮
stdln_siteD_rockpga0500_momag65	1x88	704	double array
stdln_siteE_rockpga0050_momag45	1x88	704	double array
⋮	⋮	⋮	⋮
stdln_siteE_rockpga0500_momag65	1x88	704	double array
stdln_siteF_rockpga0050_momag45	1x88	704	double array
⋮	⋮	⋮	⋮
stdln_siteF_rockpga0500_momag65	1x88	704	double array
stdln_siteG_rockpga0050_momag45	1x88	704	double array
⋮	⋮	⋮	⋮
stdln_siteG_rockpga0500_momag65	1x88	704	double array
stdln_siteH_rockpga0050_momag45	1x88	704	double array
⋮	⋮	⋮	⋮
stdln_siteH_rockpga0500_momag65	1x88	704	double array

A.8 Response spectra

Response spectral acceleration S_a describes the maximum response of a range of single-degree-of-freedom (SDOF) oscillators to a particular input acceleration (Figure A.2). They are useful in PSHA and PSRA because buildings can be approximated by SDOF oscillators where buildings of different height correspond to SDOF oscillators with different natural period T_o. Response spectral acceleration is a function of T_o and the damping ratio for each of the SDOF oscillators (Chopra 2001;Kramer 1996). In practice, the damping ratio is assumed to be the same for each oscillator and is generally set to 5%. Note that the response spectral acceleration does not characterise actual ground motion, rather it provides information on how SDOF oscillators respond to strong ground motion.

Response spectral velocity and response spectral displacement are the velocity response and displacement response, respectively.

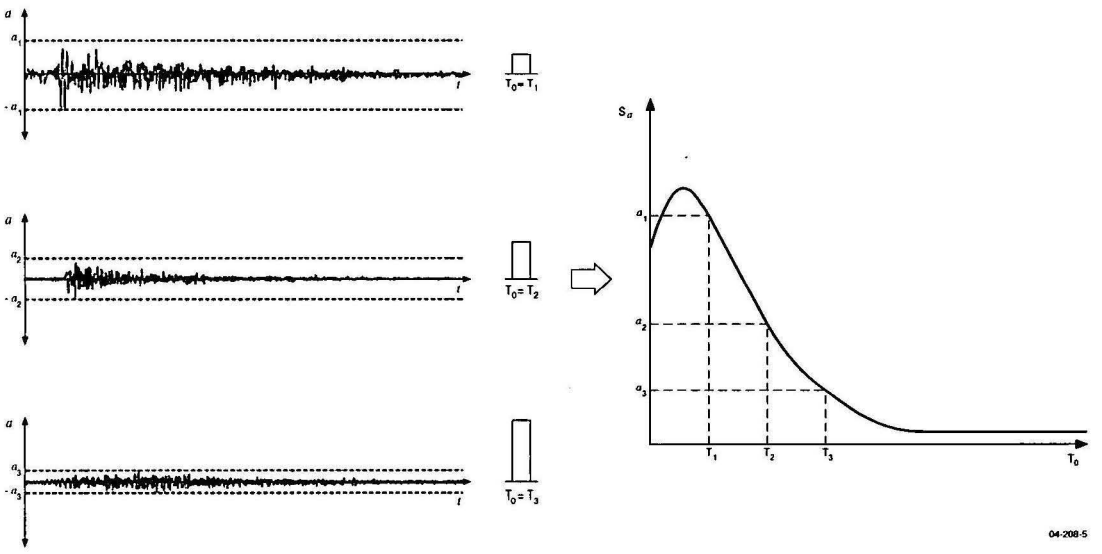

Figure A.2: Response spectral acceleration as the maximum acceleration response to an earthquake, for a family of building periods. The diagram on the left illustrates a series of time histories corresponding to the response of three buildings with different heights (or fundamental periods). The diagram on the right plots the maximum amplitude corresponding to the periods as a continuous curve. This is the Response Spectral Acceleration.

Given an input ground motion displacement, $y_g(t)$, the differential equation describing the response of a building with fundamental period T_o is

$$\ddot{u} + \gamma\dot{u} + \omega_0^2 u = -\ddot{y}_g(t), \tag{A.5}$$

where u is the displacement, $\omega_0 = \sqrt{k/m} = 2\pi/T_o$, k is the stiffness coefficient and m the mass of the oscillator. The response spectral acceleration of the building is then given by

$$S_a(T_o) = \max_{t \in T_R} \left(\ddot{u}(t) + \ddot{y}_g(t) \right), \tag{A.6}$$

where T_R is some time period that bounds the maximum response. Robinson *et al.* (2006) provide a detailed explanation on how to compute S_a. Note that a building of zero period (i.e. zero height or equivalently, infinite stiffness) corresponds to PGA (peak ground acceleration).

A.9 Tables of building parameters

This appendix lists the tables of building parameters used in the Newcastle and Lake Macquarie study (Fulford *et al.*, 2002) (Table A.1, Table A.2 and Table A.3). Further details about these parameters can be found in Edwards *et al.* (2002).

Table A.1: Table of building capacity curve parameters, as decided as part of a consultancy with University of Melbourne.

	C_s	h	T_e	α_1	α_2	γ	λ	μ
W1MEAN	0.077	13	0.275	0.9	0.7	1.75	2	7
W1BVTILE	0.063	13	0.32	0.9	0.7	1.75	2	7
W1BVMETAL	0.082	13	0.28	0.9	0.7	1.75	2	7
W1TIMBERTILE	0.069	13	0.3	0.9	0.7	1.75	2	7
W1TIMBERMETAL	0.094	13	0.26	0.9	0.7	1.75	2	7
C1LMEAN	0.2	20	0.45	0.975	0.795	1.5	1.38	3.75
C1LSOFT	0.2	20	0.45	1	0.79	1.5	1.25	3.5
C1LNOSOFT	0.2	20	0.45	0.95	0.8	1.5	1.5	4
C1MMEAN	0.1	50	0.85	0.95	0.6	1.5	1.38	2.5
C1MSOFT	0.1	50	0.85	1	0.55	1.5	1.25	2
C1MNOSOFT	0.1	50	0.85	0.9	0.65	1.5	1.5	3
C1HMEAN	0.05	120	1.6	0.925	0.55	1.5	1.38	2
C1HSOFT	0.05	120	1.6	1	0.5	1.5	1.25	1.5
C1HNOSOFT	0.05	120	1.6	0.85	0.6	1.5	1.5	2.5
URMLMEAN	0.15	15	0.15	0.75	0.75	1.5	2	2
URMLTILE	0.15	15	0.15	0.75	0.75	1.5	2	2
URMLMETAL	0.2	15	0.13	0.75	0.75	1.5	2	2
URMMMEAN	0.1	35	0.28	0.75	0.75	1.5	2	2
URMMTILE	0.1	35	0.28	0.75	0.75	1.5	2	2
URMMMETAL	0.15	35	0.23	0.75	0.75	1.5	2	2

Table A.2: Table of damage threshold parameters used for the current set of building parameters.

Damage state	S	M	E	C
Non-Structural damage drift sensitive (drift ratios)				
nonres	0.004	0.008	0.02	0.03
res	0.001	0.008	0.015	0.025
Accel. sensitive (g)				
Accel	0.2	0.4	0.8	1.6
Structural Damage drift ratios				
W1MEAN	0.001	0.004	0.008	0.015
W1BVTILE	0.0005	0.001	0.002	0.005
W1BVMETAL	0.0005	0.001	0.002	0.005
W1TIMBERTILE	0.002	0.008	0.015	0.04
W1TIMBERMETAL	0.002	0.008	0.015	0.04
C1LMEAN	0.006	0.009	0.013	0.04
C1LSOFT	0.006	0.009	0.013	0.04
C1LNOSOFT	0.006	0.009	0.013	0.04
C1MMEAN	0.005	0.007	0.01	0.03
C1MSOFT	0.005	0.007	0.01	0.03
C1MNOSOFT	0.005	0.007	0.01	0.03
C1HMEAN	0.004	0.005	0.007	0.02
C1HSOFT	0.004	0.005	0.007	0.02
C1HNOSOFT	0.004	0.005	0.007	0.02
URMLMEAN	0.0005	0.0008	0.0012	0.002
URMLTILE	0.0005	0.0008	0.0012	0.002
URMLMETAL	0.0005	0.0008	0.0012	0.002
URMMMEAN	0.0005	0.0008	0.0012	0.002
URMMTILE	0.0005	0.0008	0.0012	0.002
URMMMETAL	0.0005	0.0008	0.0012	0.002

Table A.3: Table of damping parameters used for the current set of building parametersas decided as part of a consultancy with University of Melbourne.

Type	κ_S	κ_M	κ_L	B_E
W1MEAN	0.001	0.001	0.001	0.08
W1BVTILE	0.001	0.001	0.001	0.08
W1BVMETAL	0.001	0.001	0.001	0.08
W1TIMBERTILE	0.001	0.001	0.001	0.08
W1TIMBERMETAL	0.001	0.001	0.001	0.08
C1LMEAN	0.12	0.09	0.09	0.07
C1LSOFT	0.12	0.09	0.09	0.07
C1LNOSOFT	0.12	0.09	0.09	0.07
C1MMEAN	0.105	0.08	0.08	0.07
C1MSOFT	0.105	0.08	0.08	0.07
C1MNOSOFT	0.105	0.08	0.08	0.07
C1HMEAN	0.095	0.07	0.07	0.07
C1HSOFT	0.095	0.07	0.07	0.07
C1HNOSOFT	0.095	0.07	0.07	0.07
URMLMEAN	0.001	0.001	0.001	0.05
URMLTILE	0.001	0.001	0.001	0.05
URMLMETAL	0.001	0.001	0.001	0.05
URMMMEAN	0.001	0.001	0.001	0.05
URMMTILE	0.001	0.001	0.001	0.05
URMMMETAL	0.001	0.001	0.001	0.05

Bibliography

Abrahamson, N. and W. J. Silva (1997). Empirical response spectral attenuation relations for shallow crustal earthquakes. *Seismological Research Letters 68*(1), 94–127.

Atkinson, G. M. (1995). Optimal choice of magnitude scales for seismic hazard estimates in Eastern North America. *Seismological Research Letters 66*(1), 51–55.

Atkinson, G. M. and D. M. Boore (1997). Some comparisons between recent ground–motion relations. *Seismological Research Letters 68*(1), 24–40.

Australian Bureau of Statistics (2001). Construction: Special Article - Functional classification of building. Building Approvals, Australia ABS Cat. No. 8731.0, Australian Bureau of Statistics.

Bommer, J. J., F. Scherbaum, H. Bungum, F. Cotton, F. Sabetta and N. A. Abrahamson (2005). On the use of logic trees for ground-motion prediction equations in seismic-hazard analysis. *Bulletin of the Seismological Society of America 95*(2), 377–389.

Boore, D. M. (1983). Strong-motion seismology. *Reviews of Geophysics and Space Physics 21*(6), 1308–1318.

Borcherdt, R. D. and J. F. Gibbs (1976). Effects of local geologic conditions in the San Francisco Bay region on ground motions and intensities of the 1906 earthquake. *Bulletin of the Seismological Society of America 66*, 467–500.

Brown, A. and G. Gibson (2004). A multi-tiered earthquake hazard model for australia. *Tectonophysics 390*, 25–43.

Campbell, K. W. (2003). Strong motion attenuation. In W. H. K. Lee, H. Kanamori, P. C. Jennings and C. Kisslinger (Eds.), *International Handbook of Earthquake and Engineering Seismology*, Volume B, Chapter 60, pp. 1003–1012. London: Academic Press.

Chopra, A. K. (2001). *Dynamics of Structures: Theory and Applications to Earthquake Engineering.* New Jersey: Prentice Hall. pp.844.

Cornell, C. A. (1968). Engineering seismic risk analysis. *Bulletin of the Seismological Society of America 58*(5), 1583–1606.

Dhu, T. and T. Jones (2002). Earthquake risk in Newcastle and Lake Macquarie. GA Record 2002/15, Geoscience Australia.

Dhu, T., D. Robinson, C. Sinadinovski, T. Jones, N. Corby, A. Jones and J. Schneider (2002). Earthquake hazard. In T. Dhu and T. Jones (Eds.), *Earthquake risk in Newcastle and Lake Macquarie, GA Record: 2002/15*, Chapter 4, pp. 43–76. Geoscience Australia.

Edwards, M. R., D. J. Robinson, K. J. McAneney and J. Schneider (2004, 1–6 August). Vulnerability of residential structures in Australia. In *13th World Conference on Earthquake Engineering*, Vancouver. Paper Number 2985.

Edwards, M. R., J. L. Wilson and N. T. K. Lam (2002). Review of Geoscience Australia's seismic risk assessment model. Technical Report MEI Ref: 2002-042, University of Melbourne.

EPRI (1993). Vol 2: Appendices for ground motion estimation. Guidelines for determining design basis ground motions. Technical Report EPRI TR-102293, Electric Power Research Institute, Palo Alto, California, U.S.A.

FEMA (1999). *HAZUS99: Technical Manual.* Washington DC: Federal Emergency Management Agency.

Fulford, G., T. Jones, J. Stehle, N. Corby, D. Robinson, J. Schneider and T. Dhu (2002). *Earthquake Risk*, pp. 103–122. Earthquake risk in Newcastle and Lake Macquarie, GA Record 2002/15. Geoscience Australia.

Gaull, B. A., M. O. Michael-Leiba and J. M. W. Rynn (1990). Probabilistic earthquake risk maps of Australia. *Australian Journal of Earth Sciences 37*, 169–187.

Johnstone, A. C. (1996). Seismic moment assessment of earthquakes in stable continental regions – I. Instrumental seismicity. *Geophysical Journal International 124*, 381–414.

Kircher, C. A., A. A. Nassar, O. Kustu and W. T. Holmes (1997). Development of building damage functions for earthquake loss estimation. *Earthquake Spectra 13*(4), 663–682.

Kircher, C. A., R. K. Reitherman, R. V. Whitman and C. Arnold (1997). Estimation of earthquake losses to buildings. *Earthquake Spectra 13*(4), 703–720.

Kramer, S. L. (1996). *Geotechnical Earthquake Engineering.* New Jersey: Prentice Hall. pp. 653.

McGuire, R. K. and W. J. Arabasz (1990). An introduction to probabilistic seismic hazard analysis. In S. H. Ward (Ed.), *Geotechnical and Environmental Geophysics*, Volume III, pp. 333–353. Society of Exploration Geophysicists.

Meremonte, M., A. Frankel, E. Cranswick, D. Carver and D. Worley (1996). Urban seismology - Northridge aftershocks recorded by multi-scale arrays of portable digital seismographs. *Bulletin of the Seismological Society of America 86*(5), 1350–1363.

Murphy, J. R., A. H. Davis and N. L. Weavers (1971). Amplification of seismic body waves by low-velocity surface layers. *Bulletin of the Seismological Society of America 61*, 109–145.

Newmark, N. M. and W. J. Hall (1982). *Earthquake Spectra and Design.* Oakland, California: Earthquake Engineering Research Institute Monograph. pp. 103.

Patchett, A., D. Robinson, T. Dhu and A. Sanabria (2005). Investigating earthquake risk models and uncertainty in probabilistic seismic risk analyses. GA Record 2005/02, Geoscience Australia.

Robinson, D. J., T. Dhu and J. Schneider (2006). SUA: a computer program to compute regolith Site-response and estimate Uncertainty for probabilistic seismic hazard Analyses. *Computers and Geoscience 32*(1), 109–123.

Sadigh, K., C. Y. Chang, J. A. Egan, F. Makdisi and R. R. Youngs (1997). Attenuation relationships for shallow crustal earthquakes based on California strong motion data. *Seismological Research Letters 68*(1), 180–189.

Scherbaum, F., J. Schmedes and F. Cotton (2004). On the conversion of source-to-site distance measures for extended earthquake source models. *Bulletin of the Seismological Society of America 94*(3), 1053–1069.

Sibson, R. H. (2003). Geology of the crustal earthquake source. In W. H. K. Lee, H. Kanamori, P. C. Jennings and C. Kisslinger (Eds.), *International Handbook of Earthquake and Engineering Seismology*, Volume A, Chapter 29, pp. 455–473. Academic Press.

Sinadinovski, C., M. Edwards, N. Corby, M. Milne, K. Dale, T. Dhu, A. Jones, A. McPherson, T. Jones, D. Gray, D. Robinson and J. White (2005). *Earthquake Risk*, pp. 143–208. Natural hazard risk in Perth, Western Australia - Comprehensive report, GeoCat No. 63527. Geoscience Australia.

Somerville, P., N. Collins, N. Abrahamson, R. Graves and C. Saikia (2001). Ground motion attenuation relations for the Central and Eastern United States. Technical Report Award Number: 99HQGR0098, USGS.

Standards Australia (1993). Earthquake loads. AS 1170.4–1993, Sydney.

Stehle, J., T. Jones, D. Stewart and J. Schneider (2001). Building paramaters for earthquake vulnerability - workshop proceedings and further investigation. Technical report, Geoscience Australia.

Toro, G. R., N. A. Abrahamson and J. F. Schneider (1997). Model of strong ground motions from earthquakes in Central and Eastern North America: Best estimates and uncertainties. *Seismological Research Letters 68*(1), 41–57.

Wells, D. L. and K. J. Coppersmith (1994). New empirical relationship among magnitude, rupture length, rupture width, rupture area, and surface displacement. *Bulletin of the Seismological Society of America 84*(4), 974–1002.

Index

<site_loc>_db_hzd, 106, 115
<site_loc>_db_savedecloss, 100, 102, 108, 109, 113, 115
<site_loc>_db_savedsocloss, 101
_MCRInstaller.exe, 19
setdata
    eqrm_param_T, 7

all_postcodes, 45
all_suburbs, 45, 46
amp_period, 75, 127
amp_switch, 11, 119, 122
attenuation_flag, 10, 66, 68, 70, 94, 119, 121
attn_allpervec_atkboore, 60, 69
attn_allpervec_gaull, 59, 69
attn_allpervec_sadigh, 60, 69
attn_allpervec_somerville, 61
attn_allpervec_toro, 58, 69
attn_atkboore_momag, 70
attn_mmi_gaull, 59
attn_prep_atkboore_aleatory, 60, 69
attn_prep_sadigh_uncertainty, 61, 70
attn_prepcoeff_atkboore, 60, 69
attn_prepcoeff_sadigh, 60, 69
attn_prepcoeff_somerville, 61
attn_prepcoeff_toro, 58, 69
attn_preptoro_aleatory1, 58, 69
attn_preptoro_aleatory2, 58, 69
attn_preptoro_epistemic, 59, 69
attn_region, 10, 58, 59, 61, 68, 70, 119, 121
attn_sadigh_coeff_momag_great65, 70
attn_sadigh_coeff_momag_less65, 70
attn_toro_midcontinent_momag, 70
aus_contents_flag, 14, 100, 102, 122
aus_peshnew, 59, 69
azi, 8, 38, 42, 119, 121

b_sitemat, 46
b_soil, 46
b_usage_type_flag, 11, 50, 53, 97, 121
bcap_rand, 82
bcap_var_method, 12, 122
build_cap_rand, 95
building capacity curve, 80
building database, 5, 6, 14, 15, 44–47, 49–53, 95, 99
    columns, 46
building type, 4, 12, 47, 49, 93
building usgage
    FCB, 11, 46, 50, 51, 97, 99
    HAZUS, 11, 46, 50, 52, 97, 99, 100
buildpars_flag, 12, 53, 122

calc_annloss, 111, 115
calc_annloss_deagg_distmag, 112, 115
calc_annloss_deagg_structural, 113, 115
calc_annloss_deagg_sub, 113, 115
calc_corner_periods, 85, 95
calc_event_activity, 40
calc_scen_loss_stats, 114, 115
capacity curve, 12, 13, 47, 49, 78–83, 85, 87–89, 92, 93, 95, 130, 137
capacity spectrum method, 14, 78, 79, 92, 94, 96
ci, 14, 98, 102, 122
create_gis_output, 106, 115
cvt_bfactors, 95

d_azi, 8, 38, 42, 119, 121
damp_flags, 13, 84, 85, 95, 122
Data Interrogation Tool, 18

demand curve, 78, 79, 82, 84, 85, 88, 89, 93, 95
destring, 8, 119, 121
determ_azi, 9, 41, 43, 120, 122
determ_btype, 12, 122
determ_buse, 12, 122
determ_flag, 9, 41, 42, 120, 122
determ_lat, 9, 41, 43, 120, 122
determ_lon, 9, 41, 43, 120, 122
determ_mag, 9, 41, 42, 120, 122
determ_ntrg, 9, 119, 122
determ_r_z, 9, 41, 43, 120, 122
dip, 8, 42, 119, 121
directory
*/buildingdb, 5
*/buildingpars, 5
*/c3_gui, 6, 7
*/compare_utils, 6
*/data, 7
*/datacvt/buildingdb, 53
*/datacvt/buildingpars, 53
*/datacvt/buildpars, 90, 95
*/datacvt/econsoclosspars, 53
*/dit, 6
*/dit_gui, 7
*/econsocpars, 6
*/eqrm/datacvt, 5, 44
*/eqrm/datacvt/buildingdb, 47
*/eqrm/datacvt/econsoclosspars, 99, 102
*/eqrm/datacvtbuildingpars, 49
*/eqrm/eqrm_app, 5, 6
*/eqrm/eqrm_app/m_code, 6
*/eqrm/eqrm_app/m_code/startup, 16
*/eqrm/eqrm_app/resources, 6
*/eqrm/eqrm_app/resources/data, 7, 16, 17, 21
*/eqrm/testing_harness, 5, 7
*/general, 6
*/hazard, 6, 7
*/m_code, 6
*/mcc_build_apps, 6
*/processing, 6
*/resources, 6
*/site_classes, 6
*/startup, 6
*/stats, 6
*/system, 6
*/utils, 6
*/vuln, 6, 7
DIT, 18
do_alldist, 57, 69
do_amplification, 13, 72, 77
do_analysis, 14, 56, 69, 72, 77, 78, 95
do_attenuation, 13, 56, 58, 61, 62, 69
do_build_vuln, 78, 95

effective damping, 84, 85
EQRM, 25, 28, 57
eqrm_analysis, 16
eqrm_param_gui, 6, 7, 16, 45, 53
eqrm_param_T, 7
eqrm_startup, 16
evntdb, 22, 24, 28

force_btype_flag, 12, 120, 122
fragility curves, 78, 89–93, 95
ftype, 8, 119, 121
function
attn_allpervec_atkboore, 60, 69
attn_allpervec_gaull, 59, 69
attn_allpervec_sadigh, 60, 69
attn_allpervec_somerville, 61
attn_allpervec_toro, 58, 69
attn_atkboore_momag, 70
attn_mmi_gaull, 59
attn_prep_atkboore_aleatory, 60, 69
attn_prep_sadigh_uncertainty, 61, 70
attn_prepcoeff_atkboore, 60, 69
attn_prepcoeff_sadigh, 60, 69
attn_prepcoeff_somerville, 61
attn_prepcoeff_toro, 58, 69
attn_preptoro_aleatory1, 58, 69
attn_preptoro_aleatory2, 58, 69
attn_preptoro_epistemic, 59, 69
attn_sadigh_coeff_momag_great65, 70

attn_sadigh_coeff_momag_less65, 70
attn_toro_midcontinent_momag, 70
aus_peshnew, 59, 69
bcap_rand, 82
build_cap_rand, 95
calc_annloss, 111, 115
calc_annloss_deagg_distmag, 112, 115
calc_annloss_deagg_structural, 113, 115
calc_annloss_deagg_sub, 113, 115
calc_corner_periods, 85, 95
calc_event_activity, 40
calc_scen_loss_stats, 114, 115
create_gis_output, 106, 115
cvt_bfactors, 95
do_alldist, 57, 69
do_amplification, 13, 72, 77
do_analysis, 14, 56, 69, 72, 77, 78, 95
do_attenuation, 13, 56, 58, 61, 62, 69
do_build_vuln, 78, 95
eqrm_analysis, 16
eqrm_startup, 16
fuse4_hzd, 24
fuse_4hzd, 13, 40, 42, 64
hyst_area_rand, 87, 95
inpolygon, 27, 28
ll2xy, 28
ln_site{1}_rockpga{2}_momag{3}, 75
m2grpdfb, 42
mag2rup_v, 32, 42
make_build_dam_rand, 78, 95
make_fragility, 95
mke_aseq4mat, 25, 27, 40, 42
mke_ctpdf, 41, 42
mke_evnts, 14, 20, 21, 25, 41, 42
mw2ml, 55, 69
nonlin_damp_rand, 95
per_replace_cost_wrt_bc_usage, 99, 102
pga_cutoff, 63, 70, 76, 77
plot_hzd_map, 106, 115
plot_pml, 110, 115
plot_singlesite_hzd, 107, 108, 115
prep_amps, 72, 77
prep_attn, 56, 58, 61, 69
prep_build_vuln, 78, 95
prep_locations, 95
prep_sites, 78
socloss, 102
src_zones_to_structure, 21
stdln_site{1}_rockpga{2}_momag{3}, 75
wrap_risk_plots, 110–115
Function Variable
amp_period, 75, 127
evntdb, 22, 24, 28
generation, 21, 25, 28, 39
ln_site{1}_rockpga{2}_momag{3}, 75
momag_bin, 72, 75, 76
pga_bin, 72, 75, 76
SA, 56
SArock, 56
SAsoil, 77
source, 21, 39
stdln_site{1}_rockpga{2}_momag{3}, 75
fuse4_hzd, 24
fuse_4hzd, 13, 40, 42, 64

generation, 21, 25, 28, 39
generation polygon, 25, 28, 30, 39
grid_flag, 8, 44, 45, 53, 119, 122
GUI
Data Interrogation Tool, 18
DIT, 18
eqrm_param_gui, 6, 7, 16

Harea_flag, 13, 122
hazard_map_flag, 15, 119, 121
hazus_btypes_flag, 11, 49, 53, 122
hazus_dampingis5_flag, 12, 122
hyst_area_rand, 87, 95

ieast, 8, 119, 121
ignore_post89_flag, 12

inpolygon, 27, 28
Input Manager, 8, 45, 53
inputdir, 8, 16, 21, 119, 121

ll2xy, 28
ln_site{1}_rockpga{2}_momag{3}, 75
ln_site{1}_rockpga{2}_momag{3}, 127

m2grpdfb, 42
mag2rup_v, 32, 42
make_build_dam_rand, 78, 95
make_fragility, 95
max_iterations, 13, 122
MaxAmpFactor, 11, 76, 77, 119, 122
mbnd, 9, 40, 42, 119, 121
min_mag_cutoff, 9, 30, 32, 119, 121
MinAmpFactor, 11, 76, 77, 120, 122
mke_aseq4mat, 25, 27, 40, 42
mke_ctpdf, 41, 42
mke_evnts, 14, 20, 21, 25, 41, 42
momag_bin, 72, 75, 76
mw2ml, 55, 69

nbins, 9, 42, 119, 121
newc89plothistsoc, 101, 102
nonlin_damp_rand, 95
nsamples, 9, 40, 42, 119, 121
nsigma, 9, 40, 42, 119, 121
ntrgvector, 8, 25, 42, 119, 121

output file
- <site_loc>_db_hzd, 106, 115
- <site_loc>_db_savedecloss, 100, 102, 108, 109, 113, 115
- <site_loc>_db_savedsocloss, 101

parameter file
- <site_loc>_par_ampfactors, 17, 72, 75, 127
- <site_loc>_par_site, 17, 44, 45
- <site_loc>_par_site_class_mask, 17
- <site_loc>_par_site_class_polys, 17, 53
- <site_loc>_par_site_uniform, 17, 45, 53
- <site_loc>_par_source, 21, 25, 28, 38, 39
- <site_loc>_par_sourcepolys, 17, 21, 22, 25, 28, 38, 124
- <site_loc>_par_sourcezones, 17, 21, 22, 25, 28, 29, 38, 123
- <site_loc>_par_study_region_box, 17, 53
- attn_atkboore_momag, 17, 60
- attn_sadigh_coeff_momag_great65, 17, 60, 61
- attn_sadigh_coeff_momag_less65, 17, 60, 61
- attn_somer_nonrift_hori, 17, 61
- attn_somer_nonrift_vert, 17
- attn_somer_rift_hori, 17
- attn_somer_rift_vert, 17
- attn_toro_midcontinent_momag, 15, 17, 58
- aus_mat, 17
- australia_bndy, 17
- bfactorsdb, 17
- bfactorsdb_hazus, 17
- bfactorsdb_wshop, 17
- bfactorsdb_wshop_update2, 17
- bfactorsdb_wshop_update3, 17
- buildfacts<version>, 90
- buildfacts_<version>, 95
- econ_par, 17
- factors-nonstructdam, 17
- factors-structdam, 17
- newc_par_ampfactors, 15, 72
- perth_par_site_class_polys, 45
- perth_par_study_region_box, 45
- rc_perRepl...EdwardsFCBusage, 17
- rc_perRepl...EdwardsHazususage, 17
- rc_perReplCostwrtBuildCHazusage, 17
- RcPerWrtBuildCFCBusageEdwards, 99, 102
- RcPerWrtBuildCHazususageEdwards, 99, 102
- sitedb_<site_loc>, 17, 45, 46, 53
- suburb_postcode, 17
- textbtypes, 17
- textbusageFCB, 17

textbuses, 17
peak acceleration, 79, 89
peak displacement, 78, 79, 89, 91
per_replace_cost_wrt_bc_usage, 99, 102
periods, 11, 56, 70, 72, 77, 120, 121
pga_bin, 72, 75, 76
pga_cutoff, 63, 70, 76, 77
pga_mindamage, 14, 101, 102, 122
pgacutoff, 11, 70, 77, 120, 122
plot_hzd_map, 106, 115
plot_pml, 110, 115
plot_singlesite_hzd, 107, 108, 115
prep_amps, 72, 77
prep_attn, 56, 58, 61, 69
prep_build_vuln, 78, 95
prep_locations, 95
prep_sites, 78

qa_switch_ampfactors, 13, 120, 122
qa_switch_attn, 13, 120, 122
qa_switch_fuse, 13, 120, 122
qa_switch_map, 14, 120, 122
qa_switch_mke_evnts, 14, 120, 122
qa_switch_soc, 14, 122
qa_switch_vun, 14, 95, 122
qa_switch_watercheck, 14, 120, 122

regional cost factor, 98
resp_crv_flag, 10, 122
response spectral acceleration, 10, 54, 55, 63, 64, 79, 85, 104, 106, 141
response spectral acceleration, 78
response spectral displacement, 10, 11, 54, 78, 79, 90, 95, 128
response spectral velocity, 54, 128
Rthrsh, 11, 119, 121
rtrn_per, 8, 106, 115, 119, 121
run_type, 8, 93, 95, 119, 121

SA, 56
SArock, 56
SAsoil, 77
save_deagecloss_flag, 15, 121
save_ecloss_flag, 15, 100, 102, 109, 121
save_motion_flag, 15
save_probdam_flag, 15, 121
save_socloss_flag, 15, 101, 102, 121
savedir, 8, 119, 121
Script
    newc89plothistsoc, 101, 102
SDRelTol, 13, 122
setdata
    eqrm_param_T, 7
setdata, 7, 16, 25, 38, 40, 41, 44, 49, 50, 56, 58, 66, 72, 76, 93, 97, 98, 100, 101, 106, 109
setdata, 119, 121
setdata parameter
    amp_switch, 11, 119, 122
    attenuation_flag, 10, 66, 68, 70, 94, 119, 121
    attn_region, 10, 58, 59, 61, 68, 70, 119, 121
    aus_contents_flag, 14, 100, 102, 122
    azi, 8, 38, 42, 119, 121
    b_usage_type_flag, 11, 50, 53, 97, 121
    bcap_var_method, 12, 122
    buildpars_flag, 12, 53, 122
    ci, 14, 98, 102, 122
    d_azi, 8, 38, 42, 119, 121
    damp_flags, 13, 84, 85, 95, 122
    destring, 8, 119, 121
    determ_azi, 9, 41, 43, 120, 122
    determ_btype, 12, 122
    determ_buse, 12, 122
    determ_flag, 9, 41, 42, 120, 122
    determ_lat, 9, 41, 43, 120, 122
    determ_lon, 9, 41, 43, 120, 122
    determ_mag, 9, 41, 42, 120, 122
    determ_ntrg, 9, 119, 122
    determ_r_z, 9, 41, 43, 120, 122
    dip, 8, 42, 119, 121
    force_btype_flag, 12, 120, 122
    ftype, 8, 119, 121
    grid_flag, 8, 44, 45, 53, 119, 122
    Harea_flag, 13, 122
    hazard_map_flag, 15, 119, 121
    hazus_btypes_flag, 11, 49, 53, 122

hazus_dampingis5_flag, 12, 122
ieast, 8, 119, 121
ignore_post89_flag, 12
inputdir, 8, 16, 21, 119, 121
max_iterations, 13, 122
MaxAmpFactor, 11, 76, 77, 119, 122
mbnd, 9, 40, 42, 119, 121
min_mag_cutoff, 9, 30, 32, 119, 121
MinAmpFactor, 11, 76, 77, 120, 122
nbins, 9, 42, 119, 121
nsamples, 9, 40, 42, 119, 121
nsigma, 9, 40, 42, 119, 121
ntrgvector, 8, 25, 42, 119, 121
periods, 11, 56, 70, 72, 77, 120, 121
pga_cutoff, 63
pga_mindamage, 14, 101, 102, 122
pgacutoff, 11, 70, 77, 120, 122
qa_switch_ampfactors, 13, 120, 122
qa_switch_attn, 13, 120, 122
qa_switch_fuse, 13, 120, 122
qa_switch_map, 14, 120, 122
qa_switch_mke_evnts, 14, 120, 122
qa_switch_soc, 14, 122
qa_switch_vun, 14, 95, 122
qa_switch_watercheck, 14, 120, 122
resp_crv_flag, 10, 122
Rthrsh, 11, 119, 121
rtrn_per, 8, 106, 115, 119, 121
run_type, 8, 93, 95, 119, 121
save_deagecloss_flag, 15, 121
save_ecloss_flag, 15, 100, 102, 109, 121
save_motion_flag, 15
save_probdam_flag, 15, 121
save_socloss_flag, 15, 101, 102, 121
savedir, 8, 119, 121
SDRelTol, 13, 122
site_loc, 8, 15, 16, 72, 119, 121
SiteInd, 8, 119, 121
small_site_flag, 8, 119, 121
smoothed_response_flag, 11, 122
src_eps_switch, 9, 40, 42, 62, 66, 67, 119, 121
stdcap, 13, 122
var_amp_flag, 11, 119, 121
var_amp_method, 11, 119, 121
var_attn_flag, 10, 62, 70, 119, 121
var_attn_method, 10, 62, 70, 119, 121
var_bcap_flag, 12, 122
wdth, 9, 42, 119, 121
simulated earthquake, 23, 29
simulated event, 8, 20, 22, 23, 105
simulated rupture, 23
site_classes, 45
site_loc, 8, 15, 16, 72, 119, 121
SiteInd, 8, 119, 121
SiteLocations, 44
small_site_flag, 8, 119, 121
smoothed_response_flag, 11, 122
socloss, 102
source, 21, 39
src_eps_switch, 9, 40, 42, 62, 66, 67, 119, 121
src_zones_to_structure, 21
stdcap, 13, 122
stdln_site{1}_rockpga{2}_momag{3}, 75
stdln_site{1}_rockpga{2}_momag{3}, 127
survey factor, 46
synthetic event, 39

var_amp_flag, 11, 119, 121
var_amp_method, 11, 119, 121
var_attn_flag, 10, 62, 70, 119, 121
var_attn_method, 10, 62, 70, 119, 121
var_bcap_flag, 12, 122
virtual fault, 8, 9, 23, 25, 32, 42

wdth, 9, 42, 119, 121
wrap_risk_plots, 110–115